Fall 2020

Impact of Coagulation and Ozonation Pretreatment on Ceramic Microfiltration

Meghan Rita White
University of New Hampshire, Durham

IMPACT OF COAGULATION AND OZONATION PRETREATMENT ON CERAMIC MICROFILTRATION

By

Meghan White
Bachelor of Science, Environmental Engineering, University of New Hampshire, 2018

THESIS

Submitted to the University of New Hampshire
in Partial Fulfillment of
the Requirements for the Degree of

Master of Science
In
Civil Engineering

September 2020

This thesis has been examined and approved by,

Thesis Director, Dr. James P. Malley Jr.,
Professor of Civil and Environmental Engineering

Dr.ir. Abraham J. Martijn,
Senior Technological Researcher at PWN Technologies

Dr. Johan C, Kruithof
Senior Advisor at Wetsus

Dr. Nancy Kinner
Professor of Civil and Environmental Engineering

Table of Contents

List of Figures

List of Tables

Abstract

IMPACT OF COAGULATION AND OZONATION PRETREATMENT ON CERAMIC MICROFILTRATION

By

Meghan White

University of New Hampshire

Globally drinking water sources are under pressure. In many places, there is unintended closure of the water cycle. This means that the wastewater treatment plant effluent with all its pollutants ends up in the source of drinking water treatment plants that are not designed to treat this type of water. Impacts on water sources from factors such as climate change and high population density make unintended reuse, indirect reuse, and potable reuse more accepted and explored. Known reuse schemes use high end treatment technologies such as ceramic microfiltration. While ceramic microfiltration is a beneficial treatment option, its effectiveness can be limited due to membrane fouling causing increases in energy consumption, increases in operating costs, and a loss in permeability. Coagulation and ozonation are pretreatment options that can help mitigate membrane fouling.

Using a secondary wastewater effluent reuse pilot at RWZI Wervershoof in the Netherlands, this research project evaluated the abilities of coagulation and ozonation pretreatment to improve ceramic microfiltration performance in comparison with control runs without pretreatment. This evaluation was based on performance parameters such as critical flux and sustainable flux based on a transmembrane pressure (TMP) criterion. Critical flux was defined as the flux level at which the detection of membrane fouling initially appeared, and

sustainable flux was defined as the flux level directly (25 Lmh) below the critical flux. Water quality samples were analyzed on NOM characteristics to explain ceramic microfiltration fouling

Twenty-four-hour constant flux tests were performed to determine the critical and sustainable fluxes for the three treatment options. For the coagulation pretreatment tests, two dosages of ferric chloride, 20 and 6 mg/L as Fe^{3+}, were tested to determine the more appropriate dosage to restrict ceramic microfiltration fouling. Based on the constant flux test results, a ferric chloride dosage of 6 mg/L as Fe^{3+} was chosen. For the ozonation pretreatment tests, a bench scale ozone uptake test was conducted to determine the ozone dosage for the constant flux tests. Based on this test, the selected ozone dosage was 8 mg/L as O_3.

Without pretreatment, the critical flux was 145 Lmh. Coagulation and ozonation pretreatment increased the critical flux to 195 and 270 Lmh, respectively. During coagulation pretreatment, the critical flux increase was based on NOM removal. During ozonation pretreatment, the critical flux increase was based on changing the NOM characteristics.

The results illustrated that compared to no pretreatment, coagulation pretreatment improved and ozonation pretreatment strongly improved ceramic microfiltration performance. Overall, coagulation or ozonation pretreatment enable a more economical application of ceramic microfiltration for water reuse.

Acknowledgements

This research was made possible by the funding and support from PWN Technologies in Andijk, Netherlands and the University of New Hampshire. The relationship between Dr. Joop Kruithof, Dr. Bram Martijn, Dr. James Malley and PWN Technologies allows for graduate students from the University of New Hampshire to participate in a research internship required for their MS degree research at PWNT's research facilities in Andijk.

I would like to tank PWNT for their support and guidance throughout this research opportunity. A special thanks to Dr. Bram Martijn, Dr. Joop Kruithof, and Sabine Gabriel for their mentoring and guidance throughout this project as this research would not have been possible without them. Thank you to Marco Aalders and Rob van Westen for their vital contributions to the pilot plant operating effectively during this project and to Linda Greydanus and Renske de Winter for their logistical support. A special thanks to Maria and Jaap Pennekamp for welcoming me and allowing me to stay in their lovely home.

I would also like to thank Dr. Malley for all his support, advising, and mentoring during this time. The opportunities that I have had over these years have been because of him, and I will always be truly grateful. Thank you to Dr. Kinner as well for being a part of my thesis defense committee. I would also like to thank both Dr. Malley and Dr. Kinner for inspiring me and pushing me to my highest potential during my undergraduate and graduate education at the University of New Hampshire.

Thank you to my family for all their love and support. I would not be where I am without them. A special thanks to my friends for inspiring my and encouraging me along the way.

Chapter 1

1. Introduction

1.1 Background

Globally drinking water sources are under pressure. In many places there is unintended closure of the water cycle. This means that the wastewater treatment plant (wwtp) effluent with all its pollutants (microplastics, pathogens, antibiotic resistant bacteria and micro-contamination such as medicine residues) should be removed by drinking water treatment processes that are not designed for this purpose. Impact on sources, such as climate change and high population density make unintended reuse, indirect reuse, and potable reuse more accepted and explored.

PWN Water Supply Company North-Holland takes water from the Lake IJssel and treats it with microstraining, coagulation, and rapid sand filtration. The treated water is used as process water in the steel mill industry and for dune infiltration as part of the drinking water production. The infrastructure from the Lake IJssel to the PWN dune infiltration area and the steel mills is in close proximity to the HHNK wastewater treatment plant at Wervershoof. Wervershoof wastewater treatment plant consists of a traditional treatment train consisting of bar screen and grit removal, biological treatment, secondary clarifiers, and disinfection. It is fed by a combined sewer system resulting in mixed wet weather and dry weather conditions. Therefore, the composition of the wastewater treatment plant effluent will vary over the season due to the presence or absence of rain.

PWN and HHNK represent two important parts of the domestic water cycle and it is their ambition to close the water cycle in the province of North-Holland via reuse. This results in the investigation into required treatment technologies to enable the high-end reuse. The

current water quality of conventionally treated Ijssel Lake water is the treatment target that HHNK and PWN defined for the reuse scheme.

Known reuse schemes use high end treatment technologies in series such as microfiltration, ultra-filtration, reverse osmosis, UV based AOP, and GAC. Many reuse schemes or engineered reuse schemes conduct artificial replenishment of groundwater such as in Orange County, CA or lakes such as in Singapore. Drivers for these expensive advanced technological treatments comes from the unquantified fear or risk when reuse is involved, specifically dealing with pathogenetic microorganisms and micropollutants.

Removal of microorganisms and particulates from secondary effluent is an important treatment objective for environmentally safe artificial replenishing of water using wastewater treatment plant effluent. Micropollutants in wastewater (i.e. pharmaceuticals) can be mitigated using ozonation. Ozonation/ozone based AOP of pharmaceuticals in wastewater treatment plant effluent was investigated in a previous study as well as the retention of bacteria and viruses by the ceramic microfiltration.

This project is an investigation into the feasibility of ceramic microfiltration in a reuse scheme where wastewater treatment plant effluent is pretreated using either ozonation or inline coagulation prior to ceramic microfiltration for dune infiltration or high-end reuse for industry. Pilot work focuses on improving the performance in terms of flux of ceramic membrane microfiltration by pretreatment of effluent from wastewater treatment plant Wervershoof.

1.2 Membrane Filtration

Membrane filtration systems consist of water moving through a membrane barrier, which is usually made of flat sheets or hollow fibers, that removes contaminants present in the

water. These systems are either pressure-driven or vacuum-driven. These systems are pore size-dependent processes, which is illustrated by the scheme shown in Figure 1-1. Membranes are made of either polymeric or ceramic material. Ceramic membrane made of aluminum oxide and titanium oxide ensure a narrow pore size distribution. This research applies a Metawater ceramic microfiltration membrane with a pore size of 0.1 micrometers. The narrow pore size distribution ensures, especially in combination with pretreatment systems, a constant permeate quality, and bacteria reduction. While membrane microfiltration technologies do possess advantages regarding pathogen reduction as well as reliability, the performance of the system can sharply decrease when membrane fouling occurs.

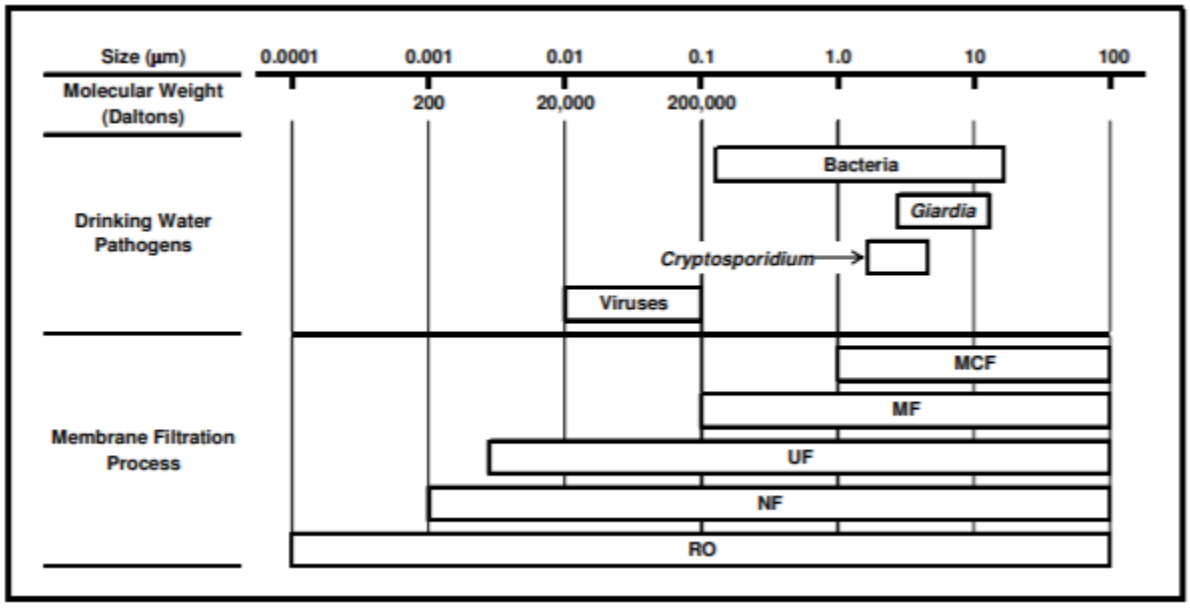

Figure 1-1 Membrane Filtration Guide (Malcolm Pirnie, Inc et al., 2005)

1.3 Membrane Fouling

There are two types of membrane fouling, physically reversible fouling and physically irreversible fouling. Physically reversible fouling is fouling that can be reversed by backwashing. It mainly refers to the cake that forms on the outside of the membrane due to

particle deposition. Irreversible fouling is the result of the preventing of the transportation of water through the membrane by particles due to the blocking of pores or the adsorbing of particulates in the pores of the membrane resulting in pore constriction. This type of fouling is often due to interaction between foulants like organic matter particles and the functional groups of the membrane. Pretreatment processes such as coagulation as well as ozonation are pursued to mitigate membrane fouling (Lee et al., 2015, Hamid et al., 2017).

1.4 Pretreatment

1.4.1 Coagulation Pretreatment

Coagulation is a pretreatment option for the reduction of membrane fouling. This pretreatment method improves the particle aggregation rate, reduces the turbidity of the feed water and the amount of dissolved organic carbon (DOC) and improves the removal of microorganisms which may be contributing to biofouling. Coagulant dose and pH control require stable operation and need to be adjusted to water composition. This can be challenging to achieve with fluctuating water quality. Disadvantages include the potential increase in fouling if the correct coagulant dosage is not used and the generation of solids.

1.4.2 Ozonation Pretreatment

Ozonation pretreatment is another effective pretreatment option for ceramic membrane microfiltration as it can lead to a larger permeate flux. This is exclusive to ceramic membrane filtration because polymeric membranes do not allow for residual ozone. Ozone pretreatment affects the water quality such as reduction of color, UV254 absorbance, and taste and odor (TAO) causing compounds. The ozone dosage can substantially affect the membrane flux without damaging the ceramic membrane.

One of the mechanisms proposed for the reduction in membrane fouling with ozonation pretreatment is ozone's reaction with natural organic matter (NOM) (Van Geluwe et al., 2011). Lehman et al. (2009) found that ozone pretreatment decreased membrane fouling through the degradation of the colloidal fraction and reduction of the whole molecular weight spectrum of NOM. It is also hypothesized that ozonation pretreatment can affect the membrane characteristics, improving membrane permeability (Hamid et al., 2017). Process conditions are essential for the beneficial application of ozonation pretreatment to improve the performance of the membrane process.

1.5 Research Partners

This research project was a joint effort between the University of New Hampshire, PWNT, PWN, and HHNK with analytical support of HWL.

Chapter 2

2. Research Description

2.1 Introduction

This chapter provides an overview of the problem statement, the research objective, and the research outline. Additionally, this chapter describes any boundary conditions that impacted the research results and the scope of work.

2.2 Problem statement

PWN and HHNK explore the possibilities of high-end reuse of further treated wastewater treatment plant effluent. The water quality reference is conventionally treated surface water from the Ijssel Lake. In previous research efforts, the contribution effect of ozonation and ceramic microfiltration on the water quality was evaluated. However, the technological optimization of ceramic microfiltration by pretreatment with ozonation and inline coagulation was not studied. The feasibility of high-end reuse consisting of ceramic microfiltration using ozonation pretreatment and inline coagulation lacks insight in membrane performance in terms of flux, pressure drop increase, and process settings for pretreatment and the benefits of pretreatment on the performance of ceramic microfiltration.

2.3 Research Objective

The objective of this research is to evaluate the impact of coagulation pretreatment and ozonation pretreatment on ceramic microfiltration performance using a secondary effluent water reuse pilot in Wervershoof.

2.4 Research Outline

This research investigates the effect of pretreatment by ozonation or inline coagulation on the flux of ceramic microfiltration in a reuse scheme. This leads to the following research intentions:

- Defining sustainable flux and critical flux
- Establishing a treatment reference (no pretreatment)
- Defining pretreatment conditions regarding coagulation and ozonation dose
- Evaluating the impact of coagulation and ozonation pretreatment on membrane performance

2.5 Boundary Conditions

The following boundary conditions apply to this research:

- The investigated water is effluent from the wastewater treatment plant in Wervershoof in the Netherlands
- Ferric salts applied by HHNK/PWN are used as coagulant
- The experimental program had to follow the available water composition
- This research was conducted using the available bench-scale setup (HWL ozone setup and PWNT jar testing setup, and a pilot with 0.4 square meter Metawater ceramic membrane module)
- The available pilot is operated in semi-batch mode
- The ozone was dosed by a venturi system installed in a recirculation loop
- This research does not examine long-term irreversible fouling, but only looks at short-term fouling

Chapter 3

3. Literature Review

3.1 Water Reuse

3.1.1 Overview

Insufficient access to sanitation is a prevalent issue plaguing people at a global level. With the increasing population and tourism, as well as developing economies, water scarcity has become a problem with increasing concern (Sgroi et al., 2018). Energy, food preparation, industrialization, as well as the condition of the natural environment relies significantly on water availability. Therefore, this issue of water scarcity plagues both industrialized nations as well as developing ones. A potential solution to this problem is water reuse (Sgroi et al., 2018).

Water reuse can provide water for irrigation, the recharge of groundwater supplies, industrial operations, as well as drinking water provisions through the employment of advanced treatment technologies. Considerations in the areas of economics, natural environment, politics, society, and technology influence the implementation of these technologies. For instance, in dry areas of the world, the application of water reuse technologies is usually for the improvement of agriculture through irrigation (Sgroi et al., 2018). Furthermore, for a successful implementation, the integration of stakeholders, such as corporations, communities, as well as individuals, along with regulations in the decision-making process is paramount (Bixio et al., 2006). Thus, the holistic approach, which considers all the components that go into reuse decisions, should be implemented (Sgroi et al., 2018).

3.1.2 Water Reuse in Developed Countries

Countries such as those within Europe, the United States, and Singapore have used water reuse to augment water supplies. In Europe, the use of water reuse has been apparent throughout history. The amount of water reuse produced in Europe was approximately 700 million cubic meters in 2004 (Angelakis et al., 2008). More than one-third of the water reuse projects taking place in Europe utilize secondary effluent. Southern Europe mainly uses wastewater reuse for irrigation to enhance agriculture as well as for urban along with environmental purposes. Northern Europe utilizes it for primarily urban, environmental as well as industrial projects (Bixio et al., 2006). The increasing acceptance of water reuse technologies has increased the potential for the implementation of more water reuse projects. Hochstrat, Wintgens, and Melin (as cited in Fawell et al.) approximated that Europe will have water savings as high as 1.5 percent by the year 2025 with the employment of such technologies (Fawell et al., 2016)

Water reuse practices are not only seen in Europe, but also in the United States, where water reuse projects are used to help mitigate drought conditions and decrease water supplies in states such as California and Florida. The biggest water reuse project in the United States is the Groundwater Replenishment System (GWRS) in Orange County, California. For more than 40 years, indirect potable water reuse systems, or potable water reuse that requires environmental buffers to facilitate the combining of reuse water with conventional water replenishments, has been used in Orange County, California. Some of the past water reuse projects utilized by Orange Country from 1976 until present include the Water Factory 21 (WF-21), Interim Water Factory 21 (IWF-21), and Groundwater Replenishment System Advanced Water Purification Facility (GWRS AWPF). GWRS AWPF is the current system

in use by Orange County and has a production capacity of 100 million gallons per day (mgd). This system consists of microfiltration, reverse osmosis as well as an advanced oxidation process in the form of UV disinfection with the addition of hydrogen peroxide. Ultimately, this system acts as a global standard for potable water reuse (Burris, 2018; Ormerod et al., 2017).

Singapore has also implemented water reuse technologies. One of the projects in Singapore was a pilot study conducted by PWNT to aid in design efforts for the expansion of Changi NEWater Facility. The pilot study was conducted from October 18th, 2013 to January 23rd, 2014. In this study, they looked at different pretreatment alternatives for ceramic membrane microfiltration such as inline coagulation, ozonation, coagulation with ozone, and no pretreatment. The tests conducted consisted of short-term runs to determine the critical flux and optimize backwashing frequency for each of the alternatives for chlorinated water and short-term runs for coagulation pretreatment on unchlorinated water. Based on the results from the tests they ran, PWNT recommended that full-scale implementation consists of coagulation pretreatment with the coagulant PACl and a dosage of 2 mg/L as Al^{3+}. They also determined that the use of ozonation pretreatment on its own was not feasible as it did not mitigate fouling and the addition of coagulation pretreatment would be needed (Zheng et al., 2014).

3.2 Ceramic Membrane Filtration

3.2.1 Overview

Membrane filtration is a pore-size dependent process that uses either pressure or vacuum-driven processes to remove particulates bigger than 1 micrometer. Pressure-driven systems involve the use of pressurized feed water and operating pressures within the range of three to

forty psi. The vacuum-driven systems employ pressure as well; however, they utilize negative pressure. The pressures used in these systems are within the range of approximately negative three to negative twelve psi. Membrane systems use a sieving process based on their pore size range to remove particulate matter. The overall process of removing particulates using a microfiltration membrane is more complicated than sieving alone. The removal of smaller particulates can occur further into the filter media, particles can adsorb to the material of the membrane, or they can adhere to the cake layer that forms as more particles run through the system and fouling occurs. (Malcolm Pirnie, Inc et al., 2005)

One type of membrane filtration system is a membrane microfiltration system. Membrane microfiltration can produce water quality effluent that has high microbial safety and sanitation quality by removing bacteria, protozoan cysts, and microorganisms (Lerch et al., 2005; Bottino et al., 2001). The membrane module of a microfiltration system is usually hollow fiber. Hollow fiber modules are composed of long and narrow tubes and can be comprised of several hundred to more than ten thousand fibers. These modules can operate in one of two ways: inside-out or outside-in. The inside-out operation signified that water enters through the center of the fiber and then penetrates through the fiber wall. The outside-in process involves the feed water filter through the fiber wall into the center of the fiber, where the filtrate is gathered. The outside-in process allows for more of the membrane surface area to be available for the filtration and prevents the clogging of the fiber's center. However, this process lacks the distinct flow path of the inside-out process. The inside-out process has a higher chance of clogging, specifically concerning the center of the fiber (Malcolm Pirnie, Inc et al., 2005).

Membrane microfiltration systems are made of polymeric materials or ceramic membrane materials. For this research, a ceramic membrane microfiltration system was used. Ceramic microfiltration membranes offer chemical and thermal durability, protection to acidity, limited environmental pollution, and improved mechanical strength when compared to conventional systems (Rakruam et al., 2014). Ceramic membranes can work during pH extremes as well as high permeate fluxes, backwashing strengths, and hydraulic pressures (Nazzal et al., 1994; Zhu et al., 2012). Ceramic membranes typically have an asymmetrical structure that consists of three layers. An outer layer provides microporous support along with mechanical strength. An inner layer enables separation, and an intermediate layer connects the outer and inner layers. Materials used in the manufacturing of ceramic membrane include alumina, Titania, glass, zirconia, silicon carbide, or some mixture of these metal oxides (Issaoui et al., 2019).

Ceramic membranes also have an electrical charge associated with them. This electrical charge develops because of the behavior of the hydroxyl group, which is located on the surface of the membrane, when it encounters an aqueous medium. Ceramic membrane's filtration capabilities are impacted by the electrochemical properties of its surface. These properties are influenced by the pH, ionic strength, as well as the constituents of the aqueous solution (Zhao et al., 2005). HHNK and PWN selected ceramic membrane microfiltration for their reuse application due to its chemical and thermal durability and its ability to remove pollutants in the water. While membrane microfiltration technologies do possess advantages regarding pathogen reduction as well as reliability, the performance of the system can sharply decrease when membrane fouling occurs. (Hamid et al., 2019; Zhu et al., 2012).

3.2.2 Membrane Fouling

Membrane fouling is a consequence of sieving and separation processes. There are two types of membrane fouling: physically reversible fouling and physically irreversible fouling. Physically reversible fouling is fouling that can be repressed by backwashing. It mainly refers to the cake formation that can form on the outside of the membrane due to particle deposition (Zhu et al., 2012). Reversible fouling can also occur when the membrane is exposed to components of natural organic matter (NOM), because of their adsorptive tendency towards the surfaces of ceramic membranes. However, the exposure to NOM can also lead to more severe membrane fouling in the form of irreversible fouling (Szymanska et al., 2014).

Irreversible fouling occurs when dissolved particles prevent the transportation of water through the membrane due to the blocking of pores or materials and particulates adsorbing onto the membrane pores resulting in pore constriction. This type of fouling is often due to the presence of organic matter as its size compared to the membrane's pore size in microfiltration is usually considerably smaller. Organic, high molecular weight particulates containing hydrophilic components are a significant source for irreversible fouling in the treatment of wastewater for reuse (Zhu et al., 2012). A depiction of the fouling mechanisms is seen below in Figure 3-1: Fouling Mechanisms (Arhin et al., 2016). Membrane fouling also signifies a rise in TMP if the microfiltration membrane system runs under constant flux (Zhu et al., 2012).

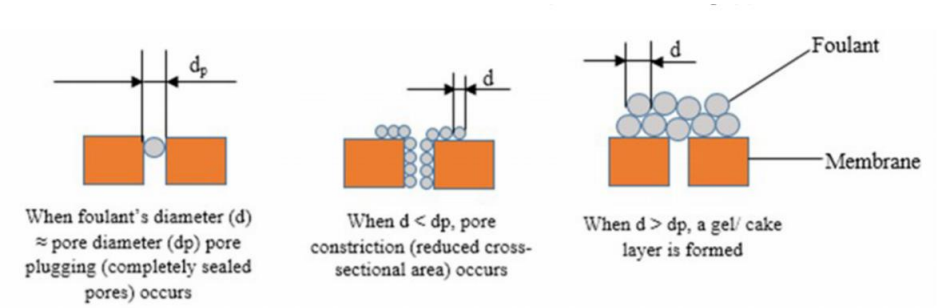

Fig. 1. The nature of fouling in low pressure membrane.

Figure 3-1 Fouling Mechanisms (Arhin et al., 2016)

Based on the literature, there are some observations seen when it comes to membrane fouling and permeability of the cake layer. The first of these observations is that when salts in the feedwater do not result in aggregation of particulates, the cake layer's permeability decreases because of electrolyte concentrations increasing. Furthermore, the cake layer's permeability can also decrease due to flux increases, which causes more compressed cake layers. On the other hand, the cake layer's permeability can increase due to increases in interparticle repulsion that results from the particle's surface potential (Petsev et al., 1993).

Strategies have been created to prolong the formation of membrane fouling and extend the operational time of a membrane filtration system. The techniques that prevent membrane fouling are split into two main categories, which are physical and chemical methods. Physical methods to prevent fouling include backwashing, working with a low TMP, and operating with a large cross velocity flow and with regards to the critical flux. However, these strategies briefly repair the membrane and require a significant amount of energy, so they are not long-term solutions. Chemical technologies include the use of chemical agents such as HCL, HNO_3, NaOCl, or NaOH in enhanced chemical backwashing. The use of such chemicals can nearly restore the membrane; however, they are costly and pose the potential threats of contaminating water, producing harmful by-products, and degrading the membrane

(Szymanska et al., 2014). Coagulation and ozonation pretreatment have also been cited in the literature as pretreatment alternatives to mitigate membrane fouling due to their ability to reduce the cake layer's hydraulic resistance. The impacts of pretreatment alternatives, as well as the importance of optimizing conditions, on low pressure membranes, such as ceramic membranes, can be seen in Figure 3-2 below (Huang et al., 2009).

Table 3-1 Effects of Pretreatment on Membrane filtration (Huang et al., 2009)

TABLE 1. List of the mechanisms, effects, and applications of major pretreatments for membrane filtration

pretreatment	coagulation	adsorption	preoxidation	prefiltration
chemicals applied	coagulants (or flocculants) at proper dose	porous or nonporous adsorbents in suspension or fixed contactor	gaseous or liquid oxidants	granular media with/without coagulants, membranes
dose effects	under-, optimal, or overdose (optimal for enhanced coagulation)	minimal effective dose if used as suspended particles	minimal effective dose	none
physical mechanisms	increases the size of aquatic contaminants to filterable level	binds small contaminants to adsorbents much larger than membrane pores	may cause dissociation of organic colloids into smaller sizes or the release of EPS by aquatic organisms	removes coarse materials that may cause cake/gel layer formation on downstream membranes
chemical mechanisms	destabilizes contaminants to cause aggregation or adsorption on coagulant precipitates or membrane surfaces	provides new interfaces to adsorb/accumulate substances detrimental to membrane performance	oxidizes and/or partially decomposes NOM, possible mineralization if VUV used	selectively removes contaminants or other particles that are sticky to filter media and downstream membranes
biological mechanisms	partially removes autochthonous NOM and hinder bacterial growth in feedwater or on membrane	may adsorb organic contaminants relevant to biofouling	suppresses microbial growth	partially removes microorganisms that can cause biofouling
targeted contaminants	viruses, humic/fulvic acids, proteins, polysaccharides with acidic groups, colloids smaller than membrane pores	humic/fulvic acids, small natural organic acids, some DBPs, pesticides and other synthetic organic compounds	viruses and organic contaminants with ozonation	particulate and colloidal organic/ inorganic substances, microbiota
effects on membrane fouling	reduces colloidal fouling and NOM fouling	may increase or decrease membrane fouling	may reduce biofouling and NOM fouling	may reduce fouling to different extents
advantages	significantly improves LPM performance (less fouling and greater rejection)	increases the removal of DBPs and DBP precursors	reduces the occurrence of biofouling; increases organic removal (ozonation)	may reduce biofouling, colloidal fouling, and/or solids loading
disadvantages	(i) requires proper dose that can be difficult to meet if feedwater quality varies rapidly/significantly, (ii) may exacerbate fouling, (iii) produce solid wastes, (iv) ineffective in mitigating the fouling by hydrophilic neutral organics	(i) possible exacerbation of LPM fouling, (ii) difficulty in removing PAC powders from treatment facilities	(i) formation of DBPs; (ii) may damage membranes incompatible with oxidants; (iii) may be ineffective in suppressing the growth of some microbiota resistant to oxidation	(i) performance of prefilters may deteriorate and be difficult to recover, (ii) may require pretreatment (e.g., coagulation or preoxidation) to enhance the efficacy

The membrane fouling discussed above is the organic type of membrane fouling; however, there is another type of fouling. The systems, where this issue seems to be of the

most concern, are reverse osmosis along with nanofiltration. Biofouling is observed when there is an increase in TMP. This increase is the effect of the depositing of bacterial cells onto the membrane. Biofouling was not a focus of this research as it mainly impacts reverse osmosis, and this research focuses on ceramic membrane microfiltration (Bucs et al., 2018).

3.3 Critical Flux

3.3.1 Overview of Critical Flux

Critical flux is the term that describes the flux level at which the detection of membrane fouling initially appears. Below this flux, there is no occurrence of membrane fouling or accumulation of particulates on the membrane surface. This flux level below the critical flux is the sustainable flux (Field et al., 2011; Bacchin et al., 2006; Howell et al., 1995). Suspension properties can impact the critical flux such as stability, concentration, and pH. Concerning stability, low suspension stability can cause the critical flux to decrease. Suspension concentration can cause the critical flux to decrease as well as when the concentration increases, the flux decreases. The pH of the water can also impact the critical flux as it can modify the solute charge. Therefore, if the pH increases, it can cause the critical flux to rise. (Bacchin et al., 2006)

The hydrodynamics of the membrane's exterior can significantly influence changes with the critical flux, as the flux is highly sensitive to these conditions. As the hydrodynamic strength increases, the critical flux can increase as well. Furthermore, membrane properties, such as porosity and materials, can impact the critical flux. Higher porosities are more evenly distributed permeate fluxes and result in a higher critical flux across the entire surface of the membrane. Regarding the membrane material, Huisman et al. (as cited in Bacchin et al.)

noted that hydrophilic membranes usually have higher porosities associated with them, which can lead to a larger critical flux as previously mentioned (Bacchin et al., 2006)

3.3.2 Methods for Determining the Critical Flux

The determination of a critical flux of a system can occur through various methods. These methods include flux stepping or conversely through pressure stepping to generate measurements for flux or TMP, profiles of flux and pressure, direct observation of the membrane (DOTM), mass balance, as well as through analysis of the fouling rate. Regardless of the measurement method implemented, the obtained critical flux is only relevant with regards to time used as well as the sensitivity of the method. Each of these methods has advantages and disadvantages associated with them as well as certain processes that they have more suitability towards (Bacchin et al., 2006).

Flux stepping is one of the methods used for determining the critical flux. The most simplistic technique for this method is to create and run a series of increasing pressure stages before a series of decreasing stages. Wu et al. (as cited in Bacchin et al.) implemented this process in two ways. The first way was through a set of increasing flux stages, and the other way was through sets of increasing and decreasing stages. The second method allowed for the detection of small differences in TMP resulting from trace fouling to be possible. In this process, the initial flux was set and once they achieved a constant TMP, they reported it. Then, Wu et al. increased the flux to a marginally larger one and recorded. If there was a difference in these TMP, it signified fouling of the membrane occurred. They kept increasing and decreasing flux to different levels to see if there was any change in fouling for seven different sets. The flux stepping procedure can measure fouling; however, resistance measurements need to occur at each stage (Bacchin et al., 2006).

The profile of flux and pressure is another applicable method for determining the critical flux. This method employs either a constant flux or pressure and measures either pressure or flux, respectively. The flux should be below the critical flux when starting the process, regardless of the set up as irreversible fouling will influence the successive measurements. With a constant flux setup, the fouling rate can be determined. The pressure ends up increasing with time when fouling is present for this arrangement. With the use of constant pressure, one can determine the flux for steady-state conditions, which allows for dependable results without reliance on time with the use of an adequate pressure step duration (Bacchin et al., 2006).

Direct observation through the membrane (DOTM) employs the use of a microscope to observe the buildup of particulates on the surface of the membrane or the absence of them. It works for particulate feeds. This process is limited to translucent membranes or ones that have translucent sections within their modules, specifically on the side where permeate exits the membrane. Furthermore, the particles on the membrane must be relatively large before they can be observed under a microscope (Bacchin et al., 2006).

Using mass balance to determine critical fluxes is only applicable when the implementation of another method is occurring as well. Kwon et al. (as cited in Bacchin et al.) implemented this procedure to determine the critical flux by measuring the particulate adsorption without the presence of flux and determining the deposition rate. They then plotted a flux versus deposition rate graph and extrapolated a critical flux from it. The critical flux is the flux on the graph associated with the deposition rate of zero. This method works for particulate feeds, but it is unable to differentiate between weak and strong critical fluxes and has no relation to reversibility (Bacchin et al., 2006).

Lastly, fouling rate analysis is a method for determining critical fluxes for a membrane. With this process, one plots the change in transmembrane pressure versus time. The critical flux is where there is no observation of fouling on the graph. This process relies on the use of constant flux experiments to create the graphs. Moreover, it is subjective and has no relation to reversibility (Bacchin et al., 2006).

The critical flux test used during this research was a twenty-four-hour constant flux test as it allowed for the evaluation of short-term membrane fouling.

3.4 Coagulation

3.4.1 Overview

Coagulation in water treatment enhances the efficiency of the entire treatment system as well continues to play a significant role in managing water quality parameters such as disinfection by-product precursors, particularly natural organic matter (Jiang et al., 2015; US EPA et al., 2001). The employment of coagulation in a treatment process leads to a reduction in turbidity and color as well as in the presence of pathogens in the water. Unfortunately, the ideal circumstances for the removal of color or turbidity are not consistently compatible with the ideal circumstances for the removal of natural organic matter. Therefore, coagulation can be set up to enhance the removal of certain water characteristics (Matilainen et al., 2010).

The operation of coagulation involves the aggregation of colloids. This process consists of three main stages, which are the addition and combining of a coagulant into the feed water, destabilization of colloid particulates, and the development of flocs. Coagulation mainly describes the beginning of the destabilization process, and then the consecutive aggregation of particulates from smaller than micrometer size into millimeter size particulates is flocculation. During coagulation, the main reaction that occurs is the reduction

in the repulsive capacity of particulates. The collisions of these particulates lead to the formation of flocs. Typical coagulants include aluminum and iron salts. These salts dissociate into Al^{3+} or Fe^{3+} and develop into soluble complexes with positive charges. The positive charge of these complexes enables them to adsorb onto colloids, which have negative charges. These mechanisms can fall into two general categories: charge neutralization or sweep coagulation (Jiang, 2001; Jiang et al., 2015; Matilainen et al., 2010).

Charge neutralization occurs when the positively charged complexes adsorb onto the negatively charged colloids. This process reduces the charge of the colloids and thus, results in the precipitation and aggregation of the particulates (Jiang, 2001). Sweep coagulation refers to the process in which the dosage of coagulant exceeds the amount necessary for the precipitation of the solid precipitates formed during the hydrolysis of aluminum and iron salts, which allows for the entrapment of particulates and dissolved organism in these solids as they assemble and settle. Some of the dissolved particulates entrapped for instance are humic acids, heavy metals, and fulvic acids.

It is important to determine the optimal coagulant dosage for the specified feed water and coagulation unit. To determine optimal coagulant dosages, jar testing can be a useful tool. These experiments mimic operating conditions and enable the manipulation of coagulant dosages, mixing speeds, and settling rates. (Prince, 1975; Calderón et al., 2001).

3.4.2 Ability of Coagulation to Remove NOM and Particulates

Coagulation's ability to reduce the NOM and destabilize particles in feedwater makes it a potential pretreatment option to mitigate membrane fouling in ceramic membrane microfiltration. NOM present in the feedwater can lead to both reversible and irreversible fouling, which is why the reduction of it makes coagulation a potential pretreatment option

for ceramic membrane microfiltration. Natural organic matter (NOM) removal by coagulation occurs through a combination of processes, such as charge neutralization, adsorption, and enmeshment (Matilainen et al., 2010). The coagulation of NOM efficiently occurs within the pH range of 5 to 6 for metal-based coagulants. This increased efficiency is due to charge neutralization as well as the decrease in charge density in NOM components, both of which benefit from low levels of pH (US EPA, 2001). With metal salts, such as aluminum or ferric-based salts, the removal of NOM occurs through charge neutralization and sweep coagulation. The cationic species formed during the hydrolysis of the aluminum and ferric salts neutralize the anionic NOM. The insoluble neutralized particles aggregate into flocs and precipitate out. Furthermore, adsorption occurs in which the NOM attaches to the surface of the metal hydroxide particulates, and sweep flocculation occurs (US EPA, 2001; Shin et al., 2008). A figure depicting the coagulation mechanisms that can impact the reduction of NOM can be seen in the Figure 3-2 below.

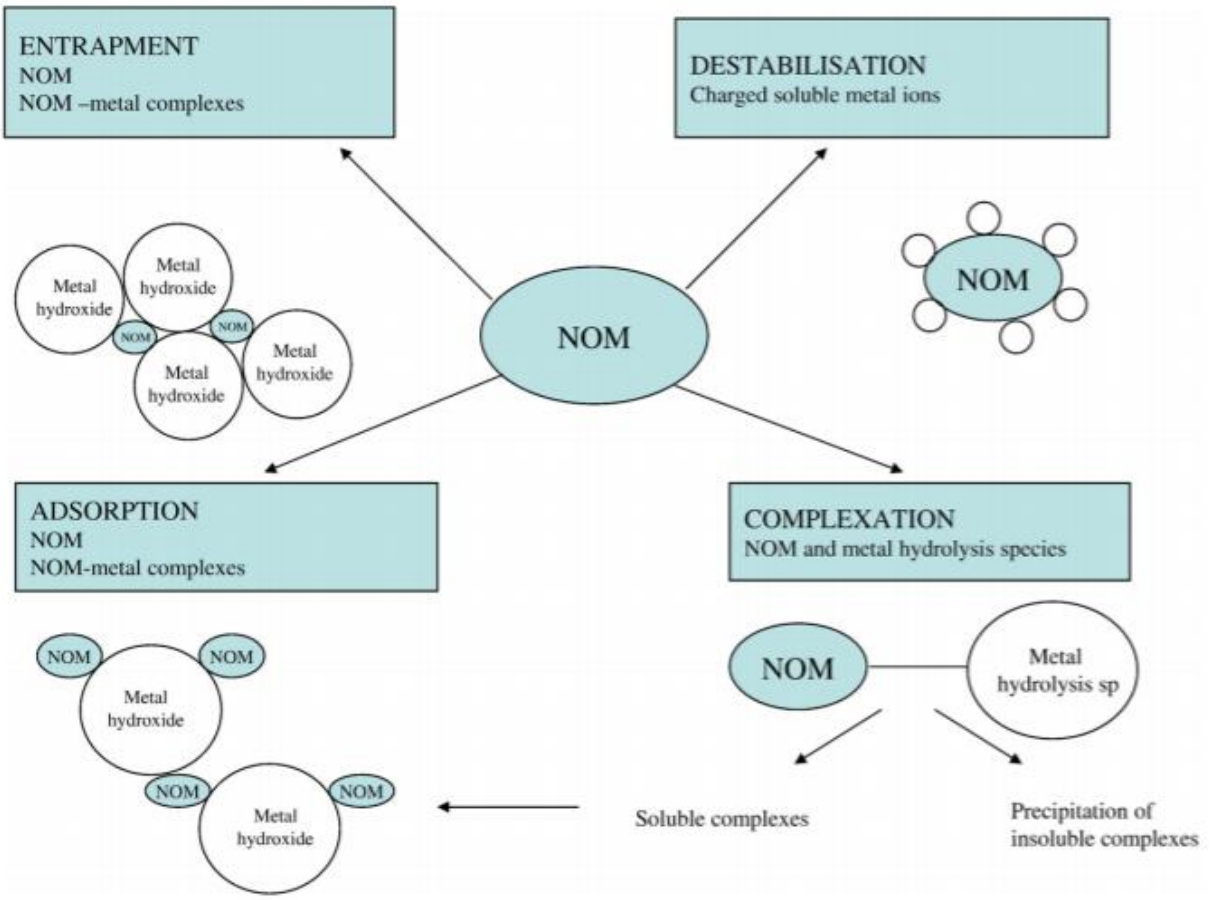

Figure 3-2 Coagulation Mechanisms that Reduce NOM (Matilainen et al., 2010)

Coagulant dosing is a crucial aspect of coagulation that determines the effectiveness of this pretreatment in mitigating membrane fouling. Underdosing generates fine flocs, which inadequately settle. These flocs are approximately the same size as the membrane pores of a microfiltration system. Therefore, if these flocs have an affinity to the surface of the membrane, then pore-blocking will likely occur. Through the application of the optimal dose, the flocs will be larger than the pore sizes in a microfiltration system, which lessens the potential of pore constriction. The main form of fouling in this scenario, especially with the use of inline coagulation, is the formation of a cake layer on the surface of the membrane. In the case of overdosing with an inorganic coagulant, it enhances NOM removal and floc

settling to some degree, which minimizes the potential of pore constriction (Arhin et al., 2016; Huang et al., 2009).

3.5 Effect of Coagulation on Ceramic Membrane Microfiltration

As previously mentioned, coagulation pretreatment can improve the particle aggregation rate, the turbidity of the feed water, the amount of dissolved organic carbon (DOC), and the removal of microorganisms. The coagulation process also improves membrane filtration operation by reducing fouling. However, it also can increase fouling without the proper coagulant dose, generates solid wastes, and is useless in reducing the fouling of organics that are neutral and hydrophilic (Arhin et al., 2016; Huang et al., 2009). Lee et al., Konieczny et al., and Hatt et al. conducted studies that evaluated coagulation pretreatment's ability to reduce fouling of ceramic membranes.

Lee et al. determined that chemical coagulation was an efficient pretreatment option for reducing membrane fouling in ceramic microfiltration. Furthermore, the physically removable fraction of membrane fouling was the more dominant form present with the ceramic microfiltration in the presence of coagulation pretreatment. In the study, Lee et al. used a hollow fiber ceramic membrane with a pore size of 0.1 μm and three sources of water, Georgia River (GR), Catawba River (SR), Lake Lanier (GL), as well as two coagulants, ferric chloride and aluminum sulfate. The evaluation of the coagulation microfiltration operations was concerning resistances and rejections. Regarding resistance, there are three types physically removable, chemically removable, and irreversible. The most significant resistance observed was physically removable fouling. Ultimately, the two coagulants used both achieved reductions in reversible, chemically removable, and irreversible fouling; however, ferric chloride delivered higher reductions (Lee et al., 2015).

Konieczny et al. concluded that to lengthen the membrane's life span and to provide a consistent and large membrane yield, the addition of coagulation pretreatment to a microfiltration system is advantageous, especially when the magnitude of organic compounds is significant in the feed water. Water quality parameters dealing with organic compounds concentrations were able to meet the regulated levels through the combination of coagulation pretreatment and microfiltration. This combined process also provides better treatment capabilities than either process can individually. To acquire these conclusions, Konieczny et al. conducted experiments using the MF-KOOW4040 ceramic membrane with a pore size of 0.1 μm and the MF-KOOW5040 ceramic membrane with a pore size of 0.2 μm, four coagulants (ferric chloride, aluminum sulfate, ALF, and PAX-16) and simulated water, which consisted of powdered humic acid and deionized water. The dosages applied were within the spectrum of 1 to 7.2 mg/dm^3 with pH values within the range of 5.5 to 8.8. They also used two different microfiltration membranes, one with a pore size of 0.1 micrometers and one with a pore size of 0.2 micrometers. The organic compounds present in the feed water during these experiments were higher than the normal levels (Konieczny et al., 2006).

Hatt et al. determined that by using a coagulant the pilot can work at higher fluxes effectively and still only have fouling rates at levels associated with lower fluxes In their study, Hatt et al. evaluated the effects five different coagulants (ferric sulfate, PAX-10, PAX-XL9, aluminum sulfate, and polyaluminum chloride) on ceramic membrane microfiltration. The type of ceramic membrane used was a Siemens Memcor CMF-S 0.04 micrometer. The source water used in this experiment was secondary effluent from a wastewater treatment plant in London. Two sets of trials were run for a week along with preliminary trials.

Regarding the preliminary runs, the coagulant dosages were 0.5, 1, and 2 mg/L. For the week-long runs, the coagulant dosage applied for the different coagulants was 0.5 mg/L but at varying fluxes, 40, 45, and 50 Lmh. With the preliminary trials, there was a linear relationship displayed between reversible fouling and irreversible fouling with turbidity, and time for intervals of constant feed water degrees of turbidity, respectively. Both linear relationships indicated that rapid shifts of the turbidity present in the feed water led to an increase in fouling rates for both reversible and irreversible fouling. Hatt et al. also determined that a coagulant dosage of 0.5 mg/L at 50 Lmh was able to diminish fouling, both reversible and irreversible. This reduction was like the one observed when the system was run without a coagulant at optimized conditions. Therefore, it was determined that the required dose to reduce fouling was only a portion of the amount required to improve the removal of organic matter. (Hatt et al., 2011).

3.6 Ozonation

3.6.1 Overview

The use of ozonation for the treatment of wastewater occurs in the areas of the enhancement of effluent water quality, sludge management, air treatment as well as pre-oxidation of polluted portions of the waste stream (Reid et al., 2009). This treatment process uses ozone gas (O3) as the disinfectant, which is relatively unstable. In natural waters, ozone's decay is initially characterized by a quick decrease followed by a decrease in terms of first-order kinetics (Von Gunten, 2007). This characterization can be seen in Figure 3-3 below.

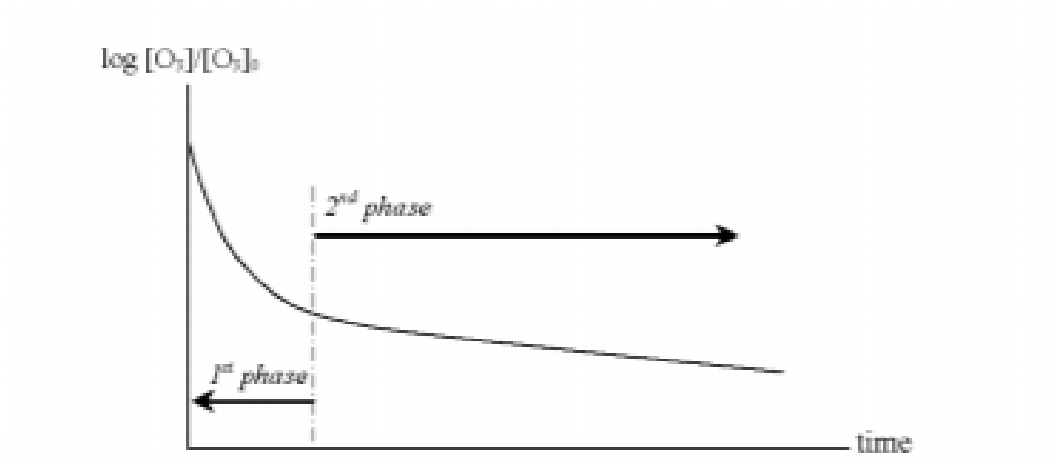

Figure 3-3 Ozone's Decay in Natural Waters and Wastewaters (Buffle, 2005)

Ozone's half-life can be in terms of seconds to hours and is largely dependent upon the water quality (Von Gunten, 2007). Factors impacting the stability of ozone include temperature, pH, and natural organic matter. In oxygen or air, the temperature can influence ozone's half-life. The half-life is approximately 20 to 100 hours when the temperature is at room level. When the temperature level is at 120°C, then the half-life substantially decreases to a range of 11 to 12 minutes. Thus, it is important to have a cooling mechanism in place with the generators to prevent the temperature from significantly affecting ozone's half-life. Furthermore, in water, lower temperatures increase ozone's solubility. This is apparent in Henry's apparent constant equation, which is Equation 3-1 (Stover et al., 1986; American Water Works Association Research Foundation et al., 1991).

Equation 3-1

$$\ln H_a = 22.3 - 4030/T$$

Ozone's half-life can also be influenced by pH. It influences the half-life of ozone due to its ability to initiate the decomposition of ozone through reactions involving hydroxide ions seen in the following reactions depicted in Figure 3-4, where k represents the rate constant.

$$O_3 + OH^- \rightarrow HO_2^- + O_2, \quad k = 70\ M^{-1}s^{-1}, \qquad (1)$$

$$O_3 + HO_2^- \rightarrow {}^{\bullet}OH + O_2^{\bullet -} + O_2, \quad k = 2.8 \times 10^6\ M^{-1}\ s^{-1} \qquad (2)$$

$$O_3 + O_2^{\bullet -} \rightarrow O_3^{\bullet -} + O_2 \quad k = 1.6 \times 10^9\ M^{-1}\ s^{-1} \qquad (3)$$

Figure 3-4 Reactions between Hydroxide Ions and Ozone (Von Gunten, 2007)

In these reactions, it illustrates that ozone initial decay can be accelerated through either increasing pH or adding hydrogen peroxide. Furthermore, this illustrates an advanced oxidation process or AOP (Von Gunten, 2003; Von Gunten, 2007).

NOM can also influence the stability of ozone in the water in one of two ways. The first way is by reacting with the ozone present in the water directly. The other way is by scavenging hydroxyl radicals present in the water. The reaction of NOM and OH radicals can be depicted in the reactions seen in Figure 3-5 below.

$$^{\bullet}OH + NOM \rightarrow NOM^{\bullet} + H_2O \text{ or } NOM^{\bullet}\text{–}OH \qquad (4)$$

$$NOM^{\bullet} + O_2 \rightarrow NOM\text{–}O_2^{\bullet} \rightarrow NOM^{+} + O_2^{\bullet -} \qquad (5)$$

Figure 3-5 Reactions between Hydroxide Ions and Ozone (Von Gunten, 2007)

These reactions can impact ozone's stability by forming carbon-centered radicals and superoxide radicals, which increase the production of OH radicals in the feed water. These reactions increase the degradation rate of ozone (Von Gunten, 2003; Von Gunten, 2007). NOM acts as a scavenger or as an inhibitor in these reactions. Scavengers cause decreases in the amount of hydroxyl radicals available for indirect reactions and decrease the ozone residual in the water. They hinder the effectiveness of ozone oxidation. As a result, higher ozone dosages are necessary to reduce the impacts of hydroxyl radical scavengers on disinfection efficiency (American Water Works Association Research Foundation et al., 1991; Papageorgiou et al., 2017).

As a strong oxidant, ozone is effective at oxidizing various organic compounds in water. However, its reactivity is highly selective, and in general, the compounds are not completely broken down into water and carbon dioxide. Ozonation mainly leads to the generation of products that possess physical and chemical characteristics that differ from the original organic compound. With regards to some of the more general pollutants, ozone can effectively reduce color as well as certain VOCs, including TCE, carbon tetrachloride, PCE, taste, and odor. It can also oxidize contaminants including pesticides, acetic acid, phenols, nitro-benzenic compounds, oxalic acids along with compounds of chloro-benzenic. However, it is not effective at reducing total organic carbon. Ozone can also react with inorganic compounds such as ions of sulfide, ferrous, manganous, nitrite along with ammonium, as well as, organic compounds such as aromatic aliphatic compounds, and humic acids (Ferguson et al., 1991, Stover et al., 1986).

3.6.2 How Ozonation Works

Ozone is mainly used for either disinfection, oxidation, or a combination of the two. It is relatively unstable and reacts with the water matrix directly through O_3 and indirectly through hydroxyl radicals. It is important to note that disinfection occurs through ozone mainly whereas oxidation occurs using oxidants, O_3, and hydroxyl radicals, which are also known as OH radicals. O_3 is a much more selective oxidant when compared to OH radicals, which are quick to react with the water matrix (Von Gunten, 2007).

The direct reactions are restricted to unsaturated compounds that are either aromatic or aliphatic along with certain functional groups. The molecular ozone during this process acts in one of three ways with the compounds in the water, either as an electrophilic agent, a nucleophilic agent, or as a dipole. An electrophilic reaction occurs on molecular sites that

have an electronic density that is strong. This characteristic is usually associated with aromatic compounds. When operating as a dipole, molecular ozone causes the addition of a 1-3 dipolar cyclo onto unsaturated bonds. This addition produces primary ozonides, which in water degrades into carbonyl compounds. Moreover, nucleophilic reactions occur only on sites that possess electronic deficits. It occurs commonly on carbons that contain electron-withdrawing components (Ferguson et al., 1991; American Water Works Association Research Foundation et al., 1991).

Indirect reactions are less selective than the direction reactions with molecular ozone. The hydroxyl radicals are stronger oxidants than the molecular ozone as well (Ferguson et al., 1991; American Water Works Association Research Foundation et al., 1991). This process is likely the only one with the ability to degrade saturated molecules that are aliphatic. The reaction rate of these radicals on numerous organic solutes present in wastewater is defined by Equation 3-2.

Equation 3-2

$$-\frac{d[M]}{dt} = k_{OH}[M][OH]$$

K_{OH} is a rate constant, and M is a compound concentration and OH is the hydroxyl radical concentration. The rate constant, K_{OH}, is within the range of 10^8 to 10^{10} $M^{-1}s^{-1}$ (American Water Works Association Research Foundation et al., 1991).

When a water matrix is exposed to ozone, there are three types of oxidation products that form. The first of these is non-halogenated organic compounds and these compounds form due to the oxidation of NOM. Examples of these compounds include carboxylic acids, ketones, and aldehydes. The other type of product is halogenates, which form when bromide and iodide completely oxidize. This type of product can cause bromate to form, and this

compound is potentially carcinogenic. The final type of compound is brominated organic compounds, which results from reactions between hypobromous acid and NOM (Von Gunten, 2007).

3.6.3 Bromate Formation

When bromide is present in the influent water, ozonation can lead to the formation of brominated disinfection by-products such as bromoform, bromate, cyanogen bromide, dibromoacetic acid as well as bromopicrin. The generation of bromate occurs because of the reactions between bromide with either hydroxyl radicals or with molecular ozone. The formation of bromate is an area of concern as it is considered a possible carcinogen. Regulations regarding its presence in water are set at 10 micrograms per liter by the United States Environmental Protection Agency along with the World Health Organization (Ferguson et al. ,1991; Lin et al., 2014). A depiction of bromate formed during ozonation can be seen in Figure 3-6 below.

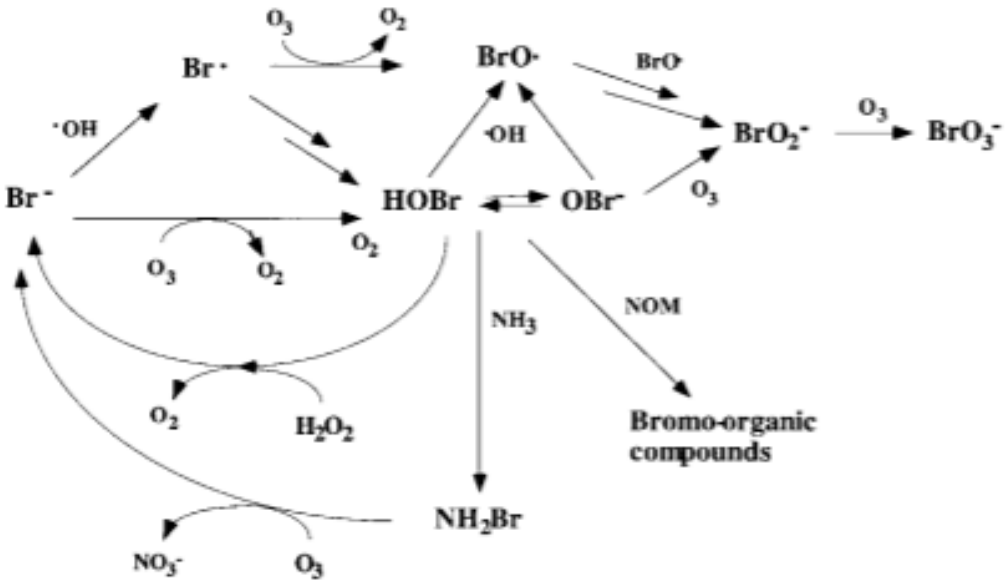

Figure 3-6 Bromate Formation Resulting from Ozonation of Water Containing Bromate (Von Gunten et al., 2000)

Bromate can potentially be reduced in a few ways based on the findings of Lin et al. and von Gunten et al. Decreasing the ozone contact time and lowering the pH can decrease the create of bromate. However, when ozone contact time decreases, the potential for brominated trihalomethanes increases. Furthermore, by lowering the pH, there was a rise in the potential production of total organic bromine and a potential decrease in the production of hydroxyl radicals from the decomposing of ozone. Adding ammonia to the feed water can also decrease bromate formation as ammonia reacts with hypobromous acid quickly and leads to the formation of bromamin. Ultimately, the impact of the bromide concentration in influent water is more significant than the impact of ozone generation on the formation of brominated disinfection by-products. (Lin et al., 2014; Von Gunten et al., 2000).

3.7 Effect of Ozonation Pretreatment on Ceramic Membrane Microfiltration

Ozonation can be a pretreatment option for ceramic membrane microfiltration as it can lead to a larger permeate flux and reduce membrane fouling. Ozone can improve membrane performance due to its ability to reduce NOM. It can react quickly with NOM, specifically with its unsaturated bonds, double bonds, and aromatic rings because it is a strong oxidant and highly reactive. Ozone can also degrade NOM into smaller molecules, increase carboxylic functions present in NOM, and convert unsaturated bonds present in the hydrophobic portion of NOM to hydrophilic byproducts like carboxylic acids. This results in rejection of the molecules by the membrane's negative exterior, products that are less inclined to adsorb onto the surface of the membrane, and reductions of cake or gel layer forming potential (Van Geluwe et al., 2011; Hamid et al., 2017).

OH radicals, which form through the decomposition of ozone, can also enhance membrane performance when the ceramic membrane is coated with titanium dioxide (TiO_2).

In a study conducted by Hu et al., they found that when OH radical interacted with the surface of the TiO_2 membrane, organic foulants on the surface of the membrane decomposed. Thus, this decomposition reduced membrane fouling. Hu et al. also found that with increasing ozone dosages, there were increasing OH radicals interacting with the surface of the membrane, which lead to the decomposition of high molecular weight foulants to low molecular weight foulants. These low molecular weight compounds can pass through the membrane (Hu et al., 2011). While ozonation pretreatment can mitigate membrane fouling; it can increase membrane fouling as it can escalate the number of larger molecules present in the water (Hamid et al., 2017). The potential increase in membrane fouling due to the use of ozone pretreatment directly corresponds to the ozone dosage. Tang et al. (as cited in Song et al., 2018) established that ozone dosages greater than 10 mg/L lead to an increase in membrane fouling when using ozone pretreatment (Song et al., 2018).

Song et al. found that low pre-ozonation dosages to some extent diminished membrane fouling and that dosages of 10 mg/L and above cause serious membrane fouling through the use of BSA raw water and a flat sheet Al_2O_3 ceramic membrane with an average pore size of 100 nm. High dosages also caused TMP to increase drastically to greater than 40 kpa compared to the control samples 1.8 kpa TMP. This result indicates that irreversible and reversible fouling for the high ozone dosage and just reversible fouling for the control affected the total fouling resistance. When observing low pre-ozonation dosages, Song et al. determined that at dosages of 1, 2, and 4 mg/L limited the TMP rise and achieved stable TMPs of 1.2, 0.9, and 1.1 kpa. When the ozone dosage increased past these values, the TMP increased as well (Song et al., 2018).

Low pre-ozonation dosages displayed a decline in resistance to reversible fouling, for instance, the decrease was 61.1 percent and 94.4 percent for 1 mg/L and 2 mg/L, respectively. At the pre-ozonation dosage of 10 mg/L, the resistance to reversible fouling was 8.3 times larger than the control's resistance. Concerning resistance to irreversible fouling, the experiments showed that pre-ozonation increased it. For dosages of 1, 2, 4, and 10 mg/L, the resistance to irreversible fouling raised to $2.25x10^{10}$, $3.59x10^{10}$, $4.49x10^{10}$, and $125.75x10^{10}$, accordingly. From the results, Song et al. deduced that, at low pre-ozonation dosages, membrane fouling decreased due to the reduction of reversible fouling. Furthermore, Song et al. concluded that, at high pre-ozonation dosages, the serious membrane fouling was the result of irreversible fouling, and the amount of reversible fouling present was high at this dosage as well (Song et al., 2018).

Hamid et al. discerned using raw secondary effluent from Melbourne Water's Western Treatment and a tubular ceramic membrane with a pore size of 100 nm that pre-ozonation enhanced membrane permeability, reduced irreversible and reversible fouling, and increased the quality of permeate. Furthermore, pre-ozonation effectively removed biopolymers and HS components as well as color and UVA_{254} by 100 percent, 84 percent, 97 percent, and 63 percent, respectively. The removal of biopolymers is connected to ozone's ability to transform them into smaller particulates. This removal did become lower after going through ceramic membrane microfiltration likely because of the combining of these degraded particulates into larger molecules. In conjunction, the reduction of HS components is a result of the high aromaticity of its components. However, Hamid et al. noted that the ceramic membrane filtration contributes less to the overall water quality as pre-ozonation transforms

particulates in the feed water, which allows the particulates to go through the membrane whereas the membrane originally would have caught them (Hamid et al., 2017).

Pre-ozonation also increased the membrane flux by 25 percent due to its ability to decompose NOM. Likewise, Hamid et al. observed a lower amount of fouling with the use of pre-ozonation. The permeability of the membrane barely reduced after seven cycles of filtration with it reducing from 1 to 0.5. The minor amount of fouling present when using pre-ozonation is apparent when looking at the total fouling index data ($UMFI_T$) reported by Hamid et al. The $UMFI_T$ for pre-ozonation slowly raised from 0.02 to 0.03 m^2L^{-1} after six cycles; whereas, the $UMFI_T$ for the raw water raised from $0.14m^2L^{-1}$ to $0.73m^2L^{-1}$ after six cycles. This result is due to the reduction in HS and biopolymers (Hamid et., 2017.) Thus, pre-ozonation had a significant effect on ceramic membrane microfiltration.

Chapter 4

4. Methods and Materials

4.1 Materials

4.1.1 PWNT Pilot in Wervershoof

The PWNT Pilot in Wervershoof is a secondary effluent reuse system that consists of ozonation, inline coagulation, and ceramic membrane microfiltration. The process trains for the various pretreatment alternatives can be seen in Figures 4-1, 4-2, and 4-3 below. Conductivity tests were run to determine the retention times of the feedwater through the static mixer, inline coagulation unit, and the ceramic membrane. Based upon the conductivity measurements conducted with a flow rate of 60 liters per hour (l/h), the time it takes for the feedwater to go through the static mixer, inline coagulation unit, and the ceramic membrane are 50 seconds, 4 minutes and 58 seconds, and 3 minutes and 28 seconds, respectively. Details of this procedure can be seen in Appendix II.

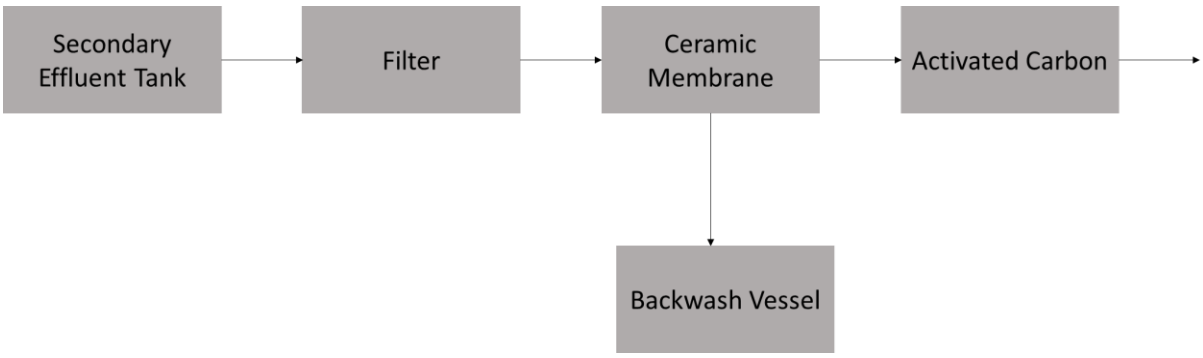

Figure 4-1 Process Train for No Pretreatment

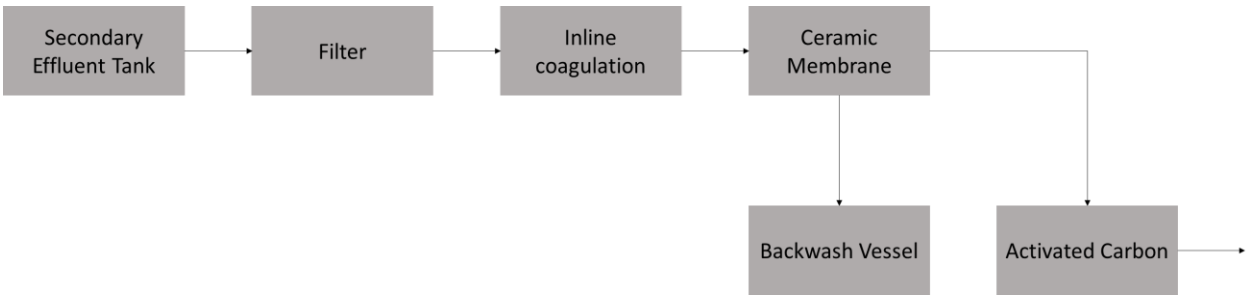

Figure 4-2 Process Train for Coagulation Pretreatment

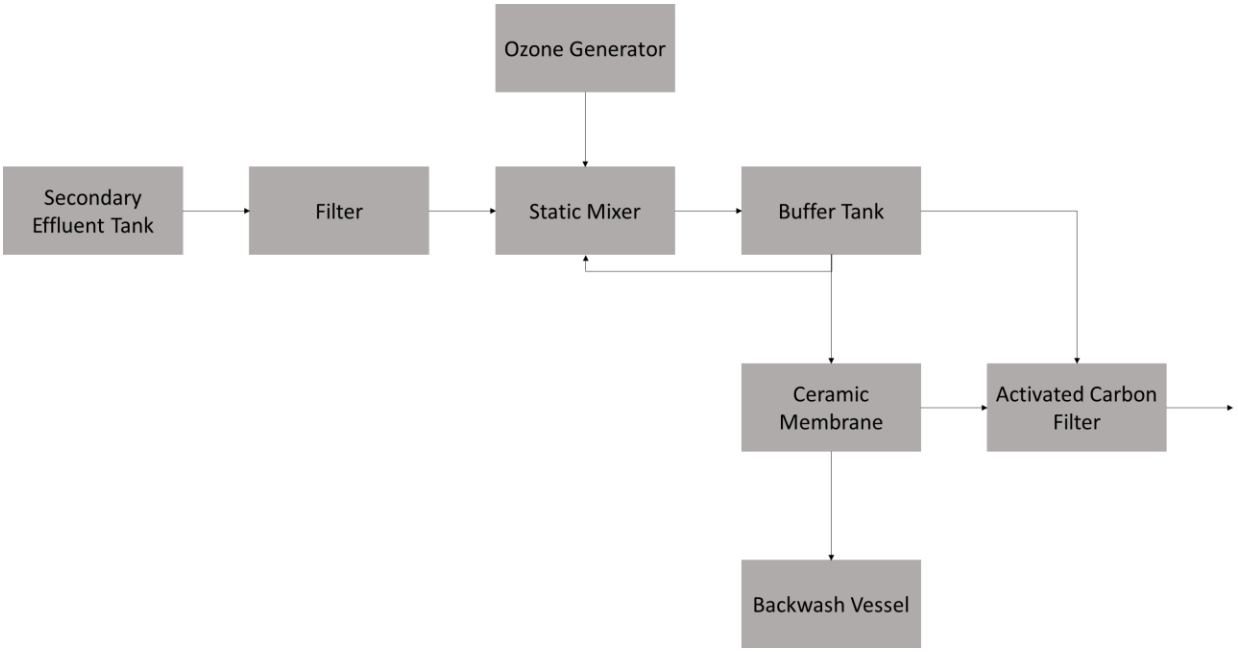

Figure 4-3 Process Train for Ozonation Pretreatment

As previously mentioned, the secondary effluent reuse pilot consists of ozonation, inline coagulation, and ceramic membrane microfiltration. The ozonation system consists of a WEDECO OCS Modular 4HC ozone generator. This generator uses oxygen produced from ambient air using the Air Sep by Topaz to generate ozone. It has an oxygen demand of 0.04 cubic meters per hour along with a power consumption of 0.1 kilowatts when the ozone production is at one hundred percent. Furthermore, it has a maximum ozone production of 4 grams per hour (WEDECO AG, 2006). The inline coagulation system is the RZR1 model created by Heidolph. This model can achieve speed ranges of 35 rotations per minute to 250

rotations per minute. (Heidolph Instruments GMBH & CO KG, 2011). The system put in place in the pilot consists of two contact chambers with each one containing a mixer. Thus, the system can have both rapid and slow mixing speeds. The ceramic membrane microfiltration system consists of one 0.4 m^2 Metawater module. It is a hollow membrane and the water flows through the membrane inside-out. The max transmembrane pressure that the ceramic membrane can handle at the pilot is 2 bar, and if this is surpassed the installation will shut down (Gabriel, 2019).

4.1.2 Water Quality Parameters

Samples were taken before each treatment train process to determine the initial water quality and potential water quality improvements. The water quality parameters analyzed were %UVT254, ammonia, bromate, bromide, chloride, nitrate, nitrite, pH, sulfate, total dissolved solids, and turbidity. A NOM characterization was also done to see what types of NOM were present in the water and have the potential to cause fouling. Total dissolved solids were an important parameter due to their potential to cause fouling as well. Bromate and bromide were a concern during ozonation pretreatment tests as bromide can be transformed into bromate when it is exposed to ozone. Ammonia, nitrate, nitrite, and sulfate were tested to determine if these treatment train processes were able to remove nutrients. Chloride was tested to determine if there was a potential for the formation of disinfection byproducts. Lastly, %UVT254, pH, and turbidity were analyzed as they are good indicators of the quality of the water.

4.1.3 Ozone Bench-Scale in Haarlem

The semi-batch ozone bench-scale setup is located at Het Waterlaboratorium in Haarlem. The apparatus consists of an oxygen gas cylinder, a WEDCO Ozone Generator, two BMT

964 ozone analyzers, a gas flow meter, the ABB FAM3255, a Hach Orbisphere 410A dissolved ozone meter, and a glass reactor. The system also has ozone destructors after each one of the BMT 964 ozone analyzers and a larger destructor following the reactor. (Delfos, 2019) The apparatus is viewable in Figure 4-3 Pilot at HWL in Haarlem below.

Figure 4-4 Ozone Bench-Scale at HWL in Haarlem

Ozone generation occurs using the WEDCO Ozone Generator and pure oxygen gas. The pressure, as well as the flow of ozone gas, is modifiable by using the reducer along with the regulator. The cylindrical glass reactor located in the center of the apparatus is the vessel that holds the water sample of interest. In this vessel, the recirculated water sample encounters gaseous ozone. The ozone enters the vessel directly underneath the diffuser plate located at the bottom of the vessel. The inflow and outflow ozone gas concentrations are monitored through the two BMT 964 ozone meters. The recording of the ozone concentration in the liquid phase occurs through the Hach Orbisphere 410A meter. Destructors located after each of the BMT 964 ozone analyzers and after the glass reactor transform the ozone back into oxygen. Thus, they neutralize the ozone gas (Delfos, 2019).

4.2 Methods

4.2.1 Jar Testing

Jar testing was conducted Jar on June 5th, 6th, 7th, and 12th 2020 to determine the mixing speeds for alternative 1- coagulation pretreatment. The following procedure was conducted to perform jar testing and was loosely based upon the procedure by Satterfield et al. (Satterfield, 2005).

1. A 1 percent, or 10,000 mg/L, ferric chloride solution was created from a 40 percent ferric chloride solution and MilliQ water.
2. The jar testing apparatus depicted in Figure 4-5 was used for the testing. Each one of the jar apparatus vessels was rinsed with secondary effluent and then filled to the 1.5-liter mark.

Figure 4-5 Jar Testing Apparatus

3. The appropriate amount of 1% ferric chloride solution was pipetted into each of the vessels for the corresponding dosage. The volume of solution for each of the coagulation dosages can be depicted in the Table 4-1 Required Volume of 1% Ferric Chloride Solution below.

Table 4-1 Required Volume of 1% Ferric Chloride Solution

Coagulant Dosage as $FeCl_3$ (mg/L)	Coagulant Dosage as Fe^{3+} (mg/L)	Required Volume of 1% $FeCl_3$ Solution (mL)
1	0.34	0.15
2	0.69	0.3
3	1.03	0.45
5	1.72	0.75
6	2.06	0.9
10	3.44	1.5
15	5.16	2.25
20	6.88	3
25	8.60	3.75
30	10.32	4.5
40	13.76	6
50	17.20	7.5
60	20.64	9

4. The mixing speeds for the specific trial can be seen in Table 4-2. The mixing speeds for trials 1 and 2 were taken from Lerch et al. and Arhin et al., respectively. The mixing speeds for trial 3 were based upon the mixing speeds used by PWNT in Andijk; however, instead of using 300 rpm, 250 rpm was used as this was the highest mixing speed that could be used at the pilot.

Table 4-2 Jar Testing Parameters for Each Trial

Trial	Parameter	Units	Coagulant Dosage (mg/L)												
			1	2	3	5	6	10	15	20	25	30	40	50	60
1	Coagulant Type	-	Ferric Chloride	Ferric Chloride	Ferric Chloride	Ferric Chloride	Ferric Chloride	Ferric Chloride	Ferric Chloride	Ferric Chloride	Ferric Chloride	Ferric Chloride	Ferric Chloride	Ferric Chloride	Ferric Chloride
	Mixing Speed Tank 1	rpm	230	230	230	230	230	230	230	230	230	230	230	230	230
	Mixing Speed Tank 2	rpm	58	58	58	58	58	58	58	58	58	58	58	58	58
2	Coagulant Type	-	Ferric Chloride	Ferric Chloride	Ferric Chloride	Ferric Chloride	Ferric Chloride	Ferric Chloride	Ferric Chloride	Ferric Chloride	Ferric Chloride	Ferric Chloride	Ferric Chloride	Ferric Chloride	Ferric Chloride
	Mixing Speed Tank 1	rpm	100	100	100	100	100	100	100	100	100	100	100	100	100
	Mixing Speed Tank 2	rpm	35	35	35	35	35	35	35	35	35	35	35	35	35
3	Coagulant Type	-	Ferric Chloride	Ferric Chloride	Ferric Chloride	Ferric Chloride	Ferric Chloride	Ferric Chloride	Ferric Chloride	Ferric Chloride	Ferric Chloride	Ferric Chloride	Ferric Chloride	Ferric Chloride	Ferric Chloride
	Mixing Speed Tank 1	rpm	250	250	250	250	250	250	250	250	250	250	250	250	250
	Mixing Speed Tank 2	rpm	40	40	40	40	40	40	40	40	40	40	40	40	40

5. Each trial then ran for a total time of four minutes and fifty-eight seconds.
6. The jars were then untouched until the particles settled. %UVT, pH, and temperature measurements were taken.
7. Zeta potential, %UVT, pH, and temperature measurements were also taken with secondary effluent samples with no coagulant in them for comparison purposes.

4.2.2 Ozone Uptake Measurements

The ozone uptake for the secondary effluent was measured to determine the ozone dosage for alternative 2. These experiments were run on June 17th, 2019 at the ozone bench-scale setup at HWL in Haarlem. The procedure for determining the ozone uptake was based upon Bram Delfos's procedure (Delfos, 2019).

1. Six liters of secondary effluent were poured into the glass reactor and ozone gas measurements were taken automatically for the ozone gas going into and out of the reactor. The time when the measurements started was the start time of the experiment.
2. The system was run until the outlet ozone concentration on the gas meter appeared to be stable. When the outlet gas meter stabilized, the time was recorded to signify the end of the experiment.
3. For each test completed, two graphs were created. These graphs included the inlet ozone and outlet ozone gas concentrations versus the time in minutes and the ozone uptake in terms of milligrams per liter versus the cumulative ozone in terms of liters.
4. To estimate the ozone dosage to use for alternative 2, the area under the ozone uptake graph was determined and then divided by the total cumulative ozone in liters. This calculation resulted in the ozone dosage with units of milligrams per liter.

4.2.3 Wervershoof Twenty-Four Hour Secondary Effluent Sample

Twenty-four-hour secondary effluent samples were taken for dry weather samples. PWNT operator Rob van Western collected these samples. 60 liters of secondary effluent was collected at a time. These samples were meant to be used for jar testing as well as ozone demand tests, however, they ended up not being used due to the timing of the experiments.

4.2.4 Twenty-Four-Hour Constant Flux Tests

Twenty-four-hour constant flux tests were conducted to determine the critical and sustainable fluxes for each of the alternatives tested. For this research, the critical flux was defined as the flux at which membrane fouling is first seen and the TMP gets near or hits the pilot system pressure limit of 200 kpa. The sustainable flux is defined as the flux below the critical flux. The following steps were taken to conduct the twenty-four-hour constant flux tests.

1. The system was cleaned before the start of the run using tap water and the cleaning method described in Appendix I.
2. A table with the flows for the twenty-four-hour runs can be seen below.

Table 4-3 Flux Settings for Twenty-Four-Hour Constant Flux Tests

Alternative	Flux (Lmh)	Flow (l/h)	Water Temperature (˚C)	Start Date (mm/dd/yy)
0 - No Pretreatment	120	48	17	05/13/19
	145	58	18	05/15/20
1 - Coagulation Pretreatment (6 mg/L)	145	58	16	10/08/19
	170	68	18	10/11/19
	195	78	17	10/14/19
	220	88	18	10/15/19
	245	98	16	10/16/19
1 – Coagulation	145	58	15	10/30/19
	170	68	15	11/04/19
	195	78	16	10/22/19

Pretreatment (20 mg/L)	220	88	16	10/23/19
	245	98	17	10/24/19
2 – Ozonation Pretreatment	120	48	26	06/25/19
	145	58	25	06/26/19
	170	68	25	07/05/19
	195	78	23	07/16/19
	220	88	23	07/17/19
	245	98	25	07/18/19
	270	108	26	07/24/19

3. The filtration time for all the twenty-four-hour tests was set to twenty-five minutes. The backwashing regime for the twenty-four-hour runs was set as a 4-1-1 which signifies 4 normal backwashes followed by a CEB1, and then four more normal backwashes followed by a CEB2. CEB 1 is a 100 ppm hypochlorite solution and CEB 2 is a 100-ppm hydrogen peroxide solution at a pH of 2 using HCl.
4. The startup, shut down, and data analysis for the twenty-four-hour runs followed the same steps outlined in Appendix I. The data was stored and organized in Excel, which can be seen in Appendix V.

Chapter 5

5. Results

5.1 Introduction

This chapter illustrates the results dealing with bench-scale experiments, critical flux tests, and water quality sampling.

5.2 Bench-Scale Experiments

5.2.1 Jar Testing

The purpose of the jar testing was to determine the impact of mixing speed and ferric chloride dosages on the wastewater pH and UVT_{254}. The mixing and settling times are derived from conditions of the pilot system. The trial settings can be viewed in Table 4-2 in the materials and methods section. The pH and $\%UVT_{254}$ results can be seen in Figure 5-1. There was no pH correction for the coagulant dosages tested as the secondary effluent reuse pilot in Wervershoof lacks the ability to control pH.

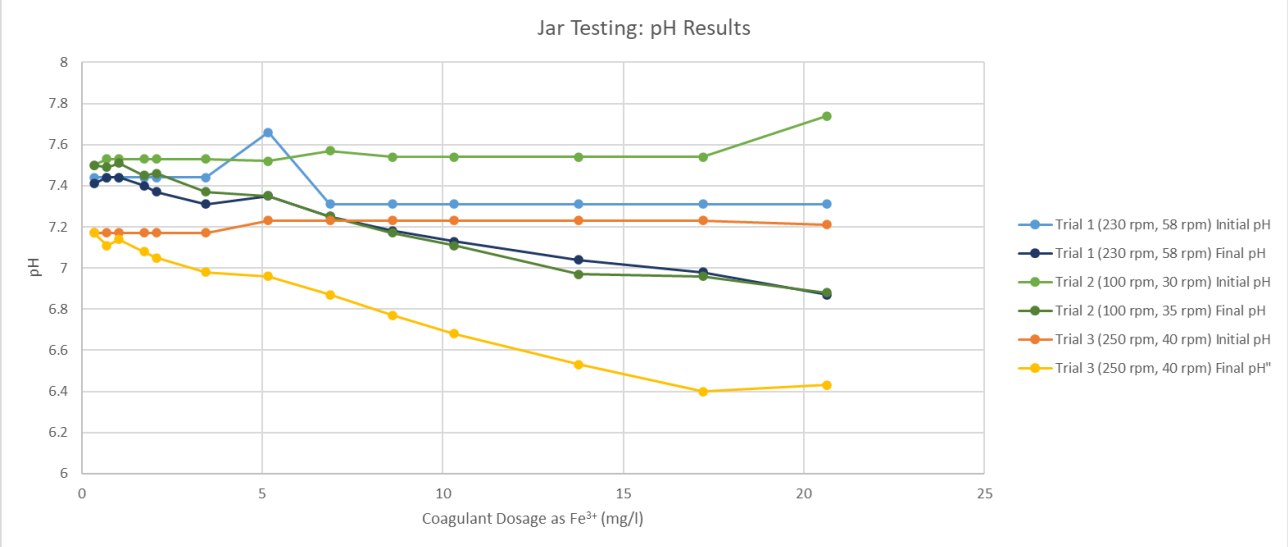

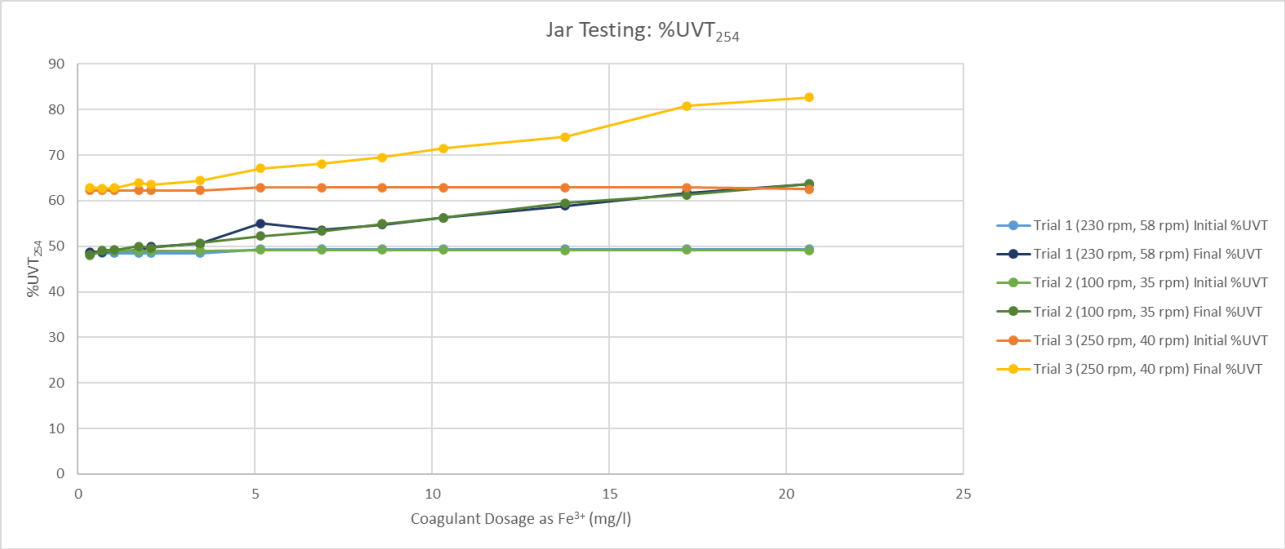

Figure 5-1 Jar Testing Results

Coagulation serves two purposes. The primary purpose is to improve performance of the membrane system and the secondary purpose is that inline coagulation may provide organic matter removal, measured by $\%UVT_{254}$ as the cause of improved membrane performance. The performance of the membrane system cannot be predicted using jar testing. To evaluate performance, coagulant needs to be dosed before the membrane system. Based on Figure 5-1, pH and UVT_{254} were hardly impacted by mixing speed, but as expected were impacted by the coagulant dose. With ferric dosage increases, the pH decreased and the $\%UVT_{254}$ increased.

Jar testing was originally scheduled to determine the optimal coagulant dosage of ferric chloride as Fe^{3+}. However, due to time limitations, these jar tests were not run. Coagulant dosages of 6 mg/L as Fe^{3+} and 20 mg/L as Fe^{3+} were used in critical flux tests for alternative 1 – coagulation pretreatment. These coagulant dosages were chosen to see the impacts of a low and high coagulant dosage on ceramic membrane performance. 6 mg/L as Fe^{3+} was the common dosage for inline coagulation used by PWNT for ceramic membrane filtration pretreatment and was used in this pilot setting. 20 mg/L as Fe^{3+} was chosen based on the dose applied for coagulation at PWN's water treatment plant in Andijk.

5.2.2 Ozone Uptake Curves

Ozone uptake bench-scale experiments were run to determine the ozone dosage for alternative 2. Two tests were conducted one for dry weather, which can be seen in Figure 5-2, and one for wet weather, which can be seen in Figure 5-3. These figures display the graphs for the inlet and outlet gas concentrations over time and the ozone uptake versus the cumulative gas volume in liters.

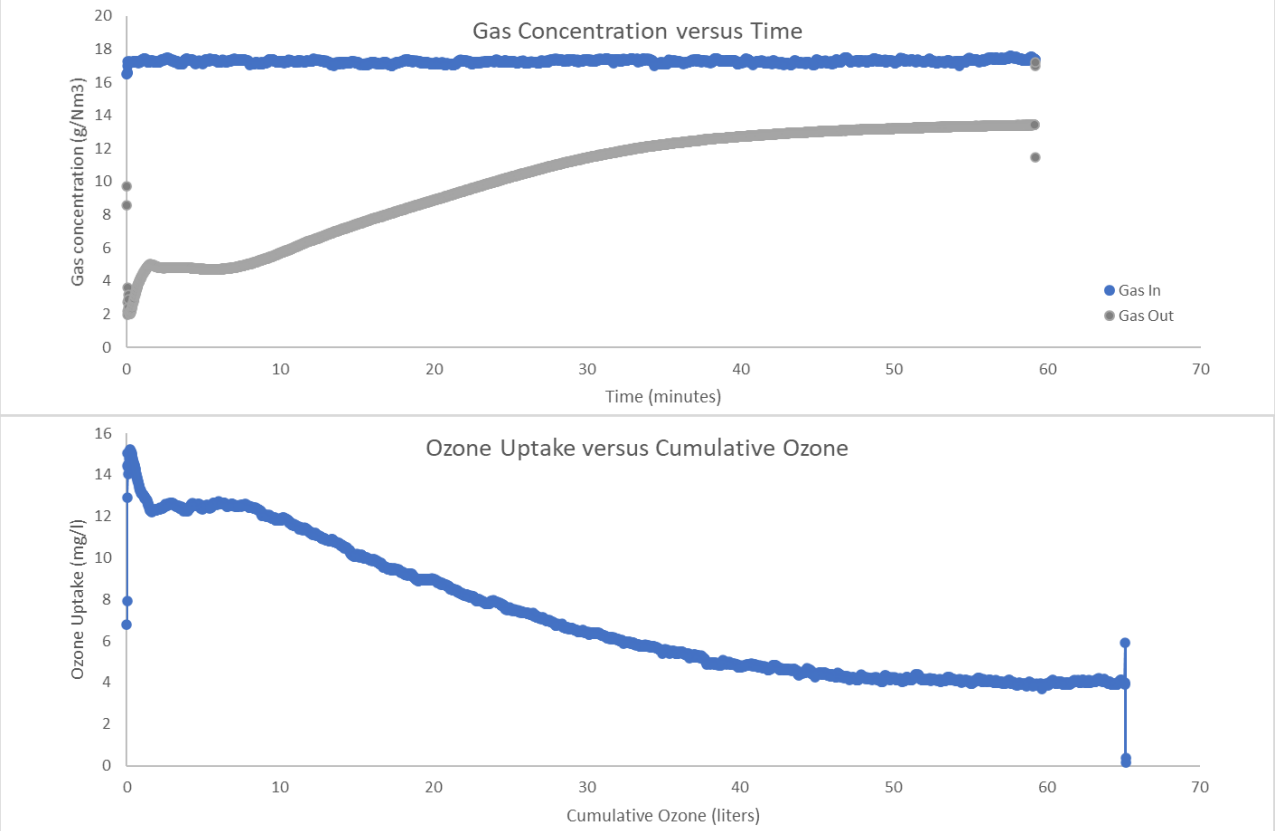

Figure 5-2 Ozone Uptake Results for Dry Weather Conditions

For the dry weather test, the experimental run lasted for a total time of 59 minutes as this was when the increase in outlet gas concentration became insignificant. The inlet ozone concentration in the gas phase remained stable throughout the experiment with an average ozone concentration of 17.3 g/m^3 and a standard deviation of 0.1 g/m^3. The outlet ozone concentration increased with time reaching a concentration of about 13.4 g/m^3 after 59 minutes. The ozone uptake was calculated by subtracting the outlet ozone concentration from

the inlet ozone gas concentration. The maximum uptake observed was 15.2 mg/L and the minimum uptake of 0.1 mg/L. By interpolating the area under the graph and dividing by the total gas volume, the ozone demand for the system was estimated to be 7 mg/L. To allow for a small residual ozone dosage, the ozone dosage for dry weather conditions for alternative 2 was set at 8 mg/L.

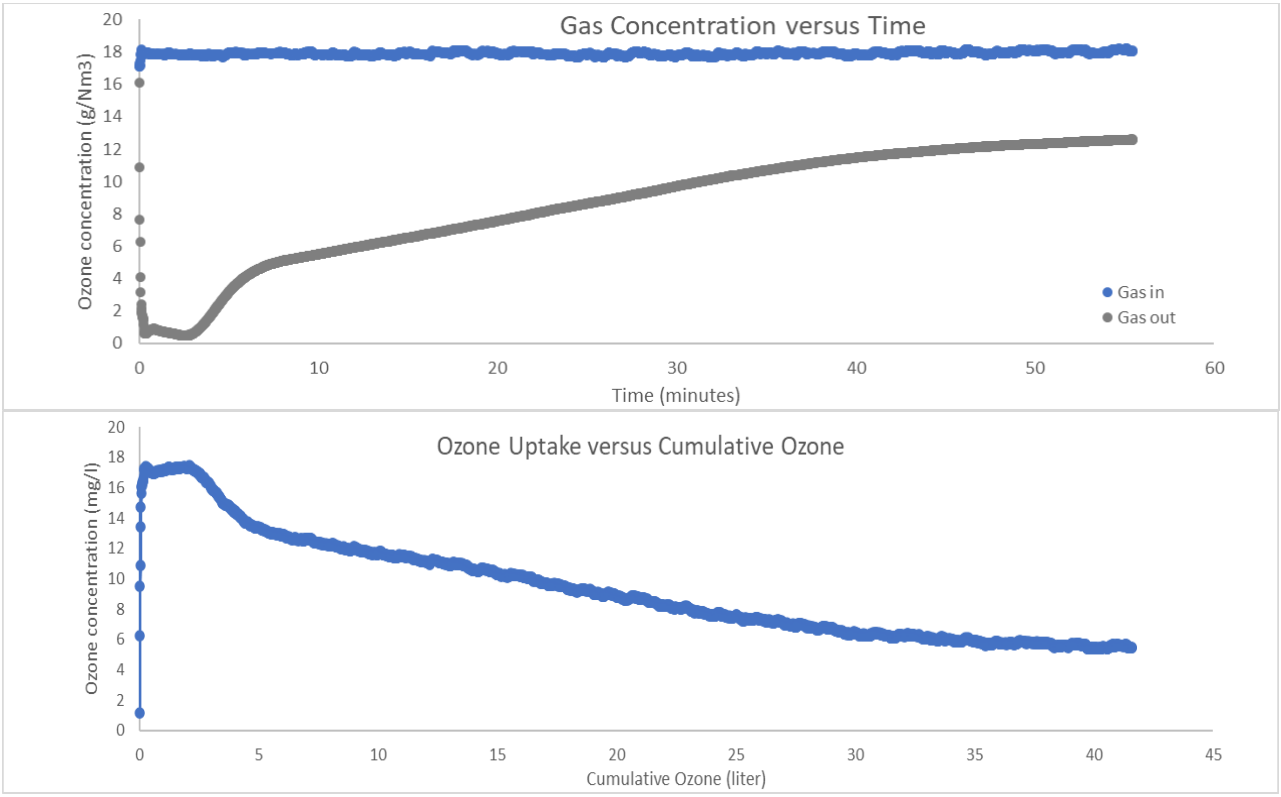

Figure 5-3 Ozone Uptake Results for Wet Weather Conditions

For the wet weather test, the experimental run lasted for a total time of 55 minutes, which is when the outlet gas concentration almost stabilized. The inlet gas concentration remained stable throughout the run with an average of 17.9 g/m3 with a standard deviation of 0.1 g/m3. The outlet gas concentration increased with time and stabilized at approximately 12.6 g/m3. The ozone uptake was calculated in the same manner as discussed before with the units of milligrams per liter. The maximum ozone uptake was 17.4 mg/L and the minimum ozone uptake was 5.4 mg/L. The ozone demand was estimated to be 7 mg/L.

A bench-scale ozone uptake test was run in May 2020 with DI water to see if there was any growth on the reactor that could cause the gap between the inlet and outlet gas concentrations. DI water was used as it does not contain any ozone or hydroxyl radical scavengers. The results of this test can be seen in Figure 5-4.

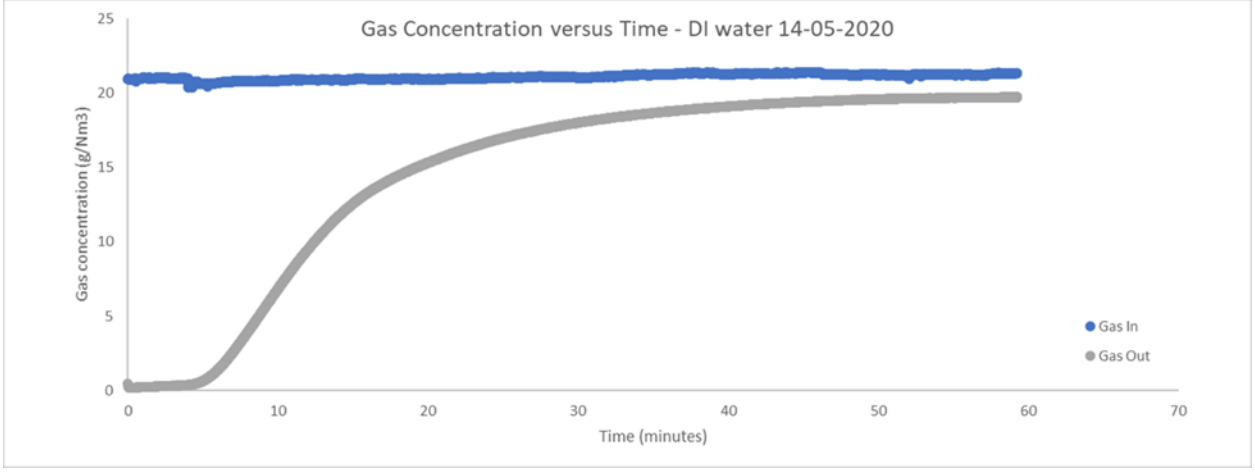

Figure 5-4 Ozone Uptake Results of DI water

The result from this uptake test illustrates that there was some growth on the biofilm as there is a gap between the inlet and outlet gas concentration. Further testing is needed to determine the mechanisms causing the gap between the inlet and outlet gas concentrations.

5.2.3 Summary of Bench-Scale Experiments

The bench-scale experiments involved jar testing and ozone uptake tests. These bench-scale experiments were used to determine the settings for the critical flux tests for alternatives 1 – coagulation pretreatment and alternative 2 – ozonation pretreatment. Jar tests were conducted to determine the mixing speeds and how ferric chloride impacted the organic matter content of the feedwater. The mixing speeds of 250 rpm and 40 rpm were chosen for pilot testing. Two coagulant dosages were run, which were 6 and 20 mg/L as Fe^{3+}, to determine the impact of low and high ozone dosages on ceramic membrane microfiltration. Ozone uptake tests were conducted to determine the ozone dosage for alternative 2 -

ozonation pretreatment. Based on these uptake tests, an ozone dosage of 8 mg/L was chosen for critical flux testing.

5.3 Critical Flux Tests

Twenty-four-hour constant flux tests were used to determine the critical and sustainable fluxes for each of the alternatives. These constant flux tests started at 120 Lmh and increased in increments of 25 Lmh until the critical flux was reached. The critical flux was defined to be the flux at which membrane fouling first occurred, which is signified by an increase in TMP. The critical flux for the purposes of this experiments was a flux at which the TMP hit 2 bar or 200 kpa within twenty-four hours, which was the pressure limit of the pilot. The sustainable flux was the flux one increment of 25 Lmh under the critical flux where the TMP remained relatively constant during the twenty-four-hour run. The TMP was normalized to a temperature of 10˚C to have comparable results. A cleaning regime of 4-1-1 was used during critical flux testing. A 4-1-1 signifies the following cleaning regime: four normal backwashes followed by a CEB 1 and then four more normal backwashes followed by a CEB 2. The CEB 1 is a 100 ppm NaOCl solution, and a CEB 2 is a 100 ppm H_2O_2/HCL solution at a pH of 2. A filtration time of twenty-five minutes occurred between each backwash and CEB. Further details regarding the twenty-four-hour constant flux test are described in section 4.6.

5.3.1 Alternative 0 – No Pretreatment

Twenty-four-hour tests were run for a flux of 120 and 145 Lmh for dry weather conditions. The TMP was analyzed to determine the critical and sustainable fluxes of the system. The TMP results for the twenty-four-hour tests are shown in Figure 5-5.

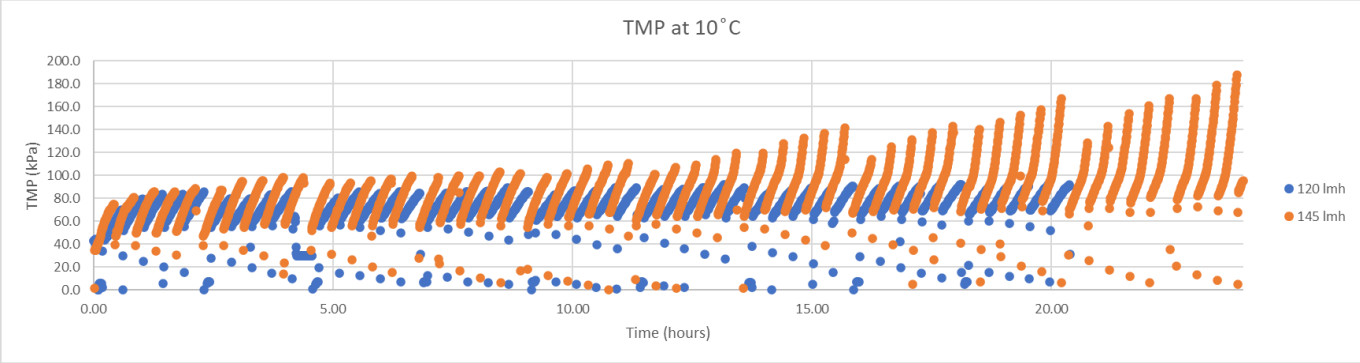

Figure 5-5 TMP Results for Alternative 0

Based upon these results, it was determined that the critical flux was 145 Lmh as there was a clear increase in TMP and the sustainable flux was 120 Lmh as it was the flux directly below the critical flux and where the TMP remained relatively constant. It is important to note that when these tests were run the NaOCl concentration for the CEB 1 was a magnitude lower than the 100 ppm concentration it was supposed to be at. The increases in the initial TMP for the fluxes of 145 and 120 Lmh can be viewed in Figure 5-6 below.

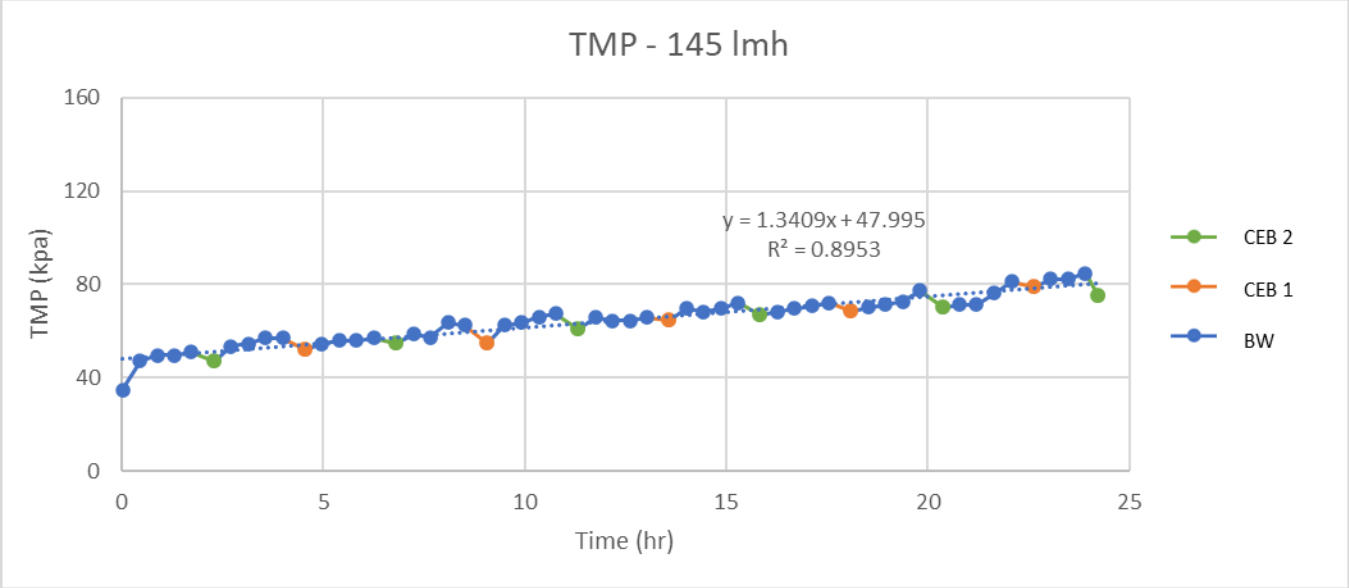

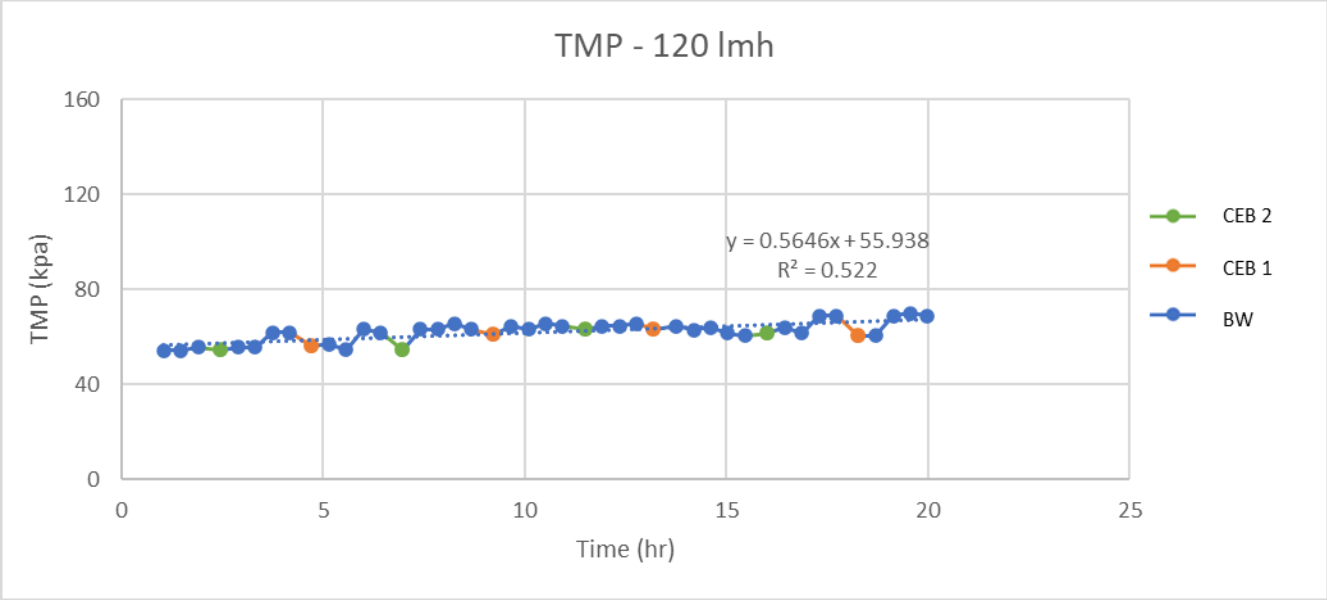

Figure 5-6 Starting TMP for Alternative 0 – No Pretreatment

Based on the initial TMP graph for a flux of 145 Lmh, the normal filtration cycles following the firstly applied NaOCl chemically enhanced backwash (CEB1), after 2.5 hours of operation, show an increased TMP after the five filtration cycles. The H_2O_2 with HCL at a pH of 2 chemically enhanced backwash (CEB2) reduced the TMP slightly, but not completely. In the cycles with regular backwashes, the TMP could not be maintained. Applying both types of CEB's and the normal backwashes, the TMP showed an increase over the duration of the twenty-four-hour test. This result is a clear indication that with no pretreatment at a flux of 145 Lmh, the CEBs, and the normal backwashes are no longer capable of mitigating fouling after twenty-four hours. Therefore, this is flux is beyond the sustainable flux and is an unsustainable situation.

The initial TMP graph for 120 Lmh provides limited information on the effect of the CEBs. The initial TMP after the CEBs and normal backwashes slightly increases over the twenty-four-hour period. In this twenty-four-hour run, the increase may seem negligible, however, extrapolating this slope till the maximum TMP of kpa indicates that it would take

approximately ten days for the initial TMP, ultimately requiring off-line clean in place to recover the system.

5.3.2 *Alternative 1 – Coagulation Pretreatment*

Twenty-four-hour constant flux tests were run for ferric chloride dosages of 6 mg/L as Fe^{3+} and 20 mg/L as Fe^{3+} to determine the optimal coagulant dosage for ceramic membrane filtration performance. The mixing speeds of the two mixing tanks involved in this pretreatment alternative were 250 rpm and 40 rpm to represent rapid and slow mixing, respectively. The individual results of the twenty-four constant flux tests with ferric chloride dosages of 6 and 20 mg/L as Fe^{3+}can be seen in Appendix V.

The TMP results of the twenty-four-hour critical flux tests for alternative 1 with an anticipated ferric chloride dosage of 6 mg/L as Fe^{3+} can be seen in Figure 5-7. The actual ferric chloride dosage for these tests ranged from 7.4 to 9.8 mg/L as Fe^{3+}. This variation in dosage is a result of the limited control possibilities at the pilot. The chemical enhanced backwash regime was followed as programmed: starting with a 100 ppm NaOCl solution followed by a 100 ppm H_2O_2 solution with HCl at a pH of 2 (pH 2). To determine the critical flux, the TMP was analyzed.

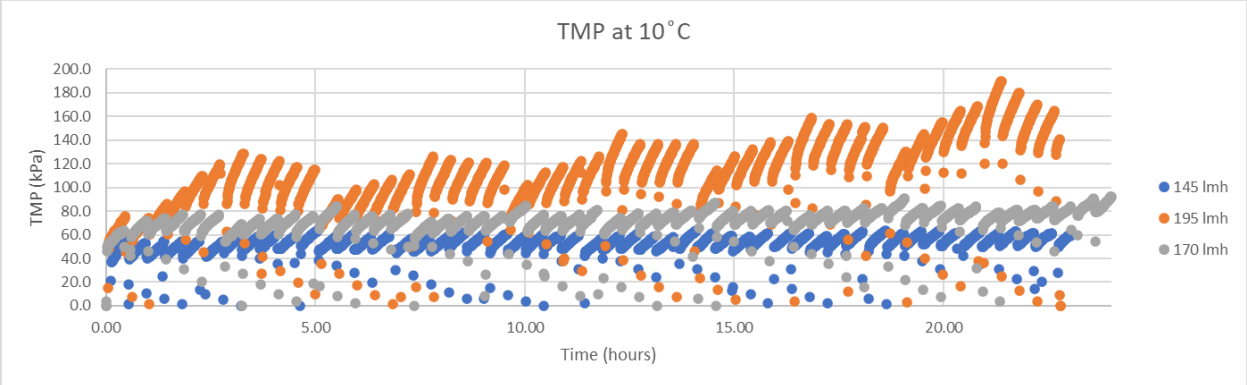

Figure 5-7 TMP Results for Alternative 1 with a Ferric Chloride Dosage of 6 mg/L as Fe^{3+}

Based upon these results and the definition of critical and sustainable flux as described in the materials and methods chapter, it was determined that the critical flux was 195 Lmh as there was a clear increase in TMP and the sustainable flux was 170 Lmh as it was the flux directly below the critical flux where TMP remained constant. The impact of the cleaning regimes on the initial TMPs for the flux levels tested can be seen in Figure 5-8.

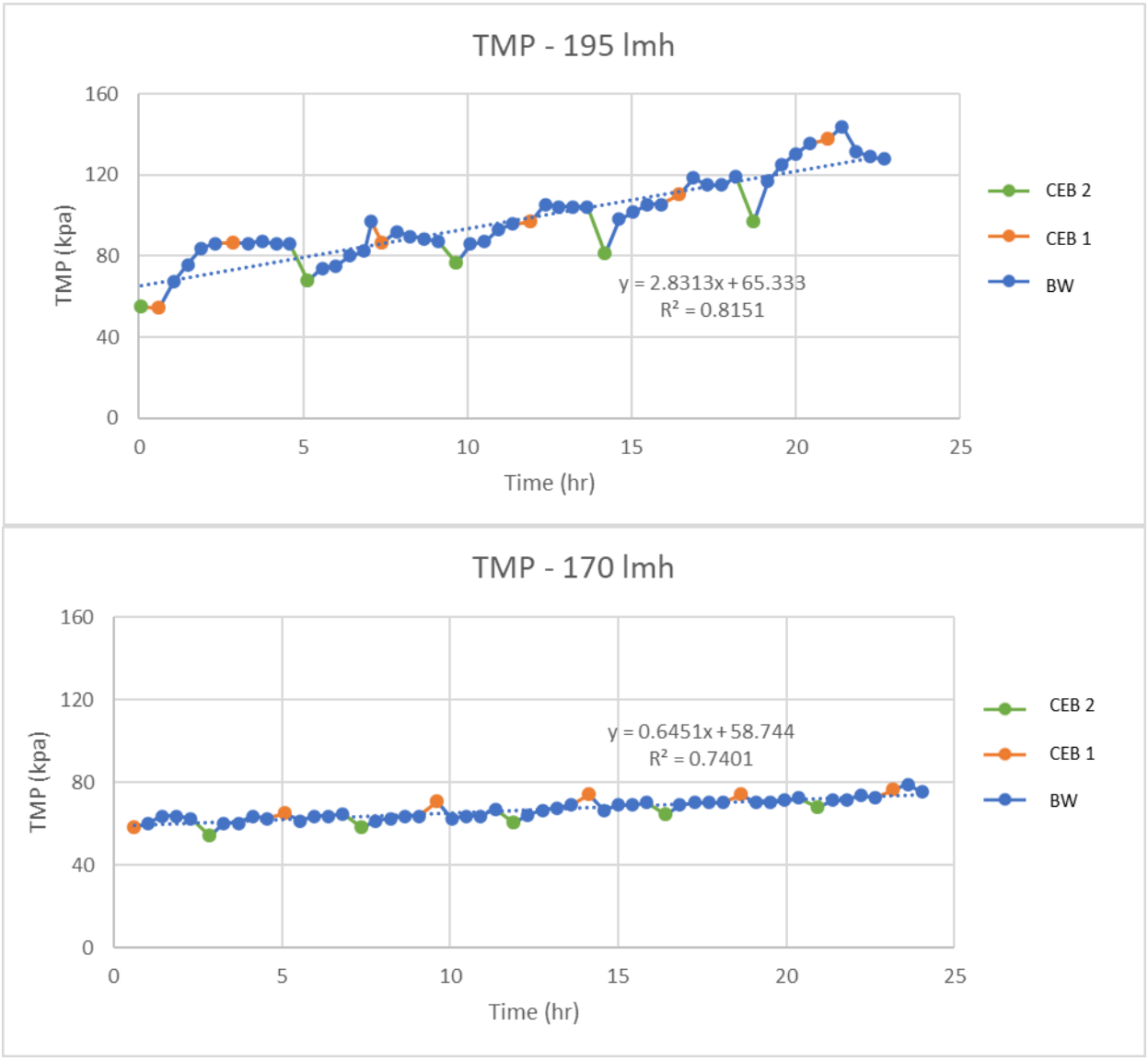

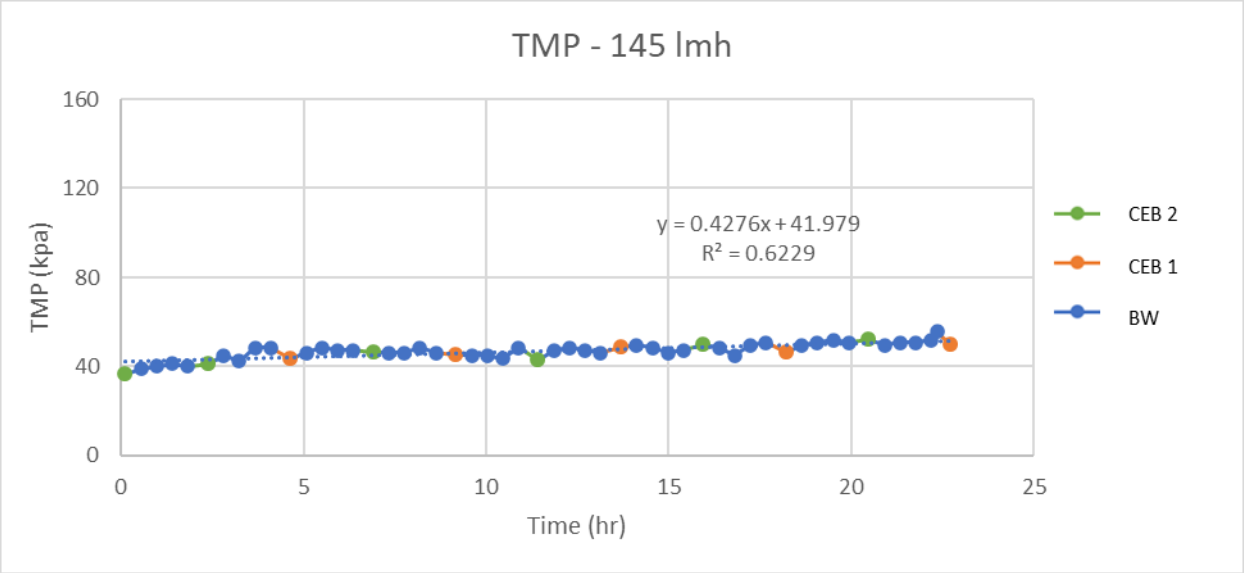

Figure 5-8 Initial TMP for Alternative 1 – Coagulation Pretreatment with a Dosage of 6 mg/L

Based on the initial TMP graph for a flux of 195 Lmh, the normal filtration cycles following the first applied NaOCl chemically enhanced backwash (CEB1), after 2.5 hours of operation, showed a stable, but high TMP after the five filtration cycles. The H_2O_2/HCL chemically enhanced backwash (CEB2) at pH 2 lowered the TMP. The development of the initial TMP after both types of CEB's and the normal backwashes shows an increase over the duration of the twenty-four-hour test. This result is a clear indication that after coagulation pretreatment with 6 mg/L Fe^{3+}, the CEBs, and the normal backwashes are no longer capable of mitigating fouling. Therefore, this is flux is beyond the sustainable flux.

The initial TMP graph for 170 Lmh provides limited information on the effect of the CEBs. CEB 1 has no impact in improving the initial TMP, while CEB 2 decreases the TMP. The initial TMP after the CEBs and normal backwashes slightly increases over the twenty-four-hour period. In this twenty-four-hour run, it may seem negligible, however, extrapolating this slope till the maximum TMP is reached indicates that it would take seven

days for the initial TMP to reach 200 kpa, ultimately requiring off-line clean in place to recover the system.

The lowest presented flux, 145 Lmh, shows a very limited TMP build up over a filtration cycle. The effect of CEB cannot be derived from the graph. Although this flux seems to be a very robust process condition, calculation of the development of the initial TMP after backwash shows a slight increase over the twenty-four-hour period. This suggests that even at this apparent robust condition, a cleaning in place can be expected when conducting long term runs.

The critical flux tests for alternative 1 with a ferric chloride dosage of 20 mg/L as Fe^{3+} consisted of the same 4-1-1 cleaning regime and a twenty-five-minute filtration time as applied for the 6 mg/L as Fe^{3+} condition. The actual ferric dosage ranged from 18.9 to 22 mg/L as Fe^{3+}. This variation in dosage is limited to the control possibilities at the pilot. The TMP results for these runs can be seen in Figure 5-9.

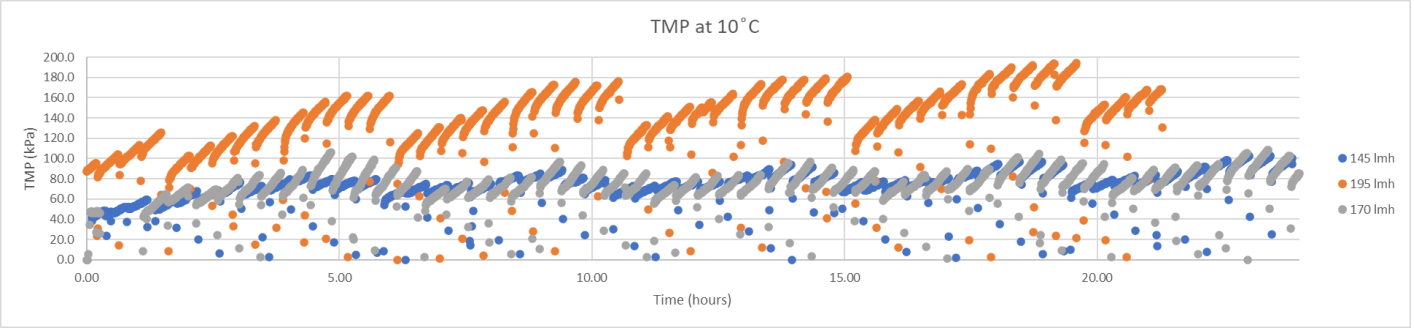

Figure 5-9 TMP Results for Alternative 1 with a Ferric Chloride Dosage of 20 mg/L as Fe^{3+}

Based on these results, it was determined that the critical flux was 195lmh and the sustainable flux was 170 Lmh. It was determined that a ferric dosage of 6 mg/L as Fe^{3+} was more optimal than a dosage of 20 mg/L as Fe^{3+}, because of a flux of 195 Lmh. The TMP

increase for the 6 mg/L dosage did not reach 200 kpa whereas the TMP associated with the 20 mg/L dosage did hit 200 kpa.

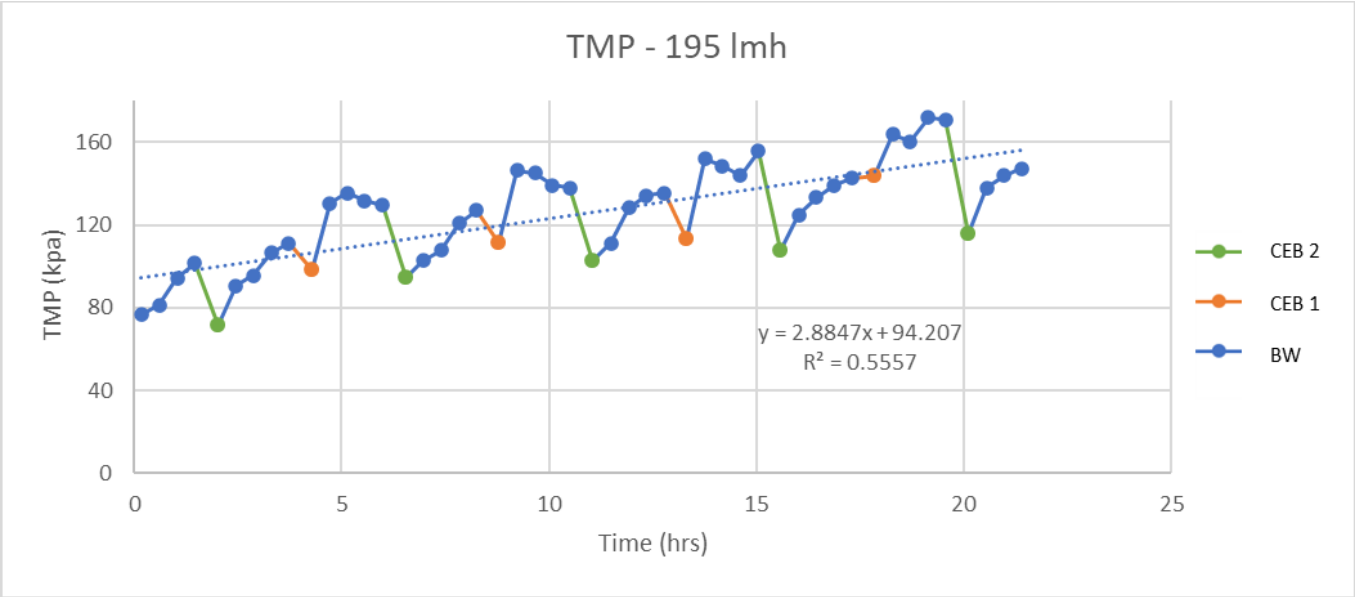

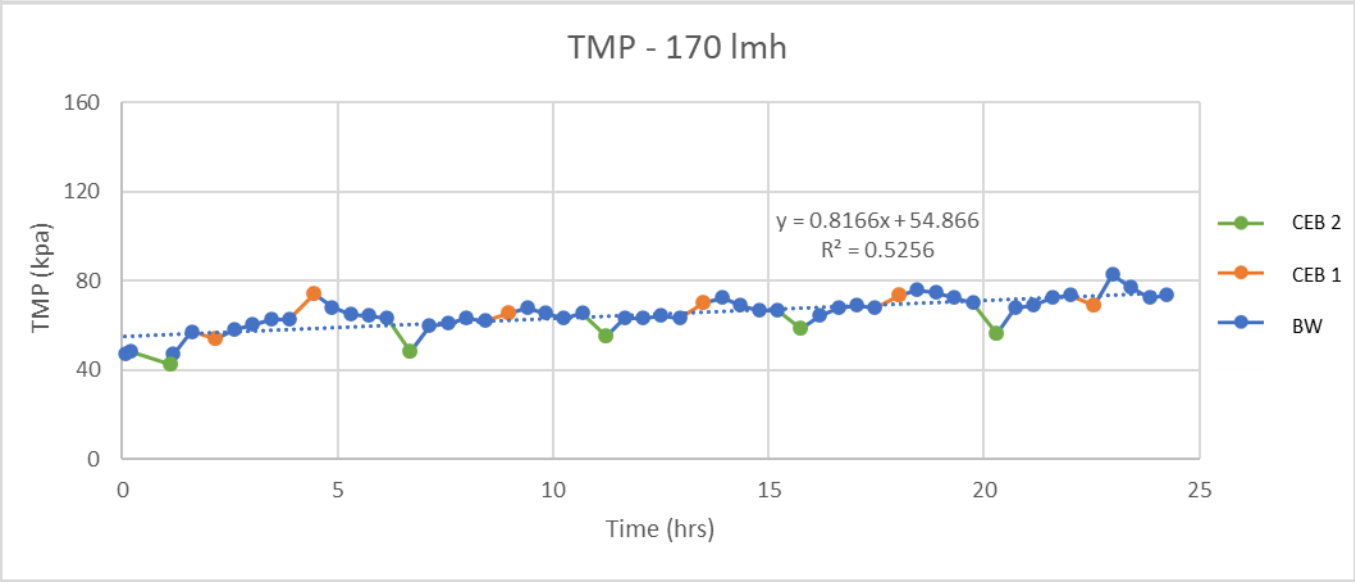

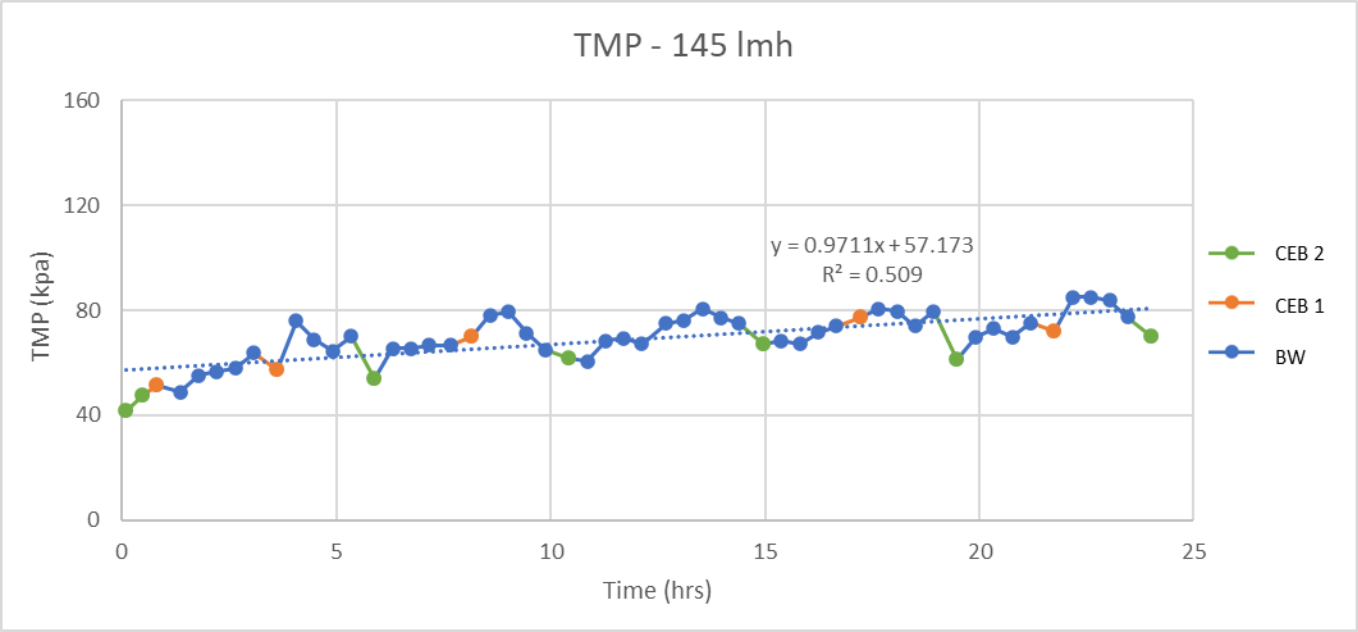

Figure 5-10 Initial TMP for Alternative 1 – Coagulation Pretreatment with a Dosage of 20 mg/L

Based on the initial TMP graph for a flux of 195 Lmh, the normal filtration cycles following the initial CEB 2 show an increase in TMP. The CEB 2s recovered the low initial TMP, however, in the normal filtration cycles, the TMP could not be maintained. The CEB 1 once lowered the TMP slightly, but in most cases only stabilized the TMP curve. The development of the initial TMP after both the two types of CEB's and the normal backwashes shows an increase over the duration of the twenty-four-hour test. This result is a clear indication that for coagulation pretreatment with 20 mg/L Fe^{3+}, the CEBs, and the normal backwashes are no longer capable of mitigating fouling. Therefore, this flux is beyond the sustainable flux and is the critical flux.

The initial TMP graph for 170 Lmh provides limited information on the effect of the CEBs. CEB 1 has no impact in improving the initial TMP while CEB 2 decreases the TMP. The development of the initial TMP after the CEBs and normal backwashes slightly increased over the twenty-four-hour period. In this twenty-four-hour run, it may seem negligible, however, extrapolating this slope till the maximum TMP is reached indicates that

it would take five days for the initial TMP to reach 200 kpa, ultimately requiring off-line clean in place to recover the system.

The lowest presented flux, 145 Lmh, shows a TMP build up over a filtration cycle like the one seen for 170 Lmh. The CEB 1 appeared to stabilize the TMP and CEB2 reduced the initial TMP. The development of the initial TMP after the CEBs and normal backwashes increased over the twenty-four-hour period. In this twenty-four-hour run, it may seem negligible, however, extrapolating this slope till the maximum TMP is reached indicates that it would take approximately four days for the initial TMP to reach 200 kpa, ultimately requiring off-line clean in place to recover the system.

Based on the twenty-four-hour tests conducted on 6 mg/L and 20 mg/L as Fe^{3+}, it can be concluded that a lower Fe^{3+} dosage seems to be more tailored in this experiment setting for a stable and balanced operation in terms of the cleaning regime. The effect of the CEB 1 is weakened in the 20 mg/L as Fe^{3+} situation and at the lower fluxes. The development of the initial TMP is not as stable as with the lower dosage. Furthermore, the increase of the TMP in one filtration cycle is higher when dosing a higher Fe^{3+} dosage than with a lower Fe^{3+} dosage. The TMP build up at the low dosage starts at a lower pressure and builds up over a larger TMP range contrary to the behavior in the higher Fe dosage setting where the initial TMP is high, but the build-up during filtration cycle is lower. From this research, application of a moderate coagulant dose, 7-10 mg/L as Fe3+ at a flux of 145 Lmh or 170 Lmh results in a process condition that is promising for further exploration in longer term tests.

5.3.3 Alternative 2 – Ozonation Pretreatment

Twenty-four-hour critical flux tests for ozonation pretreatment consisted of a 4-1-1 cleaning regime and a twenty-five-minute filtration time. The individual results for each of

the critical flux tests run for this alternative can be seen in Appendix V. To determine the critical flux, which is the flux at which membrane fouling starts to occur, the TMP was analyzed as membrane fouling leads to increases in TMP. The resulting TMP for each of the critical flux tests over time can be seen in Figure 5-11.

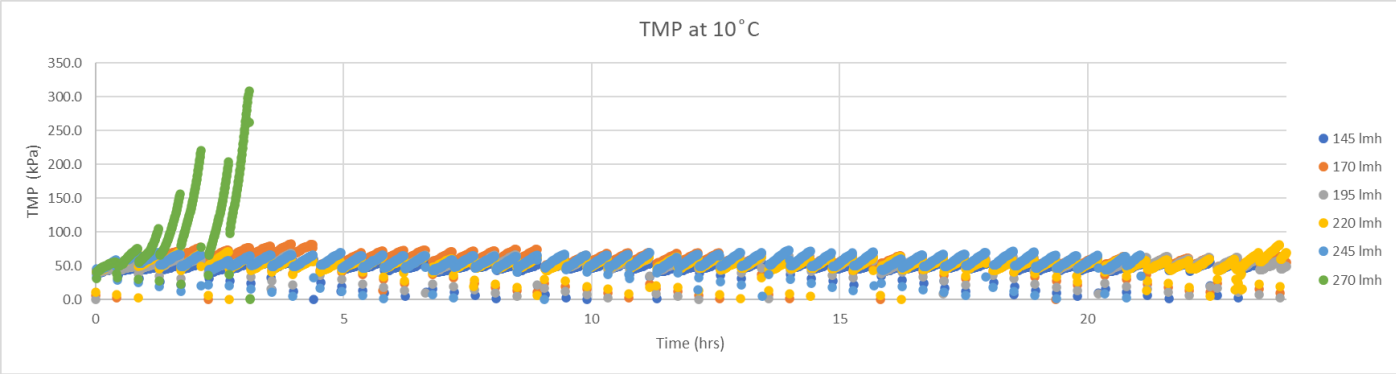

Figure 5-11 TMP Results for Alternative 2

Based on the results seen in Figure 5-11, it was determined that the critical flux was 270 Lmh as there was a very strong increase in TMP up to values much higher than 200 kpa. The sustainable flux was 245 Lmh as it was the flux directly below the critical flux where the TMP remained constant.

The baseline TMP was graphed for fluxes of 220 and 245 Lmh to see if the fluxes below 270 Lmh were behaving similarly as depicted in Figure 5-11. The results of these baseline TMP graphs can be seen in Figure 5-12. Based on this Figure, it was determined that the fluxes below 270 in particular 220 and 245 Lmh do behave similarly. Furthermore, 245 Lmh is sustainable based on the graph, but further testing would be needed to confirm this performance capability of pre-ozonation on ceramic membrane microfiltration. It is important to note that both 245 and 270 Lmh appears to be cleaning the membrane with time, which is atypical to the expected outcome. Further testing is necessary to understand the impact of ozone on the membrane.

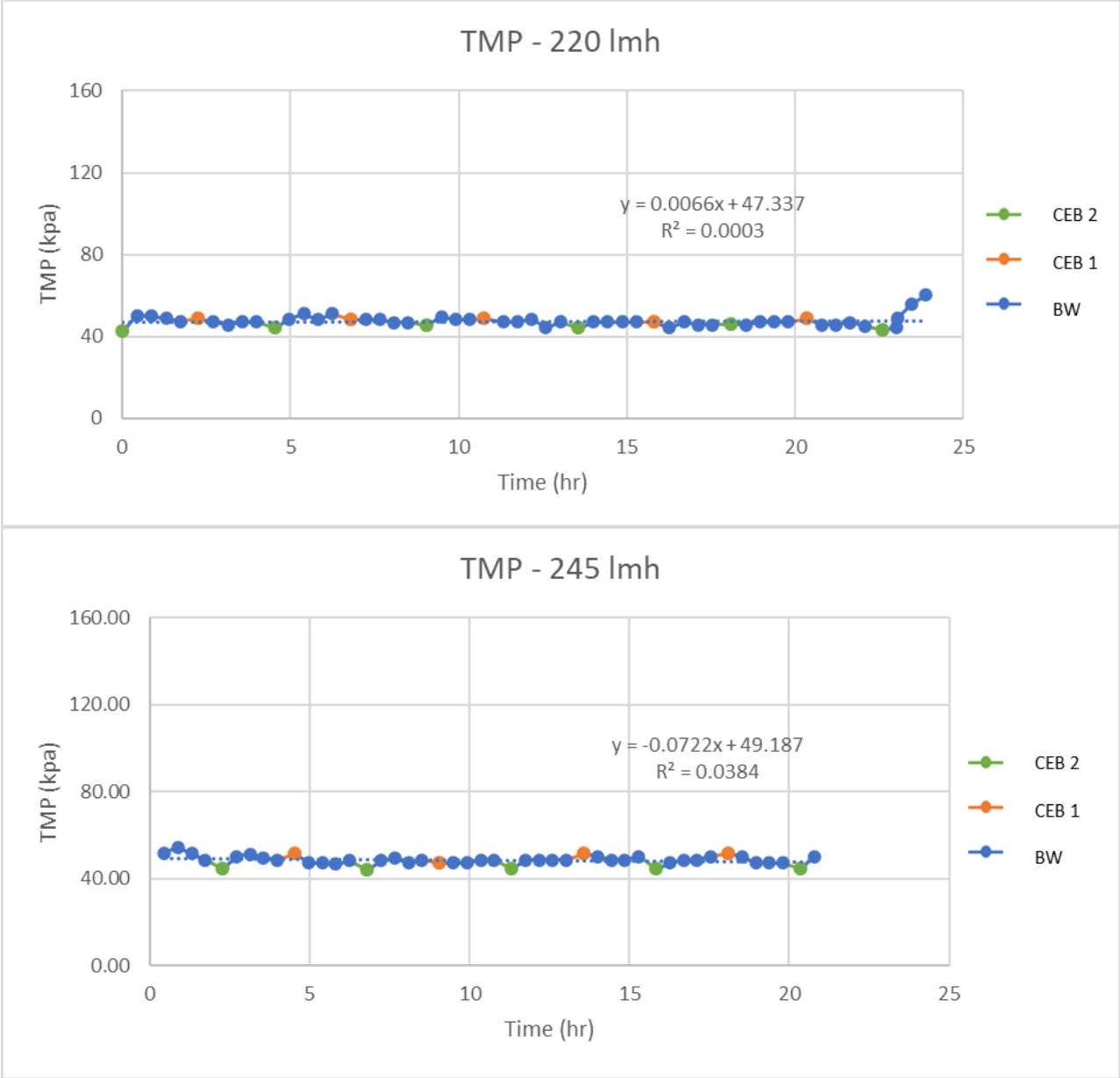

Figure 5-12 Starting TMPs for Alternative 2 – Ozonation Pretreatment

5.3.3.1 Residual Ozone Measurements

To understand how the critical flux results for alternative 2 was impacted by the ozone residual, residual ozone measurements were conducted. The results from these measurements are seen in Table 5-1.

Table 5-1 Residual Ozone Measurements

Date (mm-dd-yyyy)	Time (hh:mm)	Flux (Lmh)	Buffer Tank (mg/L)	Static Mixer (mg/L)	Before Ceramic Membrane (mg/L)	After Ceramic Membrane (mg/L)
7/22/2019	2:20	120	1.2	2.6	0.1	0
7/22/2019	1:59	145	1.9	2	0.5	0
7/22/2019	1:36	170	1.5	2.7	0.8	0
7/22/2019	1:07	195	1.2	2.2	0.9	0
7/22/2019	12:44	220	1.4	2.7	1	0
7/22/2019	12:23	245	1.2	1.4	1.2	0
7/22/2019	12:01	270	1.2	1.4	1.1	0

Even though the initial ozone readings were all around 8.0 mg/L, the measurements at each one of the sample points differed. These differing ozone measurements were the result of the differing fluxes between the experimental runs. The flux influenced the retention time of the secondary effluent in the system. With smaller fluxes, the ozone had a longer time to interact with the secondary effluent. While with larger fluxes, the ozone had less time to interact with the secondary effluent. This statement holds when analyzing the sample point directly before the ceramic membrane. There is a noticeable increase in the ozone residual measurements as the flux increases. Furthermore, for every flux, the residual ozone concentration decreased at each sampling point down the treatment train. Ultimately, these ozone residual measurements indicated that the critical flux of 270 Lmh was reached at an ozone level of 1.1 mg/L.

5.3.4 Summary of Critical Flux Tests

Twenty-four-hour constant flux tests were conducted to determine the sustainable and critical fluxes for each of the alternatives. The baseline TMP was also examined for the fluxes tested to see how many days the system could run before it needed to be shut off and have a cleaning in place (CIP). This baseline analysis involved graphing the TMP of the system after it went through either a normal backwash, CEB 1, or a CEB2, and determining

the slope based off a linear trendline through the graph. A summary of the critical flux tests and the baseline TMP analysis can be seen in Table 5-2.

Table 5-2 Results Summary Table from the Critical Flux Tests

Alternative	Flux	Slope	Dosage (mg/L)	Estimated Time until a CIP (days)	Critical Flux (LMH)	Sustainable Flux (LMH)
0	120	0.56	NA	12	145	120
	145	1.34		5		
1	145	0.43	6	16	195	170
	170	0.65		9		
	195	2.83		2		
1	145	0.97	20	7	195	170
	170	0.82		8		
	195	2.88		2		
2	220	0.01	8	996	270	245
	245	-0.07		NA		
	270	19.16		0.35		

5.4 Water Quality

Water quality measurements were taken for each of the alternatives and the results can be viewed in Appendix IV. The following parameters were tested: %UVT254, ammonium, bromate, bromide, chloride, nitrate, nitrite, pH, sulfate, total dissolved solids, and turbidity. A NOM characterization was conducted as well, which included total organic carbon (TOC), dissolved organic carbon (DOC), particulate organic carbon (POC), hydrophobic organic carbon (HOC), chromatographed DOC (CDOC), biopolymers, humic substances, building blocks, neutrals, and acids. The organic matter characteristics are described in this section.

5.4.1 Alternative 0 – No Pretreatment

Water samples were taken during the testing of this alternative at three sample locations: secondary effluent tank, before the ceramic membrane, and after the ceramic membrane. Based on the results seen in Table 5-2, there were decreases in TOC, DOC, POC, HOC, biopolymers, and neutrals. There is a significant decrease of most parameters by ceramic

membrane filtration. These decreases are good for water quality, but it may lead to membrane fouling. It is also important to note that there is a filter between the secondary effluent tank and the pilot installation. There was no measurable bromate formation with this alternative and $\%UVT_{254}$ remained constant during this alternative.

Table 5-3 Water Quality Results for Alternative 0

Parameter	Unit	Secondary Effluent Tank	Before Ceramic Membrane	After Ceramic Membrane	Change in Concentration from Influent to Effluent
TOC	µg/l C	10716	9387	8802	1914
DOC	µg/l C	10535	9411	8851	1684
POC	µg/l C	181	-25	-49	230
HOC	µg/l C	767	525	299	468
CDOC	µg/l C	9768	8886	8553	1215
Biopolymers	µg/l C	828	894	481	347
Humic Substances	µg/l C	4608	4240	4240	368
Building Blocks	µg/l C	2132	2053	2071	61
Neutrals	µg/l C	2199	1699	1760	439
Acids	µg/l C	0	0	0	0
UVT	%	51.6	51.0	51.8	-0.2

5.4.2 Alternative 1 – Coagulation Pretreatment

Water samples were taken at three sample locations: secondary effluent tank, before the ceramic membrane, and after ceramic membrane. Significant changes in the water quality from the influent to the effluent can be seen in Table 5-4. Based on the results seen in Table 5-3, coagulation caused an increase in $\%UVT_{254}$, while there were decreases TOC, DOC, CDOC, biopolymers, and humic substances. On the other hand, the removal by ceramic membrane filtration was restricted compared to no pretreatment. Therefore, coagulation pretreatment was able to reduce the NOM in the water, which helped mitigate membrane fouling. This alternative also had no measurable bromate formation.

Table 5-4 Water Quality Results for Alternative 1 at a dosage of 12 mg/L as Fe^{3+}

Parameter	Unit	Secondary Effluent Tank	Before Ceramic Membrane	After Ceramic Membrane	Change in Concentration from Influent to Effluent
TOC	µg/l C	8700	6870	6480	2220
DOC	µg/l C	8650	6790	6420	2230
POC	µg/l C	56	81	58	-2
HOC	µg/l C	571	360	557	14
CDOC	µg/l C	8080	6430	5860	2220
Biopolymers	µg/l C	466	463	184	282
Humic Substances	µg/l C	4800	3530	3250	1550
Building Blocks	µg/l C	1480	1230	1270	210
Neutrals	µg/l C	1320	1200	1160	160
Acids	µg/l C	<200	<200	<200	NA
UVT	%	55.9	60.4	66.9	-11

5.4.3 Alternative 2 – Ozonation Pretreatment

Water samples were taken during the testing of this alternative at five sample locations: secondary effluent tank, static mixer, buffer tank, before the ceramic membrane, and after the ceramic membrane. Significant changes in the water quality from the influent to the effluent can be seen in Table 5-5. Based on the results seen in Table 5-5, there were increases in building blocks, acids, and % UVT_{254}. On the other hand, there were decreases POC, HOC, and biopolymers. Thus, there was a shift in the NOM by ozonation pretreatment, which can help mitigate membrane fouling. There was significant bromate formation seen in this alternative, which is a concern as bromate is a potential carcinogen.

Table 5-5 Water Quality Results for Alternative 2

Parameter	Unit	Secondary Effluent Tank	Before Ceramic Membrane	After Ceramic Membrane	Change in Concentration from Influent to Effluent
Bromate	µg/l BrO3	<1	84	81	NA
TOC	µg/l C	10100	9330	9150	950
DOC	µg/l C	9940	9340	9130	810
POC	µg/l C	208	-8	23	185
HOC	µg/l C	379	-182	-44	423
CDOC	µg/l C	9560	9520	9170	390
Biopolymers	µg/l C	718	572	359	359
Humic Substances	µg/l C	4960	4140	4100	860
Building Blocks	µg/l C	2030	2840	2810	-780
Neutrals	µg/l C	1850	1580	1520	330
Acids	µg/l C	<200	389	384	NA
UVT	%	52.5	76.5	77	-24.5

5.4.4 Summary of Water Quality Results

Water quality measurements were taken for the three alternatives for the following parameters: %UVT254, ammonium, bromate, bromide, chloride, nitrate, nitrite, NOM, pH, sulfate, total dissolved solids, and turbidity. Based on the results, coagulation pretreatment and pre-ozonation were able to reduce the NOM in the water, which could help mitigate membrane fouling. These two alternatives also saw increases in $\%UVT_{254}$ indicating a decrease in particulates in the secondary effluent. Pre-ozonation did cause the bromide to be converted into bromate, which would need to be addressed in future work as the bromate level was above the 30 µg/L limit.

5.5 Operational Limitations

This research did have shortcomings that impacted the scope of the research as well as the results. These shortcomings included the CEB 1 chemical solution not being at the correct concentration for the alternative 0 tests, the coagulant dosage not being the optimal coagulant dosage, and the ozone uptake test not running for a long enough duration. Other

shortcomings were related to delays with pilot work. These included the air compressor leaking, the ozone generator breaking, the inline coagulation system needing to be refurbished, and another research group using the pilot system's power supply. These delays caused certain aspects of the scope to be postponed for future work, such as analyzing the alternatives for wet weather conditions and conducting an alternative that had both ozonation and coagulation pretreatment. Furthermore, long-term runs lasting five-days were attempted for each alternative using the sustainable fluxes determined by the critical flux tests. Unfortunately, none of the five-days runs were able to be completed because of either the chemically enhanced backwash solutions running out or the ozone alarm going off.

Chapter 6

6. Discussion

6.1 Introduction

The main objective of this research was to evaluate the impact of coagulation and ozonation pretreatment on ceramic microfiltration performance using a secondary effluent water reuse pilot in Wervershoof. This research was aimed at:

- defining critical and sustainable flux
- establishing a reference
- defining pretreatment conditions
- evaluating flux behavior and the impact of pretreatment on ceramic microfiltration performance and water quality parameters related to ceramic microfiltration fouling.

While trying to answer these questions, there were some boundary conditions that were in place. A summary of the research results can be seen in Table 6-1 below. The estimated time until a CIP indicates the estimated time the pilot system can run at a given flux until it will be taken offline and cleaned in place. The first number in the cells under this column indicates the time until the critical flux will need a CIP, and the second number indicates the time until the sustainable flux will need a CIP. These estimates are based on the baseline TMP.

Table 6-1 Summary of the Results

Alternative	Critical Flux (Lmh)	Sustainable Flux (Lmh)	Coagulant Dosage (mg/L as Fe^{3+})	Initial Ozone Dosage (mg/L as O_3)	Estimated Time Until a CIP (day)
0 – No Pretreatment	145	120	X	X	5 / 12
1 – Coagulation Pretreatment	195	170	6	X	2 / 9
1 – Coagulation Pretreatment	195	170	20	X	1 / 8
2 – Ozonation Pretreatment	270	245	X	8	0.35 / 999

6.2 Past Work

The research conducted in this thesis built upon the previous work conducted by Holly Shorney et al. for NEWater and Evan Owen. A pilot study conducted by PWNT from October 18th, 2013 until January 23rd, 2014 to aid in design efforts for the expansion of Changi NEWater Facility in Singapore. In this study, they looked at different pretreatment alternatives for ceramic microfiltration such as inline coagulation, ozonation, coagulation with ozone, and no pretreatment. The tests conducted consisted of short-term runs to determine the critical flux and optimize backwashing frequency for each of the alternatives for chlorinated water. Short-term runs were conducted on unchlorinated water using coagulation pretreatment as well. Based on the results from the tests, they recommended full-scale implementation consisted of coagulation pretreatment with the coagulant PACl at a dosage of 2 mg/L as Al^{3+}. It was also determined that the use of ozonation pretreatment on its own was not feasible as it did not mitigate fouling and the addition of coagulation pretreatment would be needed (Zheng et al., 2014). Research was also conducted that analyzed the impact of ozonation during ceramic microfiltration on water that contained natural organic matter. It was determined that ozone enhances the filterability as well as the permeability of the ceramic membrane because it oxidizes natural organic matter (Owen, 2019).

Daniel Farley and Bram Delfos also conducted research during this time regarding water reuse that looked at the impacts of ozone and advanced oxidation processes on organic micropollutants. In 2017, research was conducted to examine the capability of ozonation to degrade organic micropollutants in wastewater and ion exchange treated wastewater. Based on the bench-scale ozone experiments, the research illustrated that ozone can degrade organic

micropollutants; however, there were some issues with TCPP and iopromide (Farley, 2018). Further research was conducted in 2018 to 2017 evaluating the impact of ozonation and advanced oxidation regimes on pharmaceutical degradation at the ozone bench-scale setup at Het Waterlaboratorium in Haarlem. This research determined that ozonation and advanced oxidation were effective at degrading pharmaceuticals (Delfos, 2019)

6.3 Findings of the Research

6.3.1 Critical Flux Test Findings

Alternative 0 – no pretreatment served as a treatment reference for alternatives 1 and 2 to evaluate the impact of coagulation and ozonation pretreatment on ceramic microfiltration performance. Two twenty-four-hour tests were run to determine the critical flux and sustainable flux for alternative 0. For each of these tests the filtration time was set to twenty-five minutes and a cleaning regime of a 4-1-1 was run. CEB 1 (100-ppm NaOCl) helped the baseline TMP remain stable and the CEB 2 (100-ppm H_2O_2 with HCL at a pH of 2) decreased the TMP. NaOCl helps maintain the flux and H_2O_2 is an oxidant that helps break down the cake layer on the outside of the membrane, and thus, reduces the TMP (Alresheedi et al., 2019; Li et al., 2019).

Through this testing, the critical flux for alternative 0 was determined to be 145 Lmh and the sustainable flux was determined to be 120 Lmh for alternative 0. While 120 Lmh is the sustainable flux in view of the applied definition in this research effort, the system will need to be cleaned in twelve days.

The impact of coagulation pretreatment on ceramic microfiltration was studied. Two coagulant dosages, 6 mg/L and 20 mg/L as Fe^{3+}, were chosen prior to the start of critical flux tests to see the impact of higher and lower dosage on ceramic microfiltration performance

with uncorrected pH. The critical flux was estimated to be 195 Lmh and the sustainable flux was estimated to be 170 Lmh for both 6 and 20 mg/l as Fe^{3+}. A cleaning in place is necessary after 9 days for a dosage for 6 mg/L as Fe^{3+}, while for a dosage of 20 mg/L as Fe^{3+} a cleaning in place was required after four days. Therefore, compared to the 20 mg/L as Fe^{3+}, a coagulant dosage of 6 mg/L as Fe^{3+} was preferable when trying to mitigate fouling.

Based on the results for alternative 1, coagulation pretreatment improved ceramic microfiltration performance at the secondary effluent pilot in Wervershoof as it had higher critical and sustainable fluxes than alternative 0. The results from the twenty-four-hour constant flux tests for alternative 1 line up with the results seen in the literature.

The impact of ozonation pretreatment on ceramic microfiltration performance was investigated. Based on the twenty-four-hour constant flux tests and the residual ozone measurements, it was determined that the critical flux was 270 Lmh when the residual ozone prior to the membrane was 1.1 mg/L and the sustainable flux was 245 Lmh when the residual ozone prior to the membrane was 1.2 mg/L. When looking at the TMP data, there is a very strong increase in TMP. Further research is needed to understand the mechanisms causing the strong increase in TMP. A flux of 245 Lmh is promising for a sustainable flux as the TMP slightly decreases with time as the ozone residual seems to interact with the ceramic membrane surface, improving the fouling characteristics of the ceramic microfiltration. Ozonation pretreatment enhances ceramic microfiltration performance as it achieved higher critical and sustainable fluxes.

Based on a twenty-four-hour filter run both coagulation pretreatment and ozonation pretreatment enhanced ceramic microfiltration performance in terms of flux relative to no pretreatment. Based on these results, ozonation was able to mitigate membrane fouling better

than coagulation pretreatment. However, additional tests are needed to determine the optimal coagulant dosage for this system and secondary effluent. Additional research should be performed to see to what extent the combination of coagulation and ozonation offers a beneficial treatment scenario as water quality, in particular NOM content, is improved by coagulation while ozonation changes NOM characteristics and interacts with the membrane surface, thereby improving ceramic microfiltration performance.

6.3.2 Water Quality Findings

Water quality measurements were taken for $\%UVT_{254}$ and NOM as well as for other parameters that can be seen in Appendix IV. NOM was broken down into measurements for total organic carbon (TOC), dissolved organic carbon (DOC), particulate organic carbon (POC), hydrophobic organic carbon (HOC), chromatographed DOC (CDOC), biopolymers, humic substances, building blocks, neutrals, and acids. The parameters of the most concern were NOM characteristics and $\%UVT_{254}$, as NOM causes membrane fouling and $\%UVT_{254}$ is a surrogate for the organic carbon content.

For alternative 0 – no pretreatment, there was no change in $\%UVT_{254}$ before or after ceramic microfiltration. This result was expected as ceramic microfiltration is not designed to reduce the organic carbon content, but instead possesses the ability to remove bacteria (Malcolm Pirnie, Inc et al., 2005). However, there was a decrease in NOM by ceramic microfiltration, indicating NOM's ability to act as a foulant to ceramic microfiltration.

For alternative 1 – coagulation pretreatment, water quality parameters were measured at coagulant dosage of 12 mg/L as Fe^{3+}. The water quality parameters were meant to be measured at a 6 mg/L as Fe^{3+}, but because of the variations in flow the concentration of coagulant ending up being higher. Regarding $\%UVT_{254}$, there was an 11 percent increase as

coagulation aggregates particulates out of the water (Matilainen et al., 2010) . Decreases were seen in NOM were also seen as coagulation pretreatment can reduce the NOM through entrapment, destabilization, complexation, and adsorption (Matilainen et al., 2010). The removal of NOM was lower than for alternative 0 thereby reducing the CMF fouling.

For alternative 2 – ozonation pretreatment, there was a 24.5 percent increase in %UVT, which is a result of ozone and hydroxyl radicals being strong oxidants as they can react with organic compounds in the water. There were changes in NOM as pre-ozonation impacts NOM by degrading it into smaller molecules (Van Geluwe et al., 2011; Hamid et al., 2017). This change in NOM characteristics and possibly the interaction of ozone with ceramic microfiltration's surface restricted the ceramic microfiltration strongly.

Chapter 7

7. Conclusions and Recommendations

7.1 Conclusions

The aim of this research was to evaluate the impact of coagulation and ozonation pretreatment on ceramic microfiltration performance using a secondary effluent water reuse pilot in Wervershoof. Coagulation and ozonation pretreatment enhanced ceramic microfiltration performance in terms of flux relative to no pretreatment based on twenty-four hour fouling. Without pretreatment, the critical flux was 145 Lmh. By using coagulation pretreatment, the critical flux increased to 195 Lmh, while ozonation pretreatment showed a critical flux of 270 Lmh. Based on these results, it was concluded that ozonation was able to mitigate membrane fouling better than coagulation pretreatment.

7.2 Recommendations for Future Work

To address the concerns that have arisen as well as some of the limitations, the following future work is recommended.

- Tests to understand the mechanisms causing the stark increase in critical flux for Alternative 2 – Ozonation Pretreatment
- Jar tests to determine the optimal coagulant dosage for the secondary effluent in Wervershoof
- Rerun the ozone uptake tests to determine the optimal ozone dosage based on selected ozone residual directly prior to the ceramic microfiltration unit
- Determine to what extent the combination of ozonation and coagulation offers a beneficial treatment scenario

- Run twenty-four-hour constants flux tests for wet weather conditions to see the impact of weather on performance
- Rerun alternative 1 – coagulation pretreatment for an alum-based coagulant to see if it can enhance ceramic microfiltration performance better than a ferric-based coagulant

References

Abbas, A., Schneider, I., Bollmann, A., Funke, J., Oehlmann, J., & Prasse, C. et al. (2019). What you extract is what you see: Optimizing the preparation of water and wastewater samples for in vitro bioassays. Water Research, 152, 47-60. doi: 10.1016/j.watres.2018.12.049

Allen, P., & Elser, G. (1979). They said it couldn't be done - the orange County, California experience. Desalination, 30(1), 23-38. doi: 10.1016/s0011-9164(00)88430-1

Alresheedi, M., Basu, O., & Barbeau, B. (2019). Chemical cleaning of ceramic ultrafiltration membranes – Ozone versus conventional cleaning chemicals. Chemosphere, 226, 668-677. doi: 10.1016/j.chemosphere.2019.03.188

Alsheyab, M., & Muñoz, A. (2007). Optimization of ozone production for water and wastewater treatment. Desalination, 217(1-3), 1-7. doi: 10.1016/j.desal.2007.01.010

American Water Works Association Research Foundation and Compagnie Générale des Eaux. (1991). Ozone in Water Treatment: Application and Engineering (pp. 1-431). Chelsea: Lewis Publishers, INC.

Angelakis, A., & Durham, B. (2008). Water recycling and reuse in EUREAU countries: Trends and challenges. Desalination, 218(1-3), 3-12. doi: 10.1016/j.desal.2006.07.015

Annual report 2017 | De Waterketen. (2018). Retrieved from https://www.pwn.nl/jaarverslag/2017/pwn-en-haar-omgeving/de-waterketen

Annual report 2017 |About PWN. (2018). Retrieved from https://www.pwn.nl/jaarverslag/2017/pwn-en-haar-omgeving/over-pwn

Arhin, S., Banadda, N., Komakech, A., Kabenge, I., & Wanyama, J. (2016). Membrane fouling control in low pressure membranes: A review on pretreatment techniques for fouling abatement. Environmental Engineering Research, 21(2), 109-120. doi: 10.4491/eer.2016.017

Bacchin, P., Aimar, P., & Field, R. (2006). Critical and sustainable fluxes: Theory, experiments and applications. Journal Of Membrane Science, 281(1-2), 42-69. doi: 10.1016/j.memsci.2006.04.014

Bean, E., Campbell, S., & Anspach, F. (1964). Zeta Potential Measurements in the Control of Coagulation Chemical Doses. Journal - American Water Works Association, 56(2), 214-227. doi: 10.1002/j.1551-8833.1964.tb01202.x

Beier, S., & Jonsson, G. (2009). Critical flux determination by flux-stepping. Aiche Journal, 56(7), 1739-1747. doi: 10.1002/aic.12099

Bixio, D., Thoeye, C., De Koning, J., Joksimovic, D., Savic, D., Wintgens, T., & Melin, T. (2006). Wastewater reuse in Europe. Desalination, 187(1-3), 89-101. doi: 10.1016/j.desal.2005.04.070

Boost for ceramic membrane based water treatment – PWNT. (2018). Retrieved from https://pwntechnologies.com/boost-for-ceramic-membrane-based-water-treatment/

Bottino, A., Capannelli, C., Borghi, A. D., Colombino, M., & Conio, O. (2001). Water treatment for drinking purpose: Ceramic microfiltration application. Desalination, 141(1), 75-79. doi:10.1016/s0011-9164(01)00390-3

Bucs, S., Farhat, N., Kruithof, J., Picioreanu, C., van Loosdrecht, M., & Vrouwenvelder, J. (2018). Review on strategies for biofouling mitigation in spiral wound membrane systems. Desalination, 434, 189-197. doi: 10.1016/j.desal.2018.01.023

Burris, D. (2018). Groundwater Replenishment System 2017 Annual Report (pp. 1-70). Irvine: DDB Engineering, INC. Retrieved from https://www.ocwd.com/media/6822/2017-gwrs-annual-report.pdf

Calderón, A., & González, I. (2017). Some Hardware and Instrumentation Aspects of the Development of an Automation System for Jar Tests in Drinking Water Treatment. Sensors, 17(10), 2305. doi: 10.3390/s17102305

CeraMac® – PWNT. Retrieved from https://pwntechnologies.com/portfolio-item/ceramac/

Chiang, P., Chang, E., Chang, P., & Huang, C. (2009). Effects of pre-ozonation on the removal of THM precursors by coagulation. Science Of The Total Environment, 407(21), 5735-5742. doi: 10.1016/j.scitotenv.2009.07.024

Company – PWNT. Retrieved from https://pwntechnologies.com/about-us/

Delfos, B. Impact of Ozonation and Advanced Oxidation Regimes on Degradation of Micropollutants in Wastewater Treatment Plant Effluent (Masters). Water Technology at Wetsus.

Duan, J., Wang, J., Guo, T., & Gregory, J. (2014). Zeta potentials and sizes of aluminum salt precipitates – Effect of anions and organics and implications for coagulation mechanisms. Journal Of Water Process Engineering, 4, 224-232. doi: 10.1016/j.jwpe.2014.10.008

Escher, B., Allinson, M., Altenburger, R., Bain, P., Balaguer, P., & Busch, W. et al. (2013). Benchmarking Organic Micropollutants in Wastewater, Recycled Water and Drinking Water with In Vitro Bioassays. Environmental Science & Technology, 48(3), 1940-1956. doi: 10.1021/es403899t

Farley, D. (2018). Investigation into the Application of Ozonation for Reuse of Secondary Wastewater Effluent (Master of Science). University of New Hampshire.

Farvardin, M., & Collins, A. (1989). Preozonation as an aid in the coagulation of humic substances—Optimum preozonation dose. Water Research, 23(3), 307-316. doi: 10.1016/0043-1354(89)90096-1

Fawell, J., Le Corre, K., & Jeffrey, P. (2016). Common or independent? The debate over regulations and standards for water reuse in Europe. International Journal Of Water Resources Development, 32(4), 559-572. doi: 10.1080/07900627.2016.1138399

Ferguson, D., Gramith, J., & McGuire, M. (1991). Applying Ozone for Organics Control and Disinfection: A Utility Perspective. Journal - American Water Works Association, 83(5), 32-39. doi: 10.1002/j.1551-8833.1991.tb07144.x

Field, R., & Pearce, G. (2011). Critical, sustainable and threshold fluxes for membrane filtration with water industry applications. Advances In Colloid And Interface Science, 164(1-2), 38-44. doi: 10.1016/j.cis.2010.12.008

Field, R., Wu, D., Howell, J., & Gupta, B. (1995). Critical flux concept for microfiltration fouling. Journal Of Membrane Science, 100(3), 259-272. doi: 10.1016/0376-7388(94)00265-z

Gabriel, S. Personal Communication, March 2019 – August 2019

Hach Company. (2013a). User Manual Conductivity Probe: Model CDC40101, CDC40103, CDC40105, CDC40110, CDC40115 or CDC40130 [Ebook] (2nd ed., pp. 1-10). Loveland: Hach Company. Retrieved from https://www.hach.com/hqdguide-conductivity

Hach Company. (2013b). User Manual General use pH probe: Models PHC20101, PHC20103 [Ebook] (2nd ed., pp. 1-12). Loveland: Hach Company.

Hach Company. (2018). DR 6000 User Manual [Ebook] (4th ed., pp. 81-82, 100-102). Loveland: Hach Company.

Hamid, K. I., Sanciolo, P., Gray, S., Duke, M. and Muthukumaran, S. (2017). Impact of ozonation and biological activated carbon filtration on ceramic membrane fouling. Water Research, 126, pp.308-318.

Hamid, K. I., Sanciolo, P., Gray, S., Duke, M., & Muthukumaran, S. (2019). Comparison of the effects of ozone, biological activated carbon (BAC) filtration and combined ozone-BAC pre-treatments on the microfiltration of secondary effluent. Separation and Purification Technology, 215, 308-316. doi:10.1016/j.seppur.2019.01.005

Heidolph Instruments GMBH & CO KG. (2011). RZR 1 Instruction Manual (pp. 15-21). Heidolph Instruments GMBH & CO KG.

HHNK. English - Portaal - Hoogheemraadschap Hollands Noorderkwartier. Retrieved 5 April 2020, from https://www.hhnk.nl/portaal/english_41966/

Howell, J. (1995). Sub-critical flux operation of microfiltration. Journal Of Membrane Science, 107(1-2), 165-171. doi: 10.1016/0376-7388(95)00114-r

Hu, Y., Milne, N., Gray, S., Morris, G., Jin, W., Duke, M., & Zhu, B. (2011). Combined TiO2membrane filtration and ozonation for efficient water treatment to enhance the reuse of wastewater. Desalination And Water Treatment, 34(1-3), 57-62. doi: 10.5004/dwt.2011.2867

Huang, H., Schwab, K., & Jacangelo, J. (2009). Pretreatment for Low Pressure Membranes in Water Treatment: A Review. Environmental Science & Technology, 43(9), 3011-3019. doi: 10.1021/es802473r

Issaoui, M., & Limousy, L. (2019). Low-cost ceramic membranes: Synthesis, classifications, and applications. Comptes Rendus Chimie, 22(2-3), 175-187. doi: 10.1016/j.crci.2018.09.014

Jiang, J. (2001). Development of Coagulation Theory and Pre-Polymerized Coagulants for Water Treatment. Separation And Purification Methods, 30(1), 127-141. doi: 10.1081/spm-100102986

Jiang, J. (2015). The role of coagulation in water treatment. Current Opinion In Chemical Engineering, 8, 36-44. doi: 10.1016/j.coche.2015.01.008

Lee, S., & Kim, J. (2015). Effects of Coagulation on the Ceramic Membrane Fouling during Surface Water Treatment. Journal Of Environmental Engineering, 141(5), 04014087. doi: 10.1061/(asce)ee.1943-7870.0000918

Lehman, S., & Liu, L. (2009). Application of ceramic membranes with pre-ozonation for treatment of secondary wastewater effluent. Water Research, 43(7), 2020-2028. doi: 10.1016/j.watres.2009.02.003

Lerch, A., Panglisch, S., Buchta, P., Tomita, Y., Yonekawa, H., Hattori, K., & Gimbel, R. (2005). Direct river water treatment using coagulation/ceramic membrane microfiltration. Desalination, 179(1-3), 41-50. doi:10.1016/j.desal.2004.11.054

Li, K., Li, S., Huang, T., Dong, C., Li, J., Zhao, B., & Zhang, S. (2019). Chemical Cleaning of Ultrafiltration Membrane Fouled by Humic Substances: Comparison between Hydrogen Peroxide and Sodium Hypochlorite. International Journal Of Environmental Research And Public Health, 16(14), 2568. doi: 10.3390/ijerph16142568

Lin, T., Wu, S., & Chen, W. (2014). Formation potentials of bromate and brominated disinfection by-products in bromide-containing water by ozonation. Environmental Science And Pollution Research, 21(24), 13987-14003. doi: 10.1007/s11356-014-3329-2

Malcolm Pirnie, Inc., Separation Processes, Inc., & The Cadmus Group, Inc. (2005). Membrane Filtration Guidance Manual [Ebook] (pp. 1-50). Cincinnati: US EPA.

Matilainen, A., Vepsäläinen, M., & Sillanpää, M. (2010). Natural organic matter removal by coagulation during drinking water treatment: A review. Advances In Colloid And Interface Science, 159(2), 189-197. doi: 10.1016/j.cis.2010.06.007

Mezzanotte, V., Antonelli, M., Citterio, S., & Nurizzo, C. (2007). Wastewater Disinfection Alternatives: Chlorine, Ozone, Peracetic Acid, and UV Light. Water Environment Research, 79(12), 2373-2379. doi: 10.2175/106143007x183763

Michigan Department of Environmental Quality Operator Training and Certification Unit. Jar Testing of Chemical Dosages. Presentation.

Nazzal, F. F., & Wiesner, M. R. (1994). pH and ionic strength effects on the performance of ceramic membranes in water filtration. Journal of Membrane Science, 93(1), 91-103. doi:10.1016/0376-7388(94)85019-4

Ormerod, K., & Silvia, L. (2017). Newspaper Coverage of Potable Water Recycling at Orange County Water District's Groundwater Replenishment System, 2000–2016. Water, 9(12), 984. doi: 10.3390/w9120984

Papageorgiou, A., Stylianou, S., Kaffes, P., Zouboulis, A., & Voutsa, D. (2017). Effects of ozonation pretreatment on natural organic matter and wastewater derived organic matter – Possible implications on the formation of ozonation by-products. Chemosphere, 170, 33-40. doi: 10.1016/j.chemosphere.2016.12.005

Petsev, D., Starov, V., & Ivanov, I. (1993). Concentrated dispersions of charged colloidal particles: Sedimentation, ultrafiltration and diffusion. Colloids and Surfaces A: Physicochemical And Engineering Aspects, 81, 65-81. doi: 10.1016/0927-7757(93)80235-7

Price, B. (1975). Jar Tests Improve Water Quality. Opflow, 1(12), 4-4. doi: 10.1002/j.1551-8701.1975.tb00844.x

Projects – PWNT. Retrieved from https://pwntechnologies.com/projects/

Rakruam, P., & Wattanachira, S. (2014). Reduction of DOM fractions and their trihalomethane formation potential in surface river water by in-line coagulation with ceramic membrane filtration. Journal of Environmental Sciences, 26(3), 529-536. doi:10.1016/s1001-0742(13)60471-4

Richardson, N., & Argo, D. (1977). Orange county's 5 MGD reverse osmosis plant. Desalination, 23(1-3), 563-573. doi: 10.1016/s0011-9164(00)82555-2

Ried, A., Mielcke, J., & Wieland, A. (2009). The Potential Use of Ozone in Municipal Wastewater. Ozone: Science & Engineering, 31(6), 415-421. doi: 10.1080/01919510903199111

Rizzo, L. (2011). Bioassays as a tool for evaluating advanced oxidation processes in water and wastewater treatment. Water Research, 45(15), 4311-4340. doi: 10.1016/j.watres.2011.05.035

Rodríguez, F., Marcos, L., Núñez, L., & García, M. (2012). Effects of Ozonation on Molecular Weight Distribution of Humic Substances and Coagulation Processes – A Case

Study: The Úzquiza Reservoir Water. Ozone: Science & Engineering, 34(5), 342-353. doi: 10.1080/01919512.2012.710874

Rosman, N., Salleh, W., Mohamed, M. A., Jaafar, J., Ismail, A., & Harun, Z. (2018). Hybrid membrane filtration-advanced oxidation processes for removal of pharmaceutical residue. Journal of Colloid and Interface Science, 532, 236-260. doi:10.1016/j.jcis.2018.07.118

Satterfield, Z. (2005). Tech Brief Jar Testing [Ebook] (pp. 1-4). Morgantown: The National Environmental Services Center at West Virginia University.

Schneider, O., & Tobiason, J. (2000). Preozonation effects on coagulation. Journal - American Water Works Association, 92(10), 74-87. doi: 10.1002/j.1551-8833.2000.tb09025.x

Sgroi, M., Vagliasindi, F., & Roccaro, P. (2018). Feasibility, sustainability and circular economy concepts in water reuse. Current Opinion In Environmental Science & Health, 2, 20-25. doi: 10.1016/j.coesh.2018.01.004

Sharp, E., Jarvis, P., Parsons, S., & Jefferson, B. (2006). The Impact of Zeta Potential on the Physical Properties of Ferric−NOM Flocs. Environmental Science & Technology, 40(12), 3934-3940. doi: 10.1021/es051919r

Shi, Y., Fan, M., Brown, R., Sung, S., & Van Leeuwen, J. (2004). Comparison of corrosivity of polymeric sulfate ferric and ferric chloride as coagulants in water treatment. Chemical Engineering And Processing: Process Intensification, 43(8), 955-964. doi: 10.1016/j.cep.2003.09.001

Shin, J., Spinette, R., & O'Melia, C. (2008). Stoichiometry of Coagulation Revisited. Environmental Science & Technology, 42(7), 2582-2589. doi: 10.1021/es071536o

Simon, E., Schriks, M., Herbert, A., Baken, K., van der Oost, R., Van der Burg, B., & Kienle, C. EU DEMEAU project: Practical application of in vitro bioassays in water quality assessment, 1-2.

Song, J., Zhang, Z., Tang, S., Tan, Y., & Zhang, X. (2018). Does pre-ozonation or in-situ ozonation really mitigate the protein-based ceramic membrane fouling in the integrated process of ozonation coupled with ceramic membrane filtration?. Journal Of Membrane Science, 548, 254-262. doi: 10.1016/j.memsci.2017.11.031m

Stover, E., Haas, C., Rakness, K., & Scheible, O. (1986). Design Manual Municipal Wastewater Disinfection [Ebook] (pp. 113-168). Cincinnati: U.S. Environmental Protection Agency Office of Research and Development. Retrieved from https://cfpub.epa.gov/si/si_public_record_Report.cfm?Lab=NRMRL&dirEntryId=49846

Szymanska, K., Zouboulis, A., & Zamboulis, D. (2014). Hybrid ozonation–microfiltration system for the treatment of surface water using ceramic membrane. Journal of Membrane Science, 468, 163-171. doi:10.1016/j.memsci.2014.05.056

United States Environmental Protection Agency. (1999). Wastewater Technology Fact Sheet Ozone Disinfection [Ebook] (p. 3). Washington, D.C.: US EPA. Retrieved from https://www3.epa.gov/npdes/pubs/ozon.pdf

US EPA. (2001). Controlling Disinfection By-Products and Microbial Contaminants in Drinking Water (pp. 215-228) (United States of America, United States Environmental Protection Agency, Office of Research and Development). United States Environmental Protection Agency.

Van Geluwe, S., Braeken, L., & Van der Bruggen, B. (2011). Ozone oxidation for the alleviation of membrane fouling by natural organic matter: A review. *Water Research*, *45*(12), 3551-3570. doi: 10.1016/j.watres.2011.04.016

Von Gunten, U. (2003). Ozonation of drinking water: Part I. Oxidation kinetics and product formation. Water Research, 37(7), 1443-1467. doi: 10.1016/s0043-1354(02)00457-8

Von Gunten, U. (2007). The basics of oxidants in water treatment. Part B: ozone reactions. *Water Science And Technology*, *55*(12), 25-29. doi: 10.2166/wst.2007.382

von Gunten, U., & Pinkernell, U. (2000). Ozonation of bromide-containing drinking waters: a delicate balance between disinfection and bromate formation. Water Science And Technology, 41(7), 53-59. doi: 10.2166/wst.2000.0115

Waar staan we voor | PWN. Retrieved from https://www.pwn.nl/over-pwn/waar-staan-we-voor

Wang, S., Patel, M., Dunivin, B., Clark, J., Foellmi, S., & Dipietro, C. (2015). Post-treatment Optimization to Enhance Groundwater Recharge Operations. Journal - American Water Works Association, 107(5), 87-92. doi: 10.5942/jawwa.2015.107.0074

WEDECO AG (2006). WEDECO Small Ozone Systems. Herford: WEDECO, pp.1-4.

Xie, P., Chen, Y., Ma, J., Zhang, X., Zou, J., & Wang, Z. (2016). A mini review of preoxidation to improve coagulation. Chemosphere, 155, 550-563. doi: 10.1016/j.chemosphere.2016.04.003

Zhao, Y., Zhang, Y., Xing, W., & Xu, N. (2005). Influences of pH and ionic strength on ceramic microfiltration of TiO2 suspensions. Desalination, 177(1-3), 59-68. doi: 10.1016/j.desal.2004.10.032

Zheng, J., & Shorney-Darby, H. (2014). Pilot Study Report for Treating Secondary Wastewater Effluent with In-Line Coagulation and CeraMac® at the Changi NEW Facility in Singapore. PWNT.

Zheng, J., Galjaard, G., & Shorney-Darby, H. (2015). Ceramic microfiltration – influence of pretreatment on operational performance. Water Practice And Technology, 10(4), 747-760. doi: 10.2166/wpt.2015.092

Zhu, H., Wen, X., & Huang, X. (2012). Characterization of membrane fouling in a microfiltration ceramic membrane system treating secondary effluent. Desalination, 284, 324-331. doi:10.1016/j.desal.2011.09.019

Appendix I Pilot Manual

1. Overview of Pilot Setup

1.1 Overview

The PWNT Pilot in Wervershoof is a secondary effluent reuse system that consists of ozonation, inline coagulation, and ceramic membrane microfiltration. The secondary effluent is attached to the system using a filter where it is then exposed to pre-ozonation. After pre-ozonation the water goes through the static mixer, where some of the secondary effluent is recirculated through pre-ozonation. The secondary effluent then goes through the coagulation pretreatment unit, which consists of two tanks. Following coagulation, the influent water goes through the ceramic membrane where the filtrate goes through an activated carbon filter prior to being released into the environment.

The pre-ozonation system consists of a WEDECO OCS Modular 4HC ozone generator. This generator uses oxygen, produced from ambient air using the Air Sep by Topaz, to generate ozone. It has an oxygen demand of 0.04 cubic meters per hour along with a power consumption of 0.1 kilowatts when the ozone production is at one hundred percent. Furthermore, it has a maximum ozone production of 4 grams per hour. The dimensions of this unit are a height of 600 millimeters, a width of 600 millimeters, and a depth of 210 millimeters. (WEDECO AG, 2006).

The RZR1 model inline coagulation system was created by Heidolph. This model can achieve speed ranges of 35 rotations per minute to 250 rotations per minute. The power input and output of this system with regards to the motor are 77 watts and 18 watts, respectively (Heidolph Instruments GMBH & CO KG, 2011). The system put in place in the pilot consists of two contact chambers each with their own mixer. Thus, the system can have both rapid and slow mixing speeds.

A 0.4 m^2 Metawater ceramic membrane unit was the ceramic membrane system in use at the pilot. It is a hollow fiber ceramic membrane with pore size of 0.1 micrometers. Water flows through the membrane inside-out. The max transmembrane pressure that the ceramic membrane can handle at the pilot is 2 bar or 200 kpa, and if this is surpassed the installation shuts down (Gabriel, 2019).

2. Startup of Pilot

2.1 Filling Secondary Effluent Tank

The Secondary effluent tank located in the left-hand corner of the pilot room is filled using the following procedure:

1. Open hydrant for the secondary effluent, depicted in Figure 2-1, using the rusted metal apparatus depicted in the figure as well. To do this, turn the orange valve located in the ground next to the hydrant in the counterclockwise direction.

Figure 2-1 Hydrant for Secondary Effluent

2. Next, open the valve on the hydrant with the piping attached to it by turning it in the counterclockwise direction.
3. To enable the secondary effluent to flow into the tank, turn the handle of the valve on the outside of the building to the downward facing direction from the right facing direction. This valve can be viewed in the Figure 2-2 Valve for Secondary Effluent below.

Figure 2-2 Valve for Secondary Effluent

4. Since the first round of water entering the tank is relatively foul, leave the valve that allows water to exit at the bottom of the secondary effluent tank open for about 10 minutes before closing it and filling the tank.
5. Once the tank is filled, some of the secondary effluent will start flowing out of the overflow pipe. Once this starts occurring, adjust the valve in Figure 2-2 to prevent the tank from overflowing. Once this is done, the secondary effluent can be used as the feed water for the pilot system.
6. To allow the secondary effluent to be the feedwater source for the pilot, attach the secondary effluent hose to the filter, depicted in Figure 2-3. Next, attach the filter to the pilot installation by using the orange clip located at the end of the yellow tubing coming out of the filter.

Figure 2-3 Filter for Secondary Effluent

2.2 Turning on the Pilot

The procedure for starting up the pilot is the following:

1. Attach the hose for the influent feed water, which is usually secondary effluent or tap water. This is done by pulling the orange clip down on the hose and pushing to into the inlet of the pilot until a clicking noise is heard, a picture of what this ends up looking like can be seen in Figure 2-4.

Figure 2-4 Inlet Feed Water Attached to Installation

2. Turn the black switch to the upright position located on the back of the membrane portion of the installation to start up the pilot. Next, switch the red switch on the back of the ozonation portion of the pilot to the upright position.
3. Open the red and blue valves on ozonation portion of the installation. If secondary effluent is the feedwater, plug the pump into an outlet. If tap water is the feedwater, turn the valve located where the hose is stored. Next, turn the black switch located on the front of the ozonation portion of the installation of the left to start the flow of the feed water through the system.
4. If ozone is being used, the system switch at the back of the ozone portion of the pilot is turned to the right during this time. When the ozone portion of the system is turned on, the malfunction button will light up red. To turn this off, press blue release button. The ozone settings were adjusted by turning the ozone production button. The back of the ozone portion of the pilot can be viewed in Figure 2-5.
5. Once the water has been running through the system, the membrane portion of the installation is turned on. This is done by turning the switch titled voor-behandeling to on.
6. To adjust the backwash and filtration settings for the membrane filtration system according to the run use the Siemens' Simatic panel on the back of the membrane machine. The back of the membrane portion of the pilot is seen in Figure 2-5.

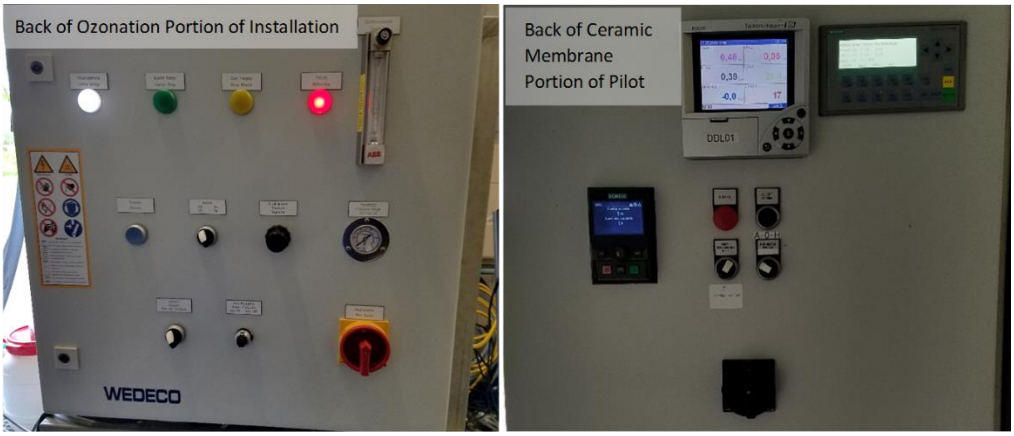

Figure 2-5 Back of Ozonation and Ceramic Membrane Portions of the Pilot

2.3 Common Problems during Pilot Startup

The startup of the pilot can be impeded by the following situations: buffer tank is empty, CEB1 levels are low, CEB2 levels are low, or the TMP exceeds 2 bar. Each of these problems is easily fixable. To fix the empty buffer tank, allow tap water to flow through the system prior to turning on system. Once the buffer tank is filled to an appropriate level, turn on the pilot and hit the accept storing button on the back of the ceramic membrane portion of the pilot. Once this storing button has been pressed, the release button on the back of ozonation portion of installation can be pushed if it has not already gone away. The system can now start running.

To increase the CEB1 and CEB2 levels, follow the description under chapter 3 of the manual. With regards to the TMP exceeding 2 bar, the installation will not allow water to flow through the membrane until the pressure is released. The releasing of pressure is done by grabbing a one- or two-liter container and placing it underneath the sample point, PAN-PIRWZI-PIL-O3, directly before the ceramic membrane. Then proceed to open the valve and allow the water and the pressure to release. Be careful as the water can spray out. Once this step has been completed the release button can be pushed on the back of the ceramic membrane portion of the installation, and the startup of the apparatus can continue.

3. Running the Pilot

3.1 Adjusting the Inlet Flow

The inlet flow can easily be adjusted by turning the black dial at the front of the ozonation portion of the pilot, which can be seen in Figure 3-1 below. To increase the flow, turn the dial to the left and to decrease the flow or shut it off completely, turn the dial to the right. When operating with tap water, the flow can fluctuate significantly with time. Thus, make sure to observe the flow and adjust as needed to ensure that the level of water in the buffer tank never gets too low. When using secondary effluent, the flow usually remains stable.

Figure 3-1 Dial for Influent Flow into Pilot System

3.2 Adjusting the Flow through the Ceramic Membrane

The flow through the ceramic membrane can be adjusted using a dial found inside the panel located on the back of the ceramic membrane portion of the pilot. The panel can be opened by using the key located right next to it. Once the panel is opened, the dial is in the upper right-hand corner and can be seen in Figure 3-2 below. To increase the flow, turn the dial to the right, and to decrease the flow turn the dial to the left. The dial is extremely sensitive so even a small turn can result in a large increase in flow. Therefore, it is recommended to move the dial in small intervals and give the flow a few minutes to adjust to this change. The adjusted flow can be viewed on the monitor on the outside of the opened panel.

Figure 3-2 Dial for the Flow of Feedwater through the Membrane

3.3 Adjusting the Ozone Concentration

The ozone gas concentration can be adjusted using the dial labeled ozone production located on the back of the ozonation portion of the pilot as depicted in Figure 3-3. To adjust the gas concentration, the dial must be unlocked, which is done by moving the switch on the side of the dial to the upright position. The dial can then be moved to the right to increase the concentration or to the left to decrease the concentration. Once the dial is set to the appropriate level, the dial should be locked again by moving the switch on the side of it to the right. A gas meter located on the top of this portion of the pilot will display the ozone gas concentration going into the water. Give the system time to adjust to the ozone gas concentration. It should usually take around 30 minutes to stabilize.

Figure 3-3 Oxone Production Dial

3.4 Filling the CEB1 Vessel

The thirty-five-liter CEB1 vessel seen in Figure 3-4 contains a 100-ppm hypochlorite solution. The system will shut down when the level of this solution is only at ten liters. To fill up this vessel, unscrew the black cap and then pour 10 liters of MilliQ, demineralized, or RO water into vessel. A 150 gram/liter hypochlorite solution is added. If the hypochlorite solution is 150 gram/liter, then 6.80 milliliters of this solution needs to be added to the vessel for every 10 liters of water. However, the concentration of the hypochlorite solution can dissipate over time, so it is recommended to test the concentration in the 100-ppm hypochlorite solution using Hach DPD Free Chlorine Reagent along with test 88 on the DR6000. When adding the hypochlorite solution, the proper personal protective equipment should be worn which includes a face shield, a lab smock, as well as thick gloves, all of which can be found at the pilot.

Figure 3-4 CEB1 Vessel

3.5 Filling CEB2 Vessel

The thirty-five-liter CEB2 vessel depicted in Figure 3-5 is filled with a 100-ppm peroxide solution. The system will shut down when the level of this solution is only at ten liters. To fill up this vessel, the black cap is unscrewed and 10 liters of MilliQ, demineralized, or RO water is poured into the vessel. Next, 2.90 milliliters of a 35 percent peroxide solution are added followed by 40 milliliters of a ten percent hydrogen chloride solution. When adding these chemicals, the proper personal protective equipment should be worn which includes a face shield, a lab smock, as well as thick gloves, all of which can be found at the pilot.

Figure 3-5 CEB2 Vessel

3.6 Common Problems Encountered

There are some common problems that can arise when using the pilot. These problems include the CEB1 or CEB2 vessels becoming too low, the inlet flow becoming too low, the TMP of the system becoming too high, and the pressure of compressor on the back of the membrane portion of the pilot decreasing. To fix the problems regarding the CEB1, CEB2, the inlet flow, along with the TMP, refer to previous sections. To increase the pressure of the compressor, there is a button on the back of the compressor needs to be pushed. This button is located on the side of the black portion of the compressor located behind the blue section. The compressor can be seen in Figure 3-6 below. Once this is button is pushed, the compressor will restart, and the pressure should increase.

Figure 3-6 Air Compressor

4. Shut Down of the Pilot

4.1 Turning off the Pilot System

The shutdown of the pilot occurs through the following steps.

1. First, change the settings of the pilot to start a CEB2 if the pilot system is not going into a CEB1 or CEB2 shortly. This is done by changing the number of times for normal BW and CEB1 to 0.
2. Once the CEB2 has entered step 3, which is the pumping of the 100 ppm Hydrogen Peroxide solution through the system, the ozone generator can be shut off if in use. Once the ozone generator completely stops, shut off the influent feed water into the system by turning the black valve located on the ozonation portion of the pilot completely to the right.
3. Once the black valve is closed, unplug the secondary effluent pump or turn off the tap water valve depending on what feedwater is being used for the designated run.
4. Once the influent flow has stopped, close the red and blue valves on the ozonation portion of the pilot. This step prevents the static mixer from draining.
5. Once CEB2 has entered step 4, shut off the membrane portion of the installation by turning the switch titled voor-behandling to zero.
6. Finally, turn the large black switch on the back of the membrane portion of the installation to completely shut off the system.

4.2 Cleaning the Membrane

To effectively clean the membrane so that the specific flux is around 400 Lmh, it is recommended that you run a 1-1-1 regime twice with ozone running through the system. A 1-1-1 regime signifies 1 normal backwash, then 1 CEB1, followed by another normal backwash, and then a CEB2. During this regime, the filtration time should be set to at least 300 seconds, or 5 minutes, to allow for adequate time for ozone to clean the membrane. An ozone gas concentration of at least 4 mg/l is also recommended. The TMP once this is completed, should be in the range of 0.3 to 0.4 bar.

4.3 Cleaning the Filter

To clean the filter, unscrew the blue cap and open it. The filter can be taken apart, so take out each section of the filter and rinse it will tap water until it appears to be clean. Once the rinsing is finished, reassemble the filter. To ensure that the filter is tight enough to prevent any leakage, extra tools may be required.

4.4 Analyzing the Pilot Data

To obtain the data from the pilot system, go to the RSG30 monitor by Endress+Hauser located on the back of the ceramic membrane portion of the pilot. Next, press on events and go to the compact disk functions. Make sure to update the compact disk first and then eject the compact disk. Once the compact disk has been removed, put the disk into the diskette reader located at the pilot and then plug the reader into your computer. Using the computer program ReadWin 2000, you will be able to save the data and export it into an excel file.

To readout the data, complete the following steps.

1. Open the ReadWin 2000 program on your laptop and have the diskette reader plugged in as well with the compact disk from the pilot monitoring system in it.
2. Click on the header titled read out.
3. Choose the option titled readout measured values using diskette. This action should result in box opening asking you to select a drive, which in this case should be d.
4. Once d is selected press ok and the data should be saved. A window will show up once the data is saved asking if you would like to delete the data off the diskette. You can choose either to delete or not to delete the data. The readout of the data is now completed, and you can proceed to exporting the data into an excel file.

To export the data into an excel file, complete the following steps on the ReadWin 2000 computer program.

1. Click on the header titled extra.
2. Select the option titled export measured values.
3. A window will pop up titled export measured values: select unit. Click on Ecograph T. This will prompt another window.
4. In the export measured values window, go to the portion titled display values and determine the period that you want. In the analogue values portion of the window, average and instantaneous value should be selected. Once these steps are completed, press continue.
5. A window dealing with channel selection will now appear. In the display channels column, you want to have Group 1 (GP1): FIT-01, Group 1 (GP1): PT-01, Group 1 (GP1): PT-02, Group 1 (GP1): PT-03, Group 1 (GP1): QIT-01 t, and Group 1 (GP1):

QIT-01/O3 to be located under this column. Once they are all under display channels, press continue.

6. A window dealing with the setup of the file will then pop up on the screen. Under file type, select text file (*.xls), For data, select replace existing, and with regards to tabular, select text in inverted commas and export status. Lastly for decimal character and format operating time, select decimal point and 0000h00:00, respectively. Once these settings are chosen, press ok.
7. One final window will now pop up, asking for a file name and the location for the file to be saved. Upon completion of this final step, press save, and your data will be exported as an excel file. The file can then be opened and analyzed.

References

CeraMac® – PWNT. Retrieved from https://pwntechnologies.com/portfolio-item/ceramac/

Gabriel, S. Personal Communication, March 2019

Hach Company. (2014). Chlorine, Free [Ebook] (11th ed., pp. 1-6). Loveland: Hach Company.

Heidolph Instruments GMBH & CO KG. (2011). RZR 1 Instruction Manual (pp. 15-21). Heidolph Instruments GMBH & CO KG.

WEDECO AG (2006). WEDECO Small Ozone Systems. Herford: WEDECO, pp.1-4.

Appendix II Detailed Procedures

Conductivity Measurements

The conductivity meter, which was the Hach Company CDC probe, was used to determine residence times for portions of the secondary effluent water reuse pilot. The meter was calibrated by Rob Van Westen prior to its use on April 10th.The steps to calibrate the meter, which can be viewed in the Hach manual for the instrument, were the following:

8. The conductivity probe was securely attached onto the Hach meter. The meter was then turned on.
9. The calibrate button was hit, and a screen popped up on the meter that signified the standard solution necessary to complete calibration. This meter used a 1000 µS/cm standard calibration solution.
10. The operator poured the standard solution into a beaker until there was enough to submerge the bottom of the probe.
11. After placing the probe into the beaker containing the standard solution, the read button was hit, and the word stabilizing appeared on the screen. A progress bar appeared as well to signify how close the probe was to achieving stabilization.
12. Once the meter stabilized, the value associated with the standard solution appeared on the screen. The done button was pushed to see the calibration synopsis, and then the store button was pushed to approve the calibration results. (Hach Company, 2013a)

After calibration, the meter was used to determine residence times for portions of the pilot in Wervershoof. The setup of this procedure at the pilot can be seen in Figure II-1 below.

Figure II-1 Pilot Setup for Conductivity Measurements

This procedure was based upon a procedure written by Daniel Farley, a previous intern at PWNT.

1. Tap water ran through the pilot; however, the pilot was not turned completely to prevent the brine solution from damaging the membrane. The recirculating pump was turned on.
2. While this was occurring, a solution of brine and tap water was created in a 10-liter bucket. This solution had a ratio of one liter of brine for every eight liters of tap water.
3. A pump was put into the bucket, and the hose attached to the pump was connected to the pilot. The pump was turned on following this connection.

4. The influent valve into the pilot was opened to allow the brine solution to go through the system and at the same time, one of the sampling locations was opened. The conductivity meter was turned on as well during this time, and the read button was hit.
5. Using a deep measuring cap with a large measuring vessel below it to catch the brine solution, continuous measurements were taken until the water coming out of the sampling point had a conductivity value close to the conductivity of the solution.
6. When the conductivity value was close to the conductivity of the brine solution, the timer stopped and the time was recorded as the time it took the brine solution to get from the inlet to the sample point, and thus was the residence time
7. Three sampling points were used to determine the residence times for pre-ozonation and coagulation pretreatment. Between the measurements at the different sampling points, the system was flushed with tap water to prevent any cross contamination and provide as accurate results as possible. (Farley, 2017) The sampling points used during this testing can be seen in Figure II-2 below.

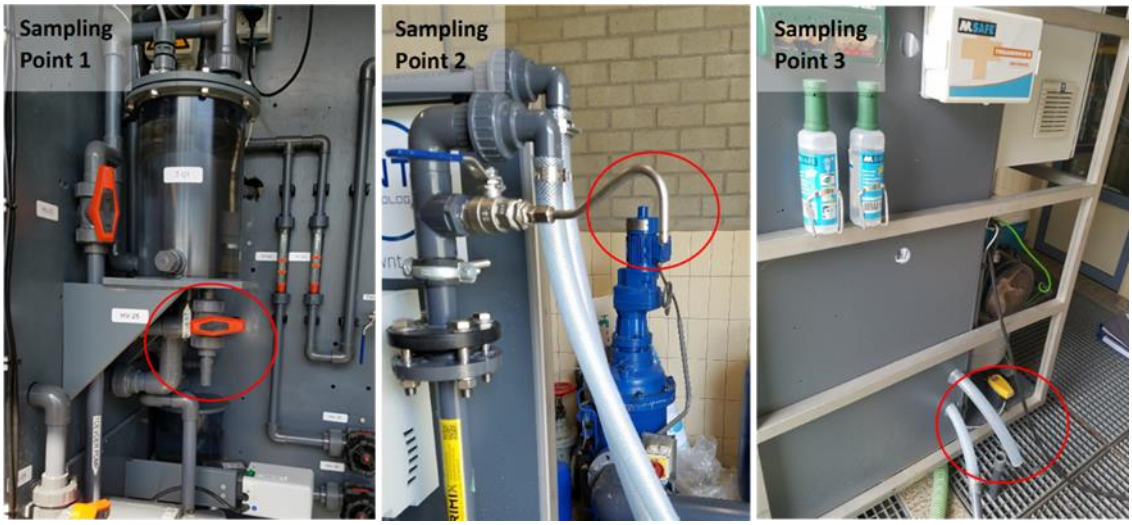

Figure II-2 Sampling Points for Conductivity Measurements

The conductivity tests to determine retention times took place on April 18th, 2019. A bine solution of 1 liter of brine for every 8 liters of tap water was used during this testing. It had an initial conductivity measurement of 47.4 millisiemens per centimeter. The conductivity measurements to determine the retention times were conducted at 60 liters per hour for sample point 1 and 2 and had a slightly higher flow of 75 liters per hour at sample point 3. These flows correspond to fluxes of approximately 150 liters per square meter per hours and 187.5 liters per square meter per hour, respectively.

PH Measurements

PH measurements were conducted using a the Hach 40d meter along with a Hach pH probe. Before use, the pH probe had to be calibrated daily. This calibration was completed through the following steps (Hach Company, 2013b):

1. Attach the pH probe securely to the Hach meter and start up the meter.
2. Once the meter is turned on, hit calibrate. The buffers needed for calibration will appear on the screen, which are standards at a pH of 4, 7, and 10. The meter along with the calibration standards can be viewed in Figure II-3 below.

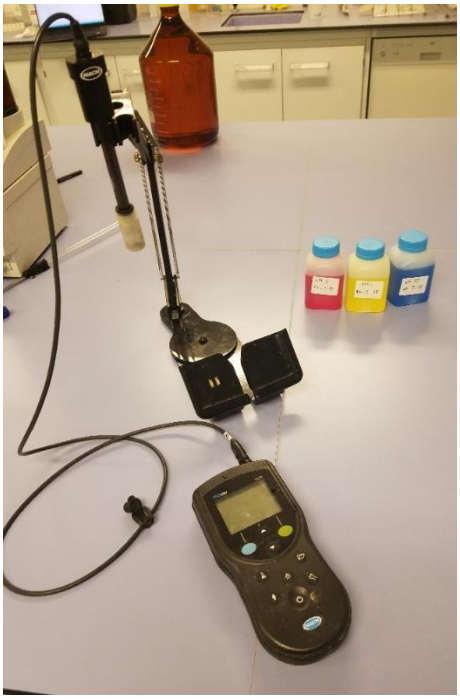

Figure II-3 Hach Meter and PH Probe along with Calibration Standards

3. Before submerging the probe into one of the buffers, it was removed from the probe soaking solution 3M KCl and rinsed with MilliQ water. After rinse, the probe was dried using a cloth that was lint free.
4. The probe was then submerged into the first standard solution of 4 and the read button was hit. The probe was left in the solution until it stabilized.
5. After stabilization, the probe was again rinsed with MilliQ water and dried using the lint free cloth. It was then submerged into the next standard solution of 7. This rinsing, drying, and submerging procedure was repeated for the standard with a pH of 10 as well.
6. Once all the calibration standards were read the done button was pushed. The results of the calibration summery were then displayed. After being looked over the stored button was pushed to approve calibration. Upon approval, the meter screen returned to the measurement one.

After calibration was completed, sample pH measurements were conducted. The procedure for using the pH meter for sample measurements is as follows (Hach Company, 2013b):

1. The probe was rinsed with MilliQ water and dried with a cloth that was lint free to prevent any previous sample or calibration standard from interfering with the results.
2. The probe was then submerged into the sample. The sample was stirred using the probe to make sure the measurement was accurate.
3. The read button was hit, and the probe was left submerged in the sample until stabilization was reached. The stabilized result was recorded
4. The probe was rinsed with MilliQ water and dried with a cloth that was lint free and then another sample could be measured.
5. Once all the desired measurements were taken, the probe was rinsed again with MilliQ water and dried. The probe was then put back into the soaking solution of 3M KCl.

UVT Measurements

UVT or UV transmittance measurements, where taken using the DR 6000 spectrophotometer. These measurements were taken as single wavelength scans at 254 nanometers. The procedure for taking these UVT measurements is the following (Hach Company, 2018):

1. The DR 6000 was turned on by pressing the switch at the back of the instrument.
2. Once the machine is turned on and finishes the system calibration, the main menu appeared on the screen. On the main menu screen, the single wavelength tab was pressed. The screen for a single wavelength scan then appeared.
3. In the upper right-hand corner, the measured wavelength setting could be viewed. The wavelength was set to 254 nanometers. This change could be completed by hitting the

wavelength scan, which would cause wavelength setting screen to appear. 254 nanometers was entered and then the next button was hit to input this change.

4. A 1 cm cuvette was rinsed with MilliQ water and then filled with MilliQ water. MilliQ water was used to zero the machine. Once the cuvette was filled, the clear sides were cleaned with a lint free cloth.
5. The blank was then inserted into the DR 6000 and the zero button was pressed. Once the blank was fully processed, 0 Abs appeared on the screen.
6. The MilliQ water was dumped out of the cuvette and into the sink. The cuvette was then rinsed and filled with sample water. A filter was attached to the syringe when filling the cuvette to get rid of any of the particulates in the sample. Once filled, a lint free cloth was used to wipe down the clear sides.
7. The cuvette filled with the sample was inputted into the DR6000 and the read button was pushed. Once the machine finished reading it the absorbance could be seen on the screen as a value with Abs next to it. To view the transmittance percentage, the option button in the bottom right hand corner was pressed and then %Trans was selected.
8. After the all the desired sample measurements were taken, the back to main menu button was hit and the machine was shut down by pressing the button at the back of the machine. The cuvette was then rinsed out with MilliQ water and dried.

The UVT transmittance measurements could also be conducted with a 5cm cuvette. However, the absorbance and UVT transmittance would have to be adjusted from the one that appears on the screen to take the size change of the cuvette into account.

Temperature Measurements

Temperature measurements were taken using Hanna Checktemp 1, which is viewable in Figure II-4 Hanna Checktemp 1 below. The temperature measurements were taken as followed.

1. The temperature meter was turned on by pressing the blue button at the back of the meter.
2. The silver temperature measuring device was submerged into the sample. It was left in the sample until the temperature appeared to no longer be changing.
3. Once the temperature measuring device was done being used, it is was cleaned with MilliQ water and dried off using a lint free cloth.

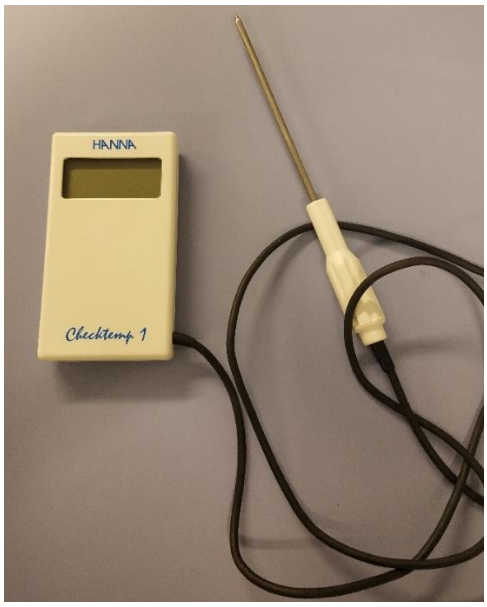

Figure II-4 Hanna Checktemp 1

Jar Testing

Jar testing was conducted to determine the optimal coagulant dosage of for alternative 1, which uses coagulation pretreatment, and alternative 3, with uses coagulation and ozonation pretreatment. The following procedure was conducted to preform jar testing and was loosely based upon the Satterfield et al. procedure outline in Tech Brief Jar Testing (Satterfield, 2005).

8. A 1 percent, or 10,000 mg/l, ferric chloride solution was created from a 40 percent stock ferric chloride solution. This solution was created using the equation $c_1v_1=c_2v_2$ in which c refers to concentration and v refers to volume and the 1 and 2 signify the starting concentration and volume along with the final concentration and volume, respectively. The 1 percent solution used MilliQ water as well as the 40 percent ferric chloride stock solution. Therefore, to create the 1% solution 17.5 ml of 40 percent ferric chloride solution was pipetted into 1000 ml of MilliQ water. The pH of this solution was 1.94. These calculations were based upon a presentation from the Michigan Department of Environmental Quality Operator Training and Certification Unit (Michigan Department of Environmental Quality Operator Training and Certification Unit, n.d.).
9. A jar testing apparatus depicted in Figure II-5 Jar Testing Apparatus was utilized. Each one of the jar apparatus vessels was rinsed with a secondary effluent sample and then filled 1.5 liters with the sample.

Figure II-5 Jar Testing Apparatus

10. The appropriate amount of 1% ferric chloride solution was pipetted into each of the jar tests for the corresponding dosage. The equation c_1v_1 was utilized to determine the

appropriate volume. The volume of solution for each of the coagulation dosage can be depicted in the Table II-1 Required Volume of 1% Ferric Chloride Solution below.

Table II-1 Required Volume of 1% Ferric Chloride Solution

Ferric Chloride Dosage (mg/L)	Required Volume of 1% Ferric Chloride Solution (ml)
1	0.15
2	0.3
3	0.45
5	0.75
6	0.9
10	1.5
15	2.25
20	3
25	3.75
30	4.5

11. The apparatus was then turned on by pressing the switch on the right side of the apparatus. The stirrers were then lowered into the vessels by pressing the blue button on the right side of the apparatus. After the stirrers were lowered into the vessels, the mixing speeds were inputted. The mixing speed for the specific trial, which can be seen in Table II-2 Jar Testing Parameters for Each Trial.

Table II-2 Jar Testing Parameters for Each Trial

Trial	Parameter	Units	Coagulant Dosage (mg/L)												
			1	2	3	5	6	10	15	20	25	30	40	50	60
1	Coagulant Type	-	Ferric Chloride	Ferric Chloride	Ferric Chloride	Ferric Chloride	Ferric Chloride	Ferric Chloride	Ferric Chloride	Ferric Chloride	Ferric Chloride	Ferric Chloride	Ferric Chloride	Ferric Chloride	Ferric Chloride
	Mixing Speed Tank 1	rpm	230	230	230	230	230	230	230	230	230	230	230	230	230
	Mixing Speed Tank 2	rpm	58	58	58	58	58	58	58	58	58	58	58	58	58
2	Coagulant Type	-	Ferric Chloride	Ferric Chloride	Ferric Chloride	Ferric Chloride	Ferric Chloride	Ferric Chloride	Ferric Chloride	Ferric Chloride	Ferric Chloride	Ferric Chloride	Ferric Chloride	Ferric Chloride	Ferric Chloride
	Mixing Speed Tank 1	rpm	100	100	100	100	100	100	100	100	100	100	100	100	100
	Mixing Speed Tank 2	rpm	35	35	35	35	35	35	35	35	35	35	35	35	35
3	Coagulant Type	-	Ferric Chloride	Ferric Chloride	Ferric Chloride	Ferric Chloride	Ferric Chloride	Ferric Chloride	Ferric Chloride	Ferric Chloride	Ferric Chloride	Ferric Chloride	Ferric Chloride	Ferric Chloride	Ferric Chloride
	Mixing Speed Tank 1	rpm	250	250	250	250	250	250	250	250	250	250	250	250	250
	Mixing Speed Tank 2	rpm	40	40	40	40	40	40	40	40	40	40	40	40	40

12. The mixing speed was adjusted on the apparatus by going to the main menu and pressing on 3, which corresponds to program. The number 12 was then entered as this was the program that was manipulated. The screen then changed to a table that had a column from segments, minutes, seconds, and rpm. Segment 1 was used for rapid mixing and

segment 2 corresponded to slow mixing. The run time for each of these segments was 2 minutes and 29 seconds. The rpm was then inputted for the trial being run. Once this was completed, the end button was pressed and then 1 was pressed to save the results and return to the main menu.

13. To start the run, 1 which corresponds to synchro run was pressed. The number 12 was then inputted, which was the program that was run. The button corresponding to enter was then pressed and then start. The trial then ran for the designated period and settings.
14. Once the run stopped, the stirrers were taken out of the system by pressing the red button on the right side of the jar testing apparatus.
15. The jars were then left till the particles settled. %UVT, pH, and temperature measurements were taken.
16. Once all the measurements were completed, the jar testing vessels were rinsed out with tap water. If another run was occurring, steps 2 through 8 were then repeated. If it was the final run, the jar test vessels were dried, and the apparatus was shut off again by pressing the on and off button on the right side of the apparatus.
17. %UVT, pH, and temperature measurements were also taken for the 24 secondary effluent sample for comparison purposes as well. No coagulant was added when these measurements were taken.

Ozone Demand at Pilot in Haarlem

Startup of Pilot

The procedure for the startup of the pilot is outlined below and is based upon the procedure written up by Bram Delfos.

1. The reactor along with the tubing was cleaned. The cleaning of the tubing occurred by disconnecting the tubing from the reactor and putting it is a glass beaker, which was filled with demineralized water. The valves were opened, and the pump was turned on with the speed set to five. The demineralized water was run through the tubing in both the forward and reverse direction for a couple of minutes. It was run in both directions a total of two times. Any air bubble present in the tubing were removed.
2. The reactor was cleaned by rinsing it was demineralized water in the sink and closing all the sampling ports prior to rinsing.
3. After both the reactor and tubing were cleaned, the reactor was reconnected to the tubing and valves 7, 8, and 9 were closed. Six liters of secondary effluent was poured into the reactor by opening the top of the reactor. Red tape present on the reactor indicated the six liter mark on the vessel.
4. The ozone generator was then turned on by flipping the main switch on and any malfunction alarms were turned off by hitting the release button.
5. Valve 1 was closed and the valves for the oxygen cylinder as well as the regulator were opened. The manometer on the oxygen cylinder was verified to have a pressure reading of 0.5 bar.
6. With the manometer reading 0.5 bar and valve 2 closed, the ozone generator was started. It was run for an hour prior to the use of the apparatus for experimentation purposes. This step was done to attain stable ozone generation.
7. During the warming up of the system, the settings for both the ozone gas meters as well as the dissolved ozone meter were adjusted to be identical with regards to date and time. The settings for the ozone gas concentration meters were adjusted on the computer. The

settings for the dissolved ozone meter were adjusted on the meter screen, which had to be unlocked using codes.

8. Once the settings of both meters were set, the ozone gas meters, and the dissolved ozone meter were linked to the laptop.
9. The recirculation of the secondary effluent was then started once valve 8 was opened and 3 was closed. It was started using the liquid pump and was put in the forward direction with the setting of 1185.
10. Upon the startup of the recirculation, the ozone gas meters were reset to zero by hitting the zero button. During this time, valves 4 and 2 were opened and 3 and 5 were closed. The ozone generator was run until the ozone levels on the gas meters appeared stable.
11. When the system was running, it was inspected for any leakages. This inspection was conducted using potassium iodide starch paper that was wetted prior to use. The experimentation run could only be continued when no leakages existed. (Delfos, n.d)

Determining Ozone Demand

The ozone demand for the secondary effluent was measured to determine the optimal ozone dosage for alternative 2 as well as alternative 3. The procedure for determining the ozone dosage by using the pilot system at Het Waterlaboratorium in Haarlem is as follows.

5. With the startup of the pilot apparatus completed, the recording of data from both the ozone gas meters as well as the dissolved ozone meters was started. For the ozone gas meters, this startup was done on the computer using the same program that was turned on to manipulate the settings of the meters. To start recording the data, options was clicked on and then the log button was clicked followed by the clicking of start. For the

dissolved ozone meter, the startup was also done on the computer by double clicking the program associated with this meter.

6. Once the data started logging, valve five was opened followed by the opening of valve 3 and the closing of valve 4. The time that this step occurred was recorded and considered to be the official starting point.
7. The system was run until the outlet ozone concentration on the gas meter appeared to be stable. Based on the results, this could take up to an hour to stabilize. Once this duration was completed, valve 3 was opened and valve 4 was closed. The time was recorded to signify the end of the experiment.
8. After the experiment was completed, the recording of data for the ozone gas meters along with the dissolved ozone meter stopped and the data was saved on the computer under the experiment map folder. (Delfos, n.d.)
9. For each test completed, three ozone uptake graphs were created. The first was the ozone uptake with units of milligrams per minutes versus the time in minutes and the other one was the ozone uptake in terms of milligrams per liter versus the cumulative ozone in terms of liters. A graph of the inlet ozone gas concentration and the outlet ozone gas concentration versus the time in minutes was also created.
10. To estimate the ozone demand, the area under the ozone uptake graph was determined and then divided by the total cumulative ozone in liters. This calculation resulted in the ozone demand with units of milligrams per liter. To estimate the area under the graph, grids were inserted behind the ozone uptake graph. Then shapes were created to determine areas of small sections, and then added together to determine the entire area.

Shutdown of Pilot

Once the experiments were conducted, the subsequent procedure was undertaken to shut the system down.

1. The ozone generator was shut off following the closing of valve 3.
2. The bypass of the system was then rinsed with oxygen by turning the generator off and opening valves 1, 2, 4, and 5. Following this cleaning, the reactor was flushed by opening valve 3 after valve 4 was closed. Once this flushing was completed, valve 3 was closed followed by valves 2 and then 1.
3. Before continuing the shutdown process, the ozone gas meters as well as the dissolved ozone meter were checked to determine if the ozone levels had adequately diminished. Once this decrease was verified, the regulator valve as well as the main valve of the oxygen tank were closed.
4. The reactor was then drained by reversing the flow of the pump along with closing valve 8 and opening valve 9. Once the reactor was fully drained, the pump was turned off and valve 9 was closed.
5. The tubing was disconnected and then cleaned with demineralized water by running the pump in both the forward and reverse in the same manner that was conducted during the startup of the pilot. During this time, the reactor was also cleaned with demineralized water.
6. Once the cleaning was completed, the tubing was left with demineralized water in it while the reactor was left empty. (Delfos, n.d.)

Appendix III Spreadsheet Template for Twenty-Four Hour Constant Flux Tests

Blue･･･Collected Data (Please copy and paste the data from mailed excel sheet)																		
Red･･･Calculated Data																		
Membrane Surface Area	0.4	m^2/Membrane			Run	RUN08 critical flux	11/20/2018		temperature measured manually									
	0.4	m^2/Module			flux	variabel												
Membrane Number	1	Membrane			BW Regime	4-1-1												
Bias (Height Difference)	8.829	kPa			filtration time	variabel												
Datum/Tijd	Status	FIT-01	PT-01	PT-02	PT-03	QIT-01 t	QIT-01/O3	Time	Time	TMP	corrected TMP (10 C)	corrected TMP (20 C)	Flux	specific flux (10C, 100kPa)	specific flux (20 C, 100 kPa)	Volume treated per membrane surface area	Viscosity	Backwash
		Mittelwert	Mittelwert	Mittelwert	Mittelwert	Momentanwert	Mittelwert											
		l/h	bar	bar	bar	°C	mg/l	min	hour	kPa	kPa	kPa	L/h/m2	(L/m^2/hr)	(L/m^2/hr)	L/m2	PaS	

Appendix IV Water Quality

Water Quality

The following water quality parameters were tested for each alternative: %UVT254, ammonium, bromate, bromide, chloride, nitrate, nitrite, NOM, pH, sulfate, total dissolved solids, and turbidity. The water quality results for the alternatives can be viewed in tables III-1, III-2, III-3.

Table IV-1 Water Quality Results for Alternative 0

Parameter	Unit	Secondary Effluent Tank	Before the Ceramic Membrane	After the Ceramic Membrane
Sampling Time	-	11:09	10:43	10:21
Temperature	°C	20.0	20.0	20.0
Turbidity	FTE	2.1	0.80	0.12
Acidity	pH	7.4	7.56	7.55
Acidity, calculated based on the current temperature	pH	7.51	7.45	7.44
Temperature pH meter	°C	11.2	12.0	11.8
Ammonium	mg/l N	0.99	1.1	1.1
Ammonium	mg/l NH4	1.3	1.4	1.4
Chloride	mg/l Cl	201	199.00	201.00
Nitrate	mg/l N	0.31	0.27	<0.20
Nitrate	mg/l NO3	1.36	1.2	<0.89
Nitrite	mg/l N	0.04	0.061	0.060
Nitrite	mg/l NO2	0.132	0.199	0.196
Sulfate	mg/l SO4	88	88	90
Bromide	µg/l Br	360	360	360
Bromate	µg/l BrO3	<0.5	<0.5	<0.5
TOC	µg/l C	10716	9387	8802
DOC	µg/l C	10535	9411	8851
POC	µg/l C	181	-25	-49
HOC	µg/l C	767	525	299
CDOC	µg/l C	9768	8886	8553
Biopolymers	µg/l C	828	894	481
Humic Substances	µg/l C	4608	4240	4240
Building Blocks	µg/l C	2132	2053	2071
Neutrals	µg/l C	2199	1699	1760
Acids	µg/l C	0	0	0
NOM	rap. code	2019-080	2019-080	2019-080
UV-extinction, 254 nm	ext/m	28.7	29.2	28.5
UVT	%	51.6	51.0	51.8

Table IV-2 Water Quality Results for Alternative 1 at a Dosage of 12 mg/l as Fe^{3+}

Parameter	Unit	Secondary Effluent Tank	Before Ceramic Membrane	After Ceramic Membrane
Sampling Time	-	8:15	8:15	8:15
Turbidity	FTE	0.53	5.5	<0.03
Acidity	pH	7.49	7.22	7.16
Temperature pH meter	°C	10.2	10.6	10.50
Ammonium	mg/l N	0.86	0.81	0.82
Ammonium	mg/l NH4	1.1	1.0	1.1
Chloride	mg/l Cl	128	143	146
Nitrate	mg/l N	1.98	2.21	2.20
Nitrate	mg/l NO3	8.77	9.77	9.76
Nitrite	mg/l N	0.094	0.092	0.094
Nitrite	mg/l NO2	0.307	0.303	0.307
Sulfate	mg/l SO4	73	72	73
Iron	mg/l Fe	NA	12.2	0.064
Iron	µg/l Fe	NA	12200	64
Bromide	µg/l Br	280	NA	NA
Bromate	µg/l BrO3	NA	<5	NA
TOC	µg/l C	8700	6870	6480
DOC	µg/l C	8650	6790	6420
POC	µg/l C	56	81	58
HOC	µg/l C	571	360	557
CDOC	µg/l C	8080	6430	5860
Biopolymers	µg/l C	466	463	184
Humic Substances	µg/l C	4800	3530	3250
Building Blocks	µg/l C	1480	1230	1270
Neutrals	µg/l C	1320	1200	1160
Acids	µg/l C	<200	<200	<200
NOM	rap. code	2019-184	2019-184	2019-184
UV-absorbance, 254 nm	ext/m	25.3	21.9	17.5
UV Transmission	%	55.9	60.4	66.9

Table IV-3 Water Quality Results for Alternative 2

Parameter	Unit	Secondary Effluent Tank	Static mixer	Buffer Tank	Before the ceramic membrane	After the ceramic membrane
Sampling Time	-	10.23	10.47	10.57	11.08	11.18
Temperature	°C	23.3	23.3	23.1	23.1	23.1
Turbidity	FTE	0.73	0.25	0.23	0.47	0.04
Acidity	pH	7.51	7.52	7.42	7.44	7.43
Acidity, calculated based on the current temperature	pH	7.36	7.37	7.28	7.30	7.29
Temperature, pH meter	°C	11.6	11.8	11.4	11.5	11.4
Ammonium	mg/l N	1.3	1.2	1.2	1.2	1.2
Ammonium	mg/l NH4	1.7	1.6	1.6	1.6	1.6
Chloride	mg/l Cl	198	198	198	207	200
Dry matter	%	<1.0	<1.0	<1.0	<1.0	<1.0
Nitrate	mg/l N	0.39	0.61	0.64	0.62	0.63
Nitrate	mg/l NO3	1.74	2.69	2.82	2.74	2.78
Nitrite	mg/l N	0.184	0.005	0.005	0.004	0.004
Nitrite	mg/l NO2	0.606	0.017	0.015	0.014	0.014
Sulfate	mg/l SO4	97	100	99	98	101
Bromide	µg/l Br	350	300	300	310	310
Bromate	µg/l BrO3	<1	79	67	84	81
TOC	µg/l C	10100	9410	9450	9330	9150
DOC	µg/l C	9940	9410	9430	9340	9130
POC	µg/l C	208	1	14	-8	23
HOC	µg/l C	379	-8	45	-182	-44
CDOC	µg/l C	9560	9420	9390	9520	9170
Biopolymers	µg/l C	718	544	556	572	359
Humic Substances	µg/l C	4960	4110	4180	4140	4100
Building Blocks	µg/l C	2030	2900	2790	2840	2810
Neutrals	µg/l C	1850	1470	1490	1580	1520
Acids	µg/l C	<200	396	375	389	384
NOM	Rap. Code	2019-119	2019-119	2019-119	2019-119	2019-119
UV,extinction, 254 nm	ext/m	28.0	11.3	11.3	11.6	11.3
UV Transmission	%	52.5	77.1	77.1	76.5	77.0

Appendix V Twenty-Four-Hour Constant Flux Test Results

Alternative 0 – No Pretreatment

120 Lmh

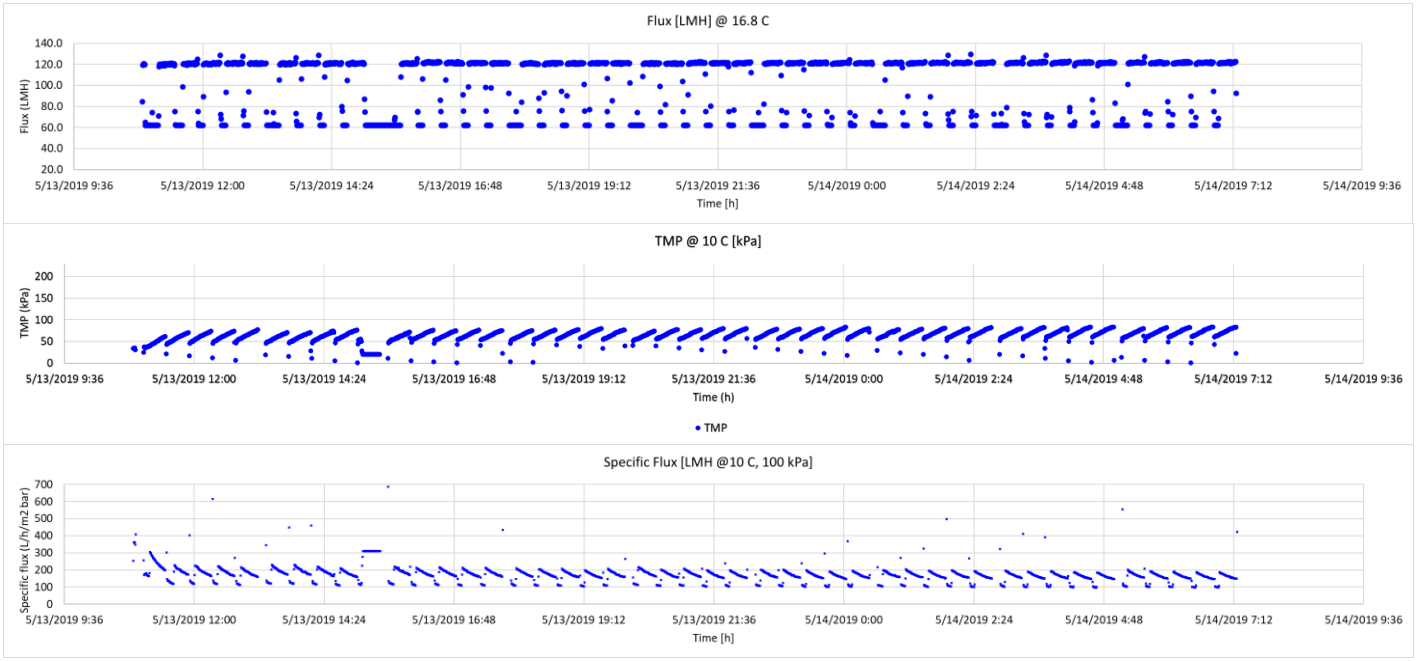

145 Lmh

Alternative 1 – Coagulation Pretreatment with a Dosage of 6 mg/l as Fe^{3+}

145 Lmh

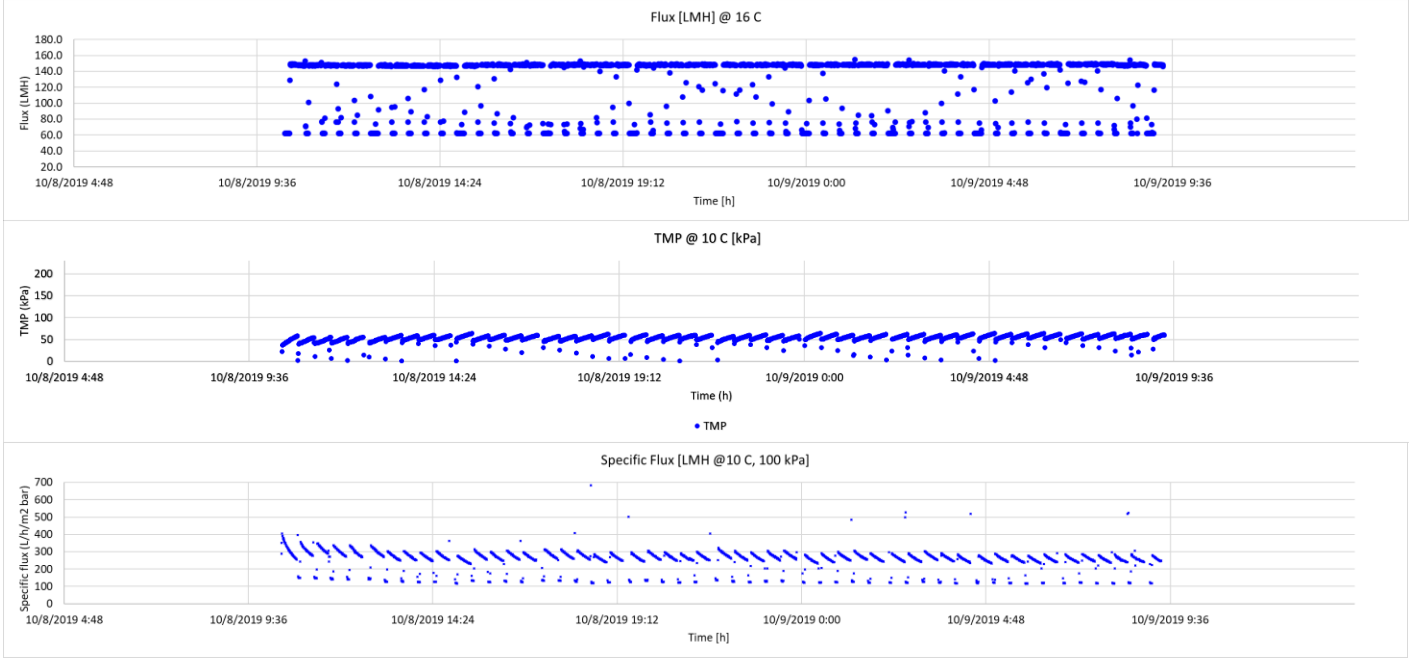

170 Lmh

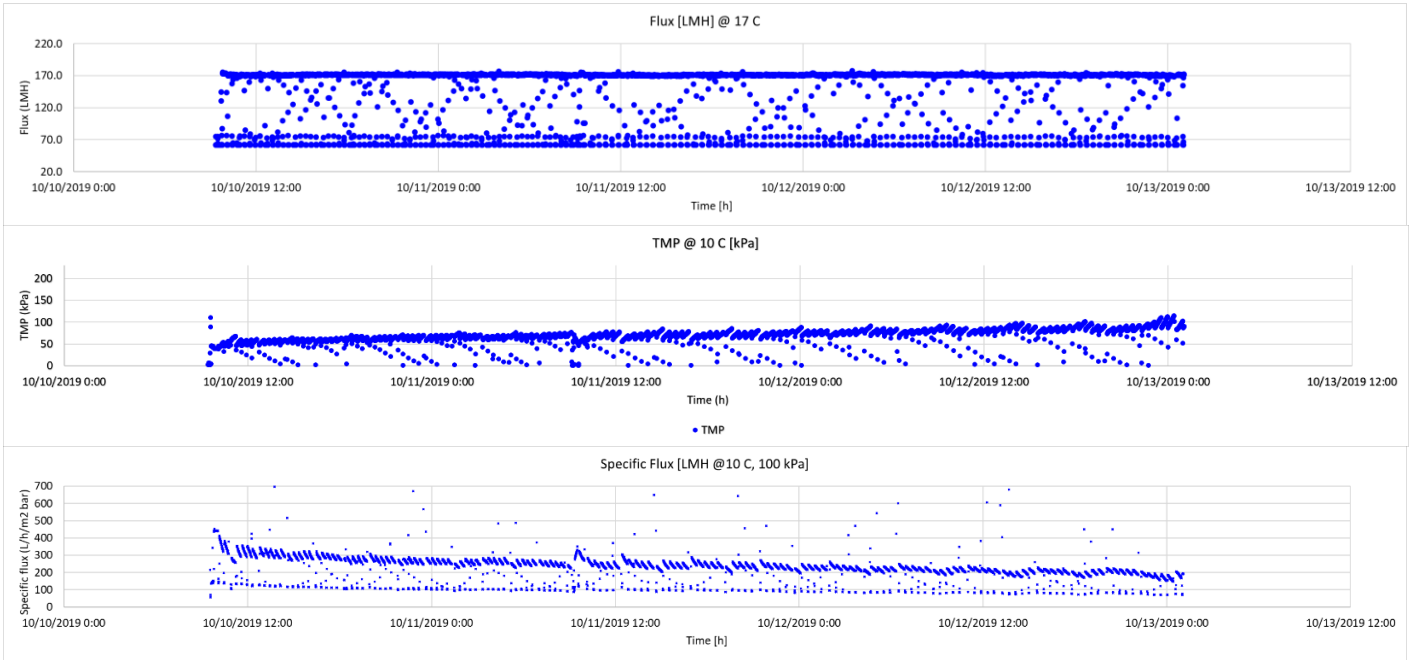

195 Lmh

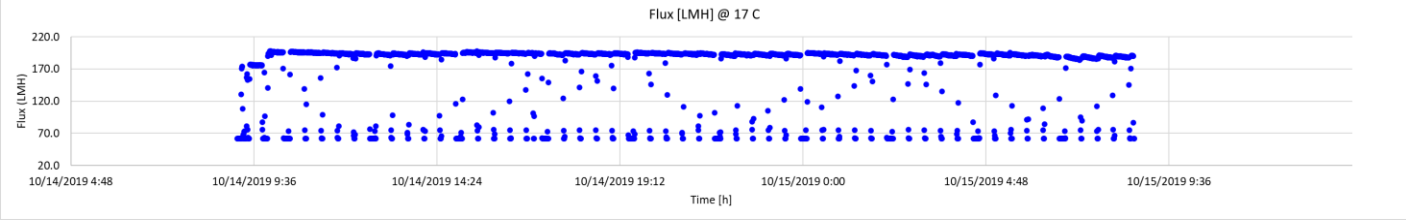

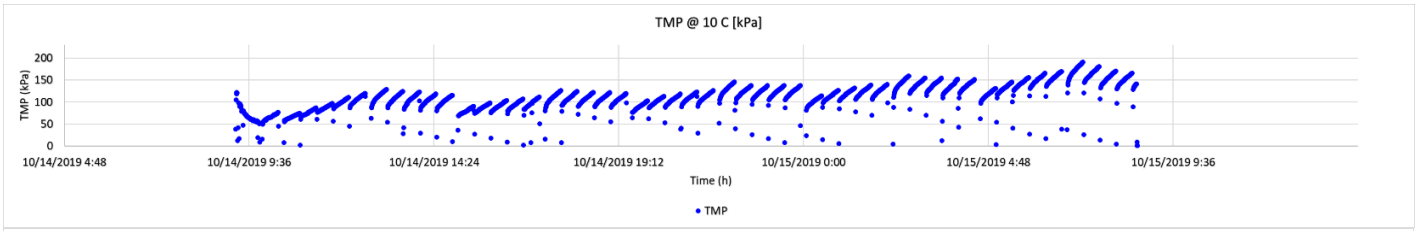

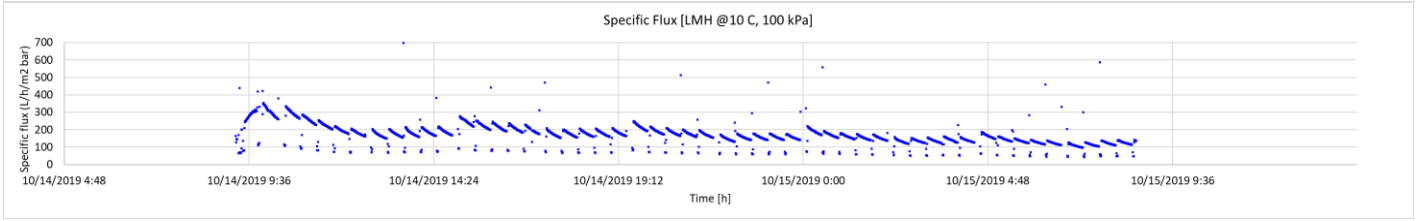

220 Lmh

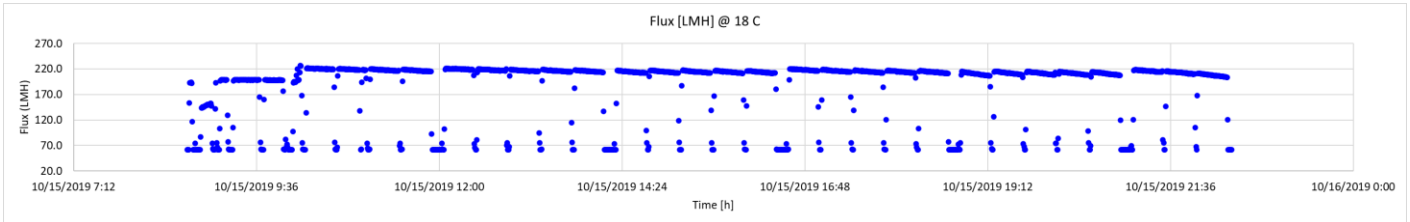

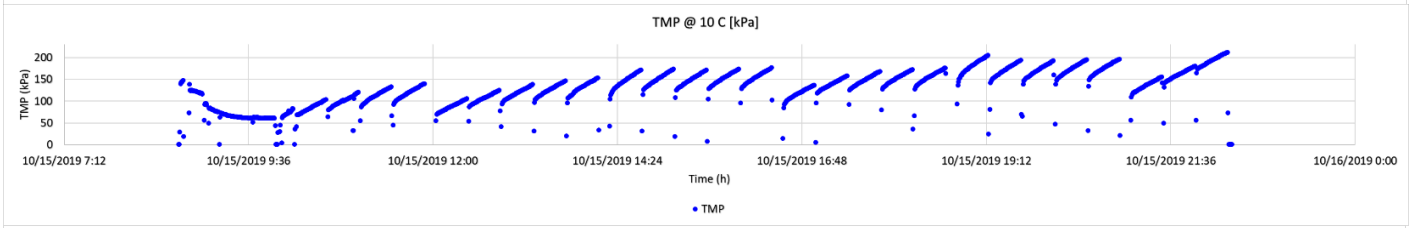

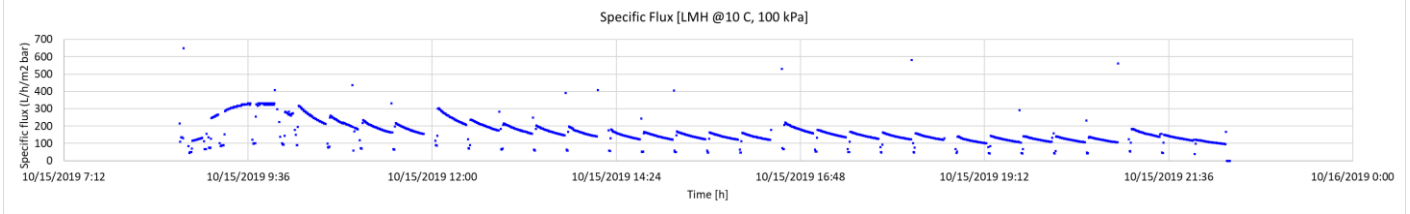

245 Lmh

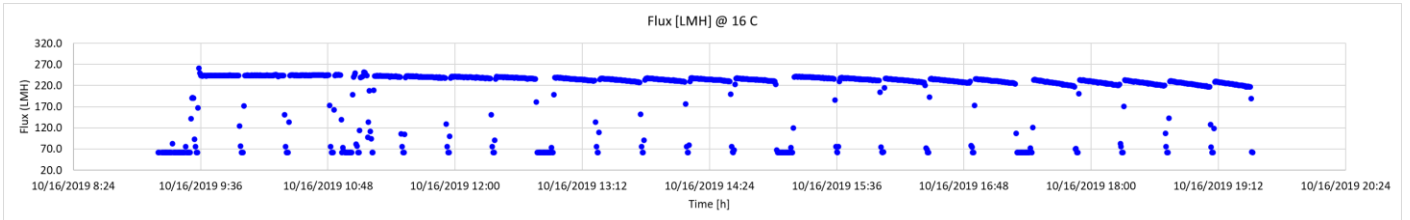

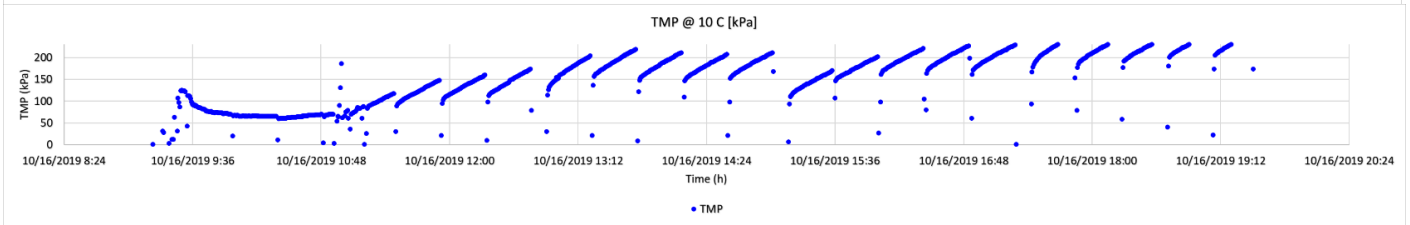

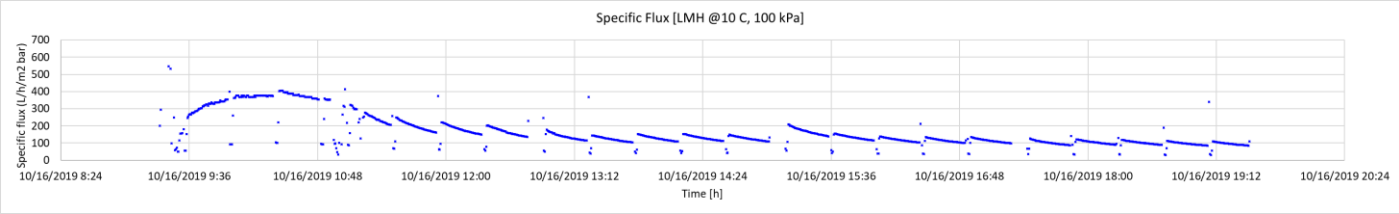

Alternative 1 – Coagulation Pretreatment with a Dosage of 20 mg/l as Fe^{3+}

145 Lmh

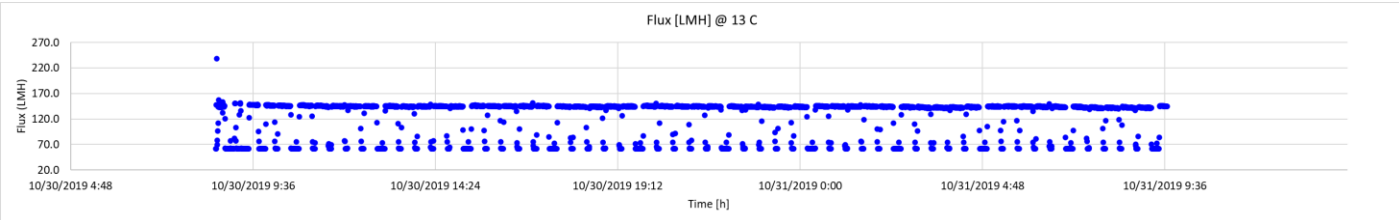

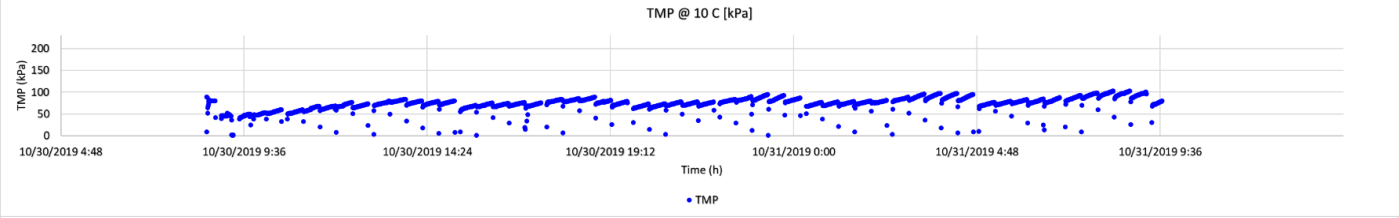

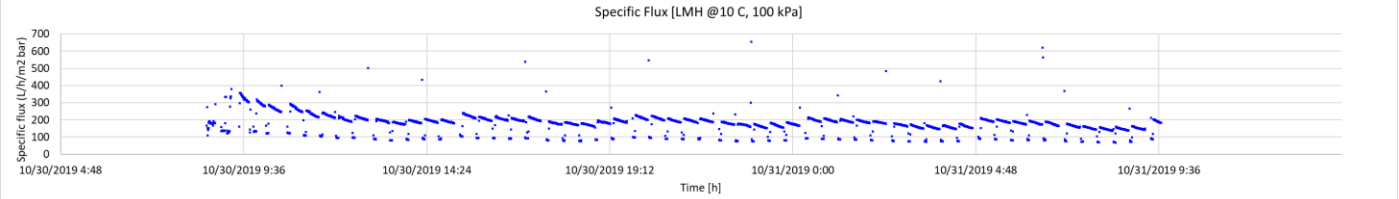

170 Lmh

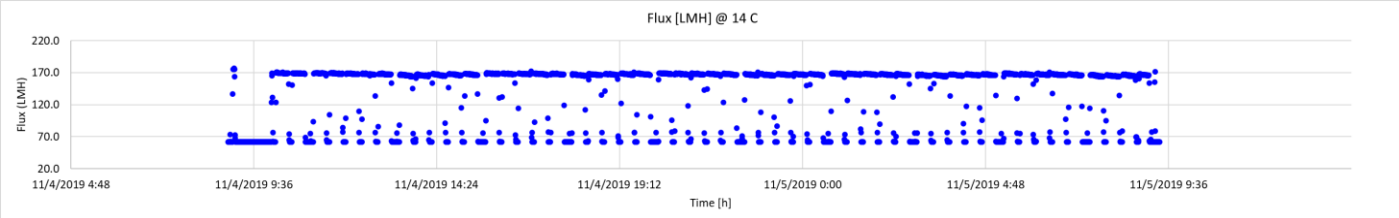

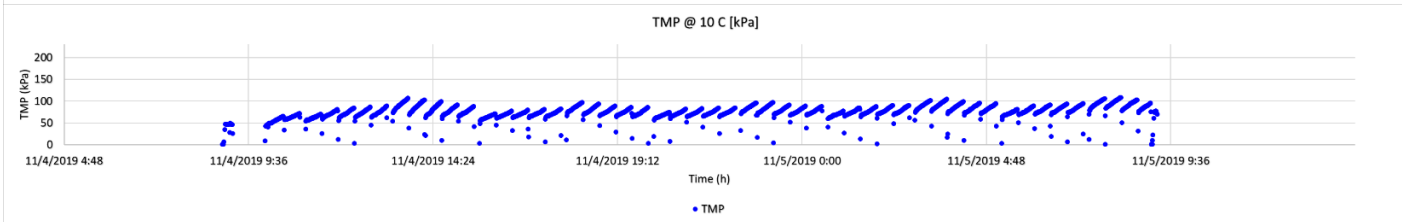

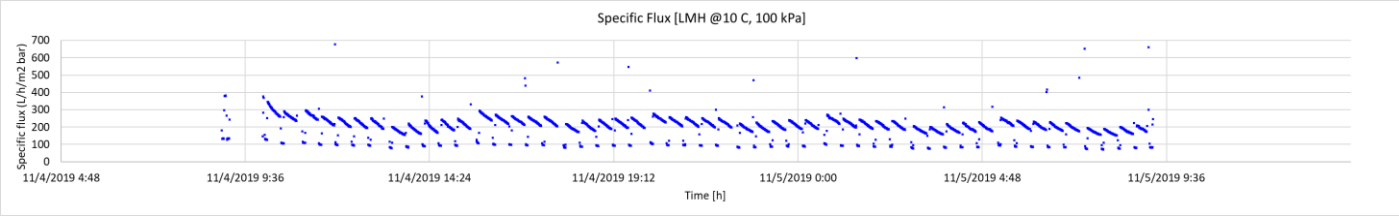

195 Lmh

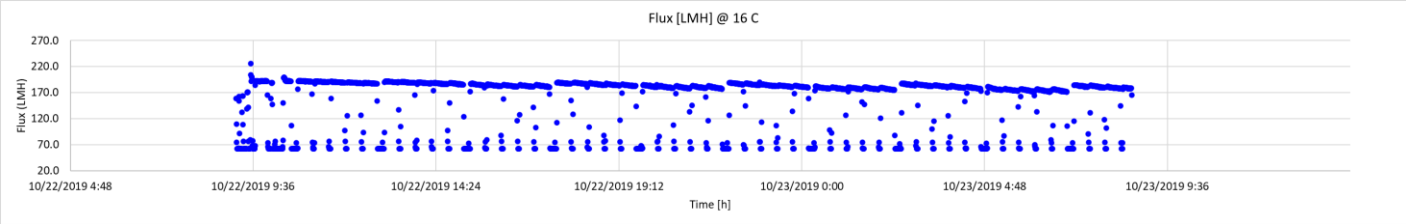

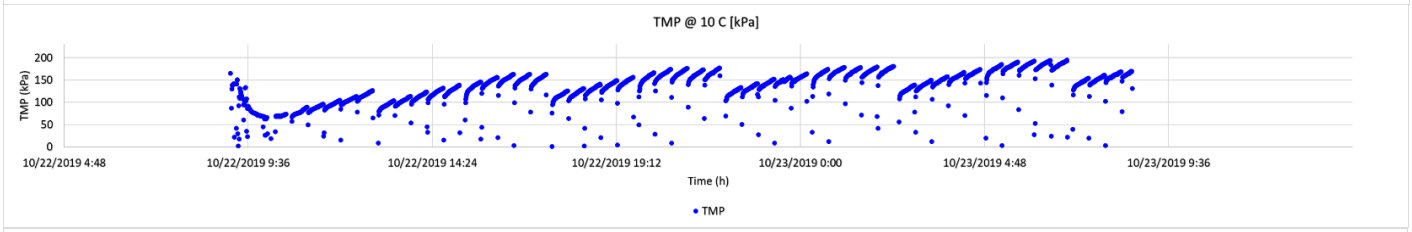

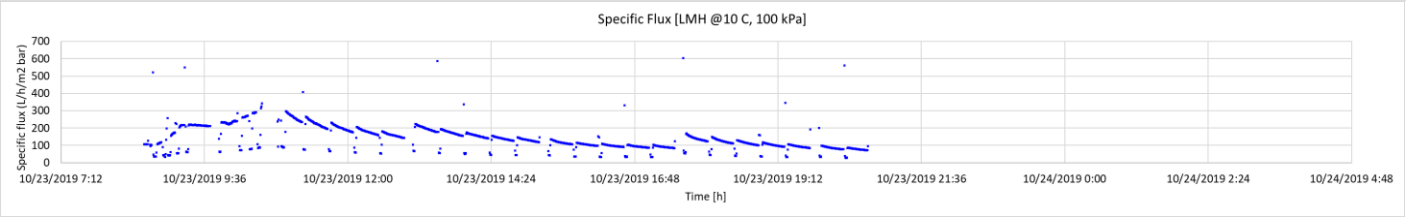

220 Lmh

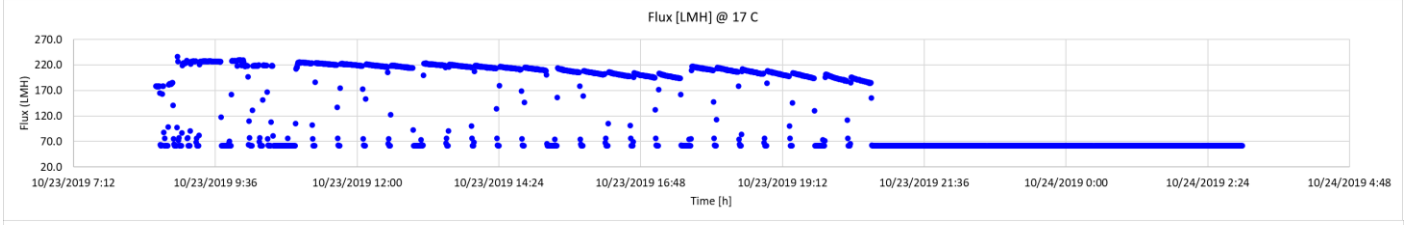

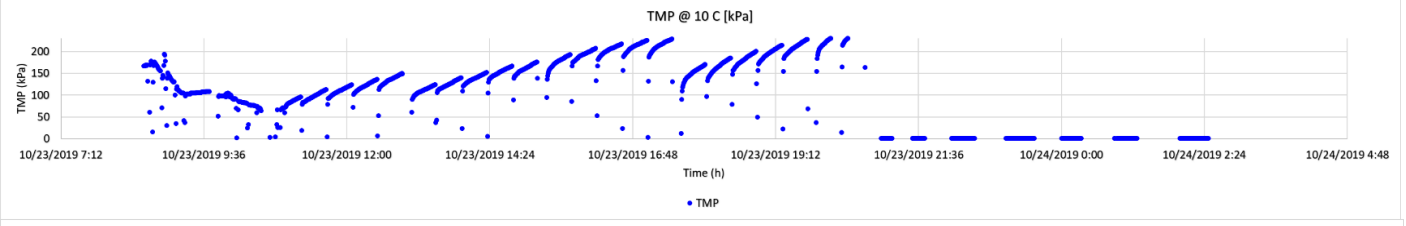

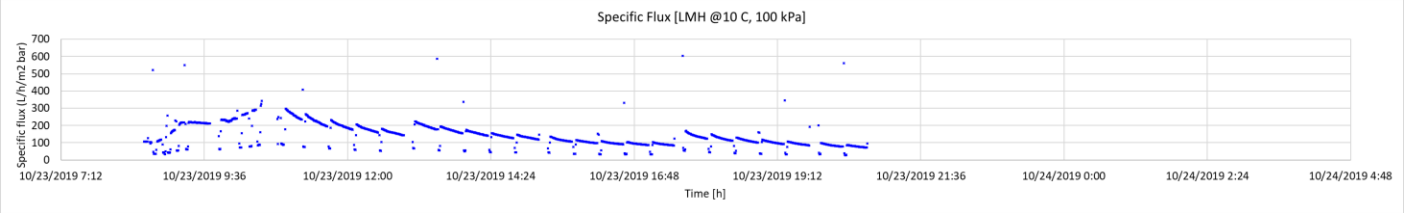

245 Lmh

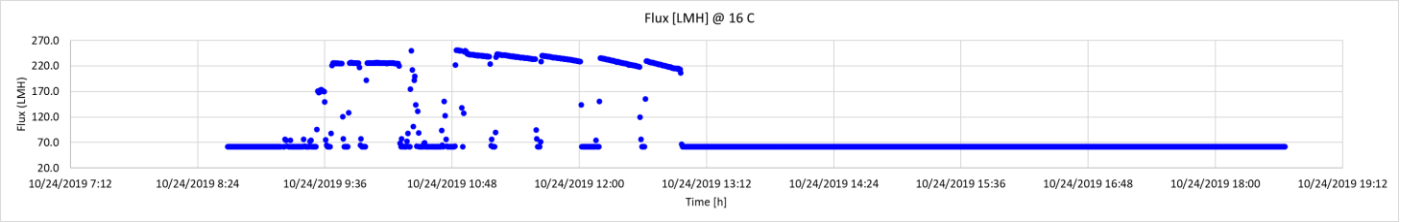

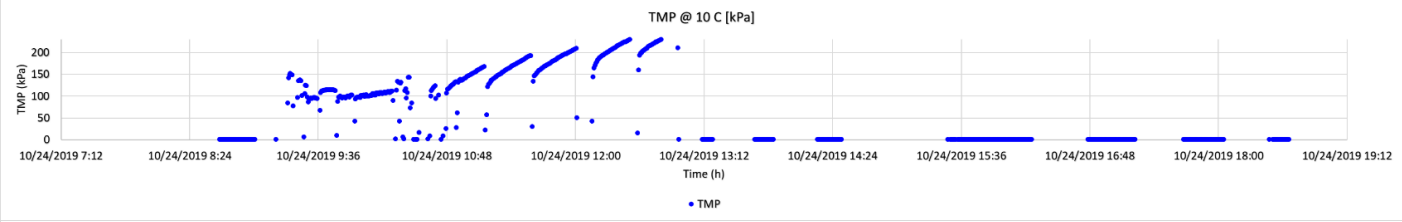

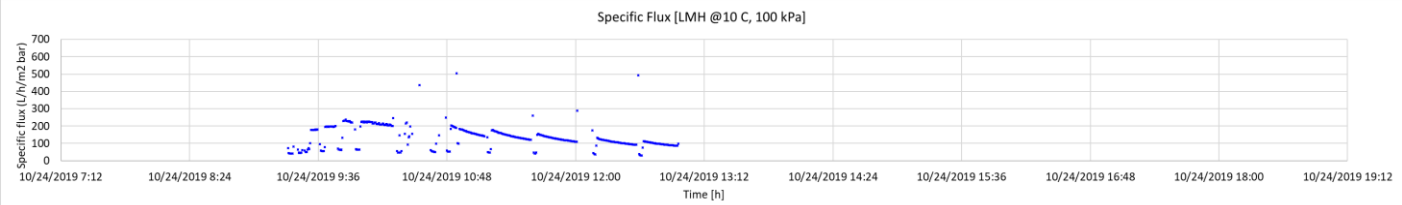

Alternative 2 – Ozonation Pretreatment

120 Lmh

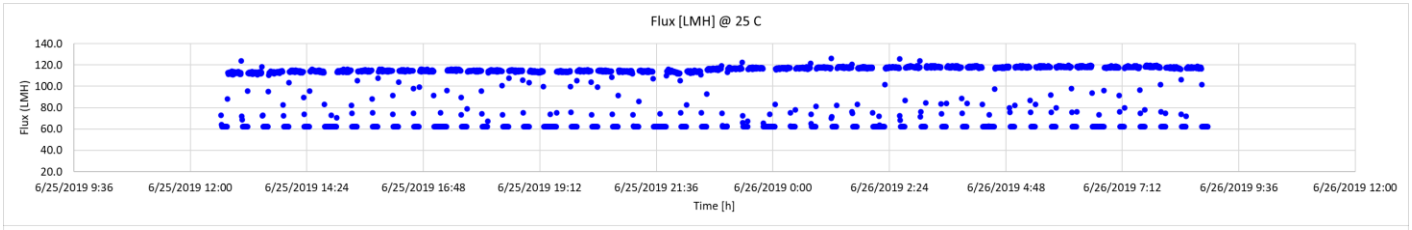

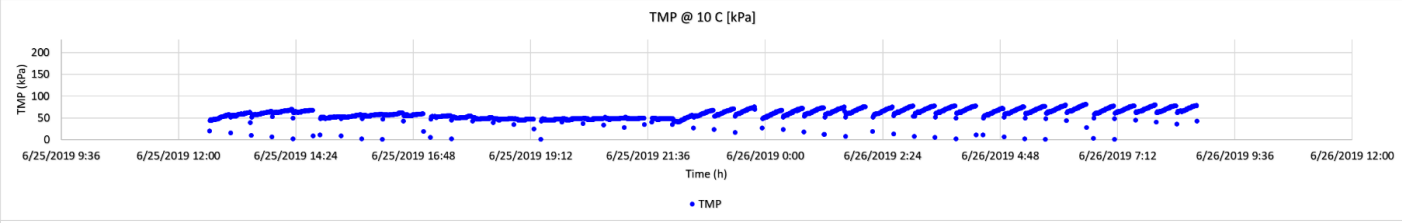

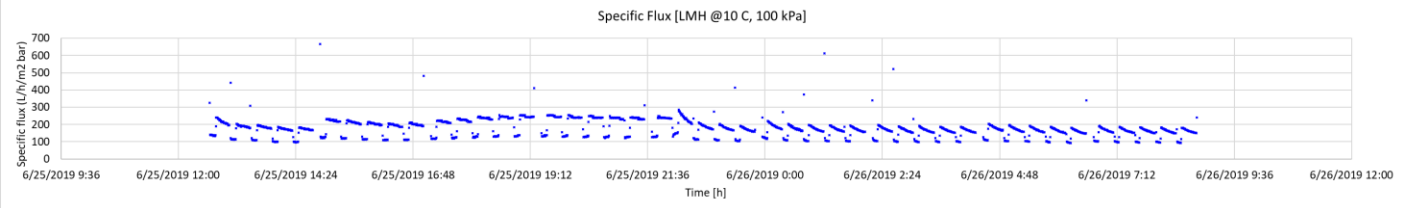

145 Lmh

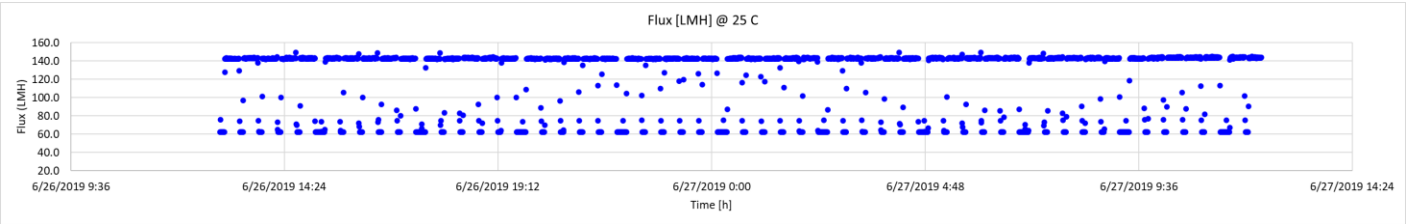

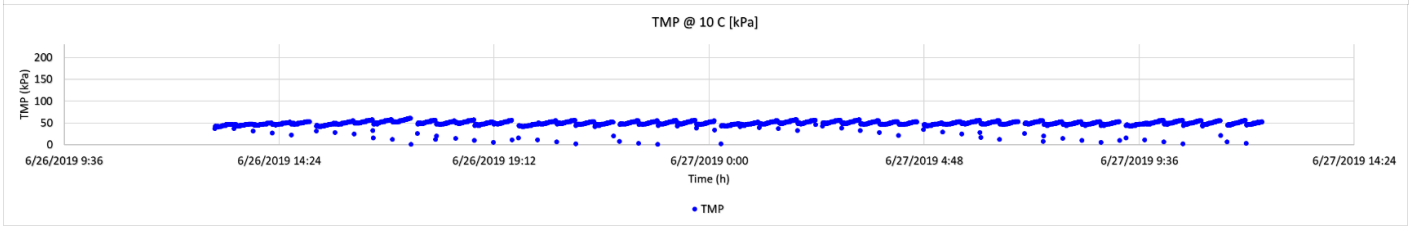

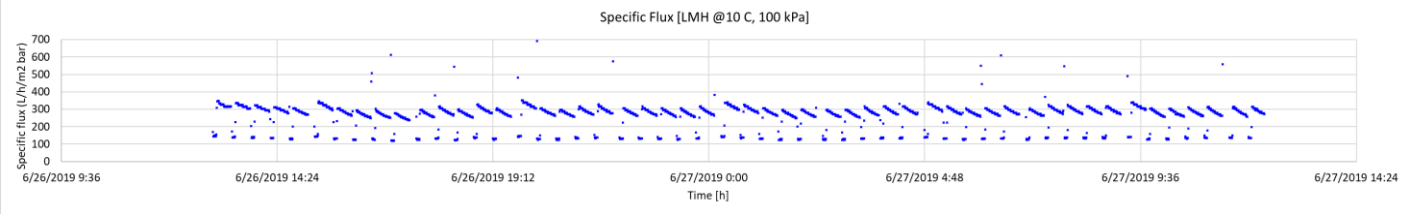

170 Lmh

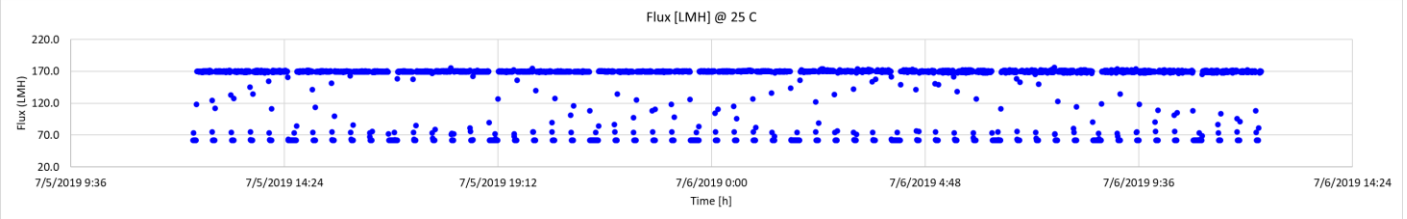

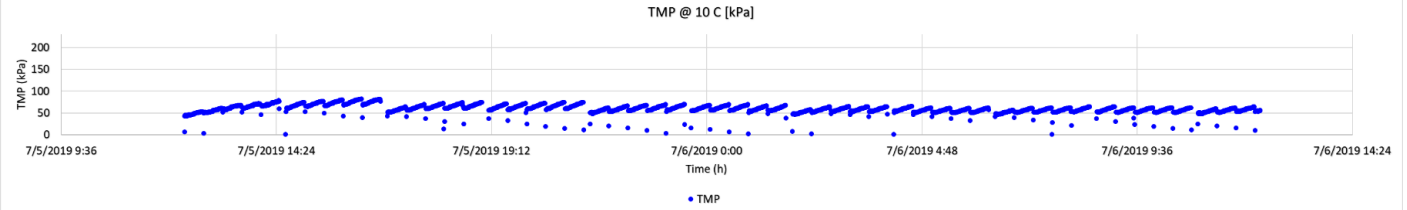

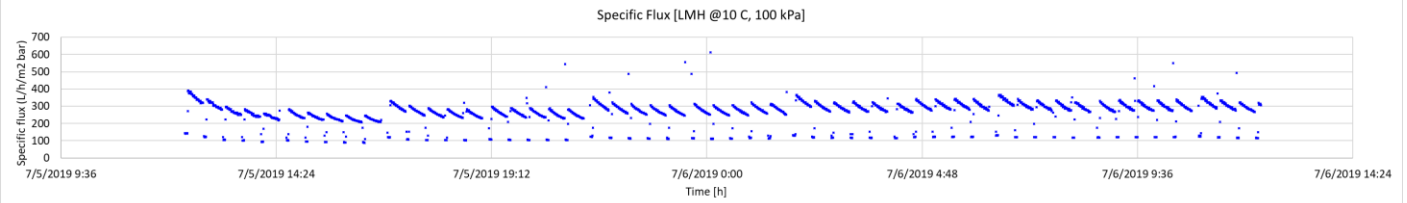

195 Lmh

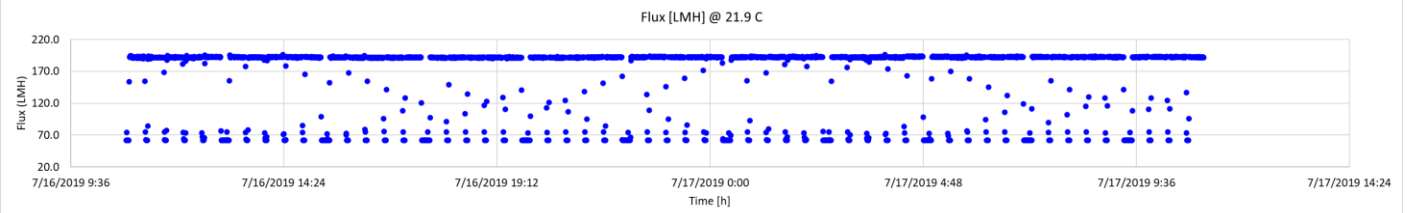

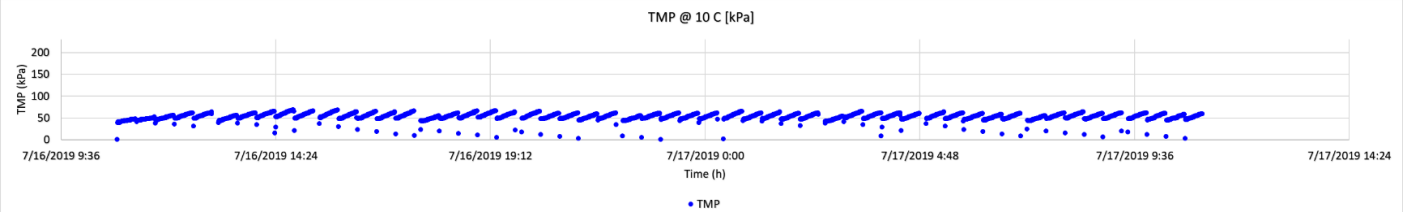

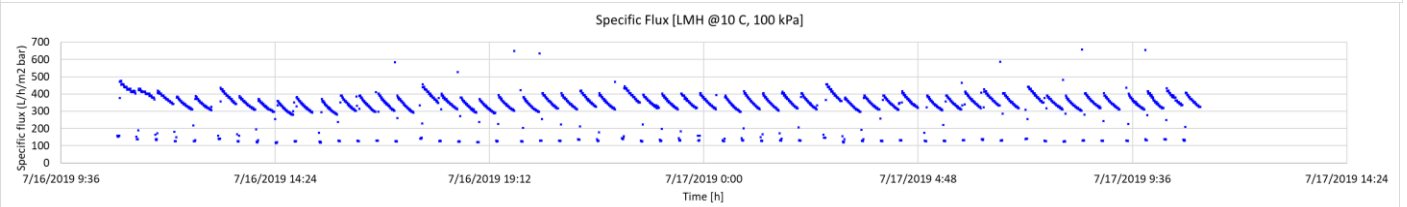

220 Lmh

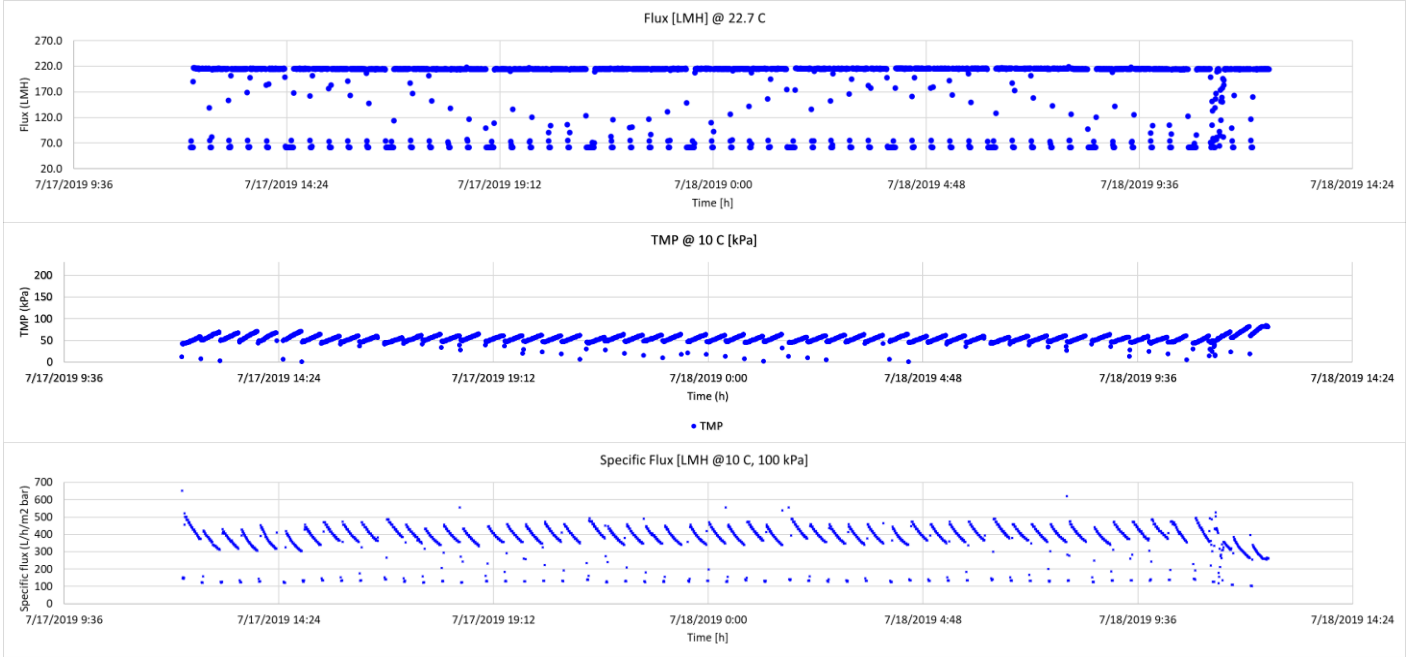

245 Lmh

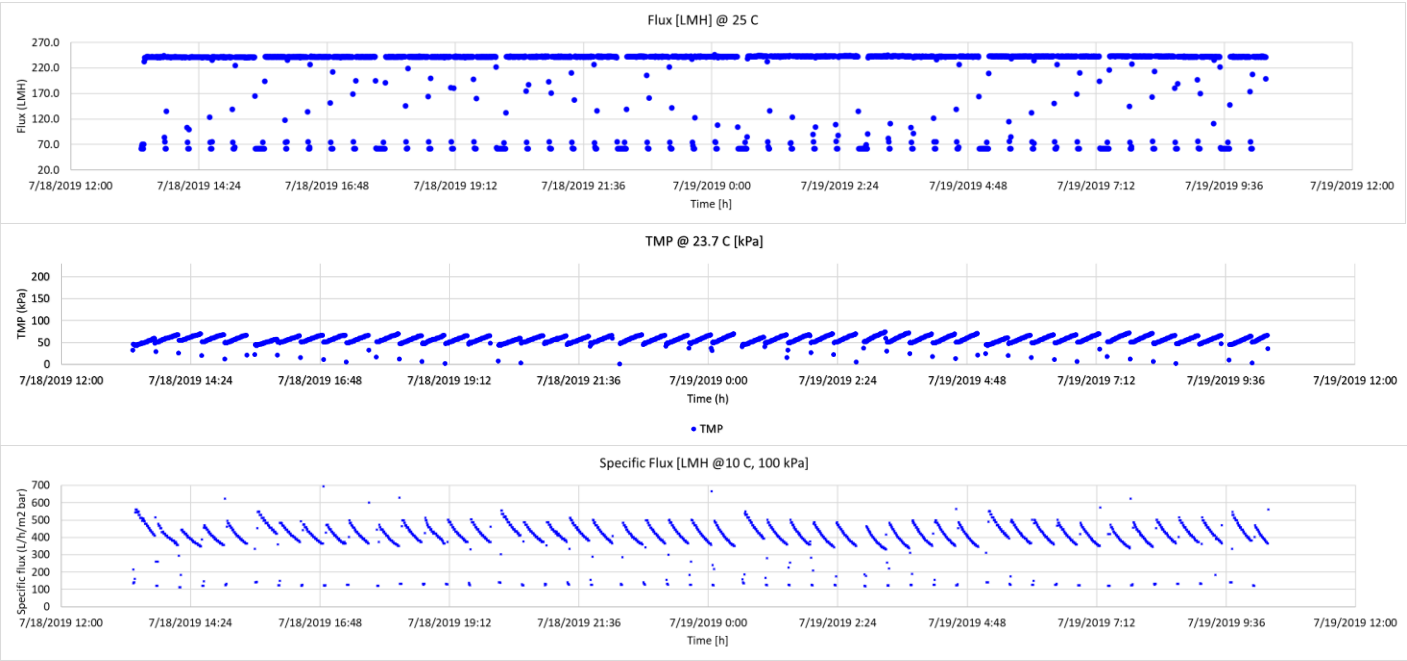

270 Lmh

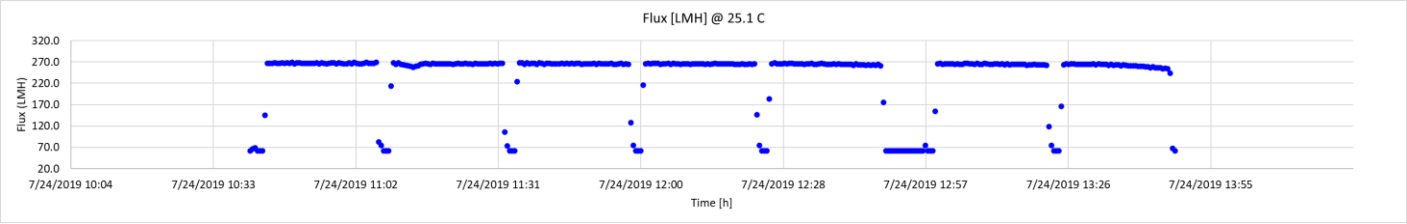

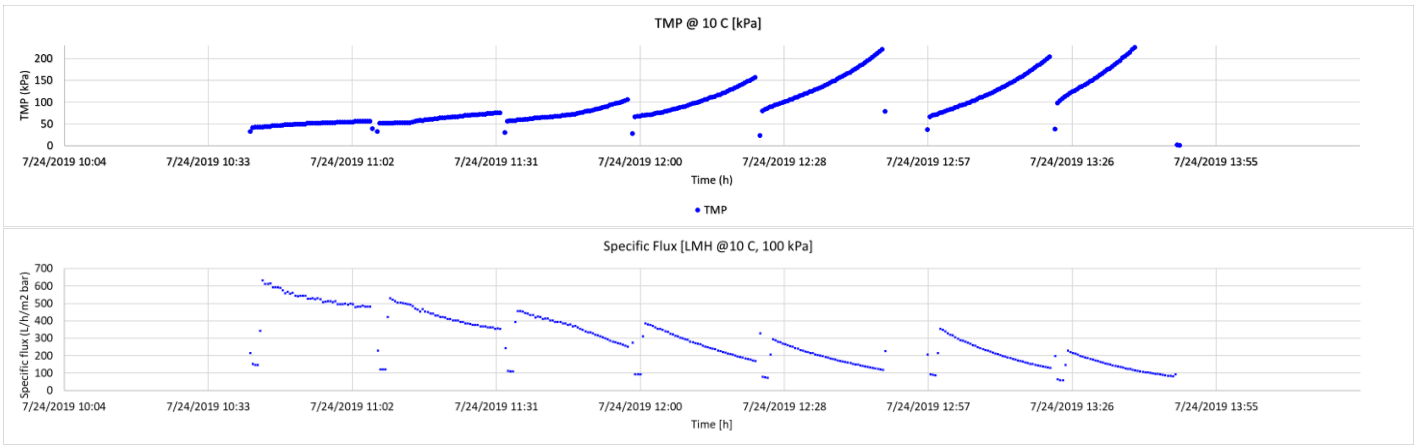
TMP @ 10 C [kPa]
TMP (kPa)
200
150
100
50
0
7/24/2019 10:04
7/24/2019 10:33
7/24/2019 11:02
7/24/2019 11:31
7/24/2019 12:00
7/24/2019 12:28
7/24/2019 12:57
7/24/2019 13:26
7/24/2019 13:55
Time (h)
TMP

Specific Flux [LMH @10 C, 100 kPa]
Specific flux (L/h/m2 bar)
700
600
500
400
300
200
100
0
7/24/2019 10:04
7/24/2019 10:33
7/24/2019 11:02
7/24/2019 11:31
7/24/2019 12:00
7/24/2019 12:28
7/24/2019 12:57
7/24/2019 13:26
7/24/2019 13:55
Time [h]

Appendix VI Additional Literature

I. Water Reuse in Europe

Countries within the European Union would benefit greatly from the widespread use of water reuse systems as it strengthens water availability, diminishes eutrophication, lowers cost as well as reduces energy demands (Angelakis et al., 2008). The economy would benefit as well as Hochstrat, Wintgens, and Melin (as cited in Fawell et al.) approximated that Europe ill have water savings as high as 1.5 percent by the year 2025 with the employment of such technologies (Fawell et al., 2016) The implementation of water reuse systems has been apparent throughout history in Europe. In particular, the Ancient Romans along with the Ancient Greeks implemented water reuse systems. These practices were also seen in Germany, Poland, Valencia Huerta, Great Britain as well as Milanese Marcites during the fourteenth as well as fifteenth centuries (Angelakis et al., 2008).

In Europe, like most parts of the world, there is room for growth with the amount of water reuse taking place. In particular, the amount of water reuse generated in the Netherlands in 2005 was 5 million cubic meters. Furthermore, in 2004, the amount of water reuse produced in Europe was approximately 700 million cubic meters. This amount was estimated to be lower than one-fifth of the approximated water reuse potential. Based on the AQUAREC project, a modeling procedure determined the European Union's overall potential for water reuse using secondary effluent. These potentials are estimates of how much reuse is possible to reach if the capacity for it is fully utilized. Spain had the highest level of potential for reuse purposes with the estimated amount of water reuse being greater than 1,300 million cubic meters per year. Mediterranean counties also demonstrated large reuse potential with Italy having approximately 550 million cubic meters per year and France

having 120 million cubic meters per year. Germany also displayed high potentials with an approximated amount of reuse capability being 150 cubic meters per year. Overall, the European Union along with EUREAU, which signifies the "Union of National Associations of Water Suppliers and Wastewater Services from countries within the EU and EFTA", has a reuse potential of approximately 2,455 million cubic meters per year (Angelakis et al., 2008).

More than one-third of the water reuse projects taking place in Europe utilize secondary effluent. Southern Europe mainly uses wastewater reuse for irrigation to enhance agriculture as well as for urban along with environmental purposes. Northern Europe utilizes it for primarily urban, environmental as well as industrial projects (Bixio et al., 2006). Angelakis et al. reported that Spain had over 150 secondary effluent reuse projects. The Canary Islands along with Murcia, Barcelona, Cost Brave, and Vitoria are home to some of these projects. Wastewater reuse in Barcelona is acting as a mitigation solution to salt-water intrusion by recharge the aquifers located in the river basin. The project in Vitoria is supplying 35,000 cubic meters per day to the irrigation system for agriculture over approximately 3,500 hectares. This agriculture field is expanding to 6,500 hectares in which wastewater reuse will feed a 7 million cubic meter reservoir (Angelakis et al., 2008).

Angelakis et al. also discussed water reuse projects occurring in Cyprus, Germany, Belgium, and Malta. In Cyprus, the expected use of roughly 25 million cubic meters per year will facilitate irrigation as well as the preservation of recreational facilities such as golf courses, gardens along with parks. Berlin, Germany manages wastewater reuse to help recharge aquifers for drinking purposes using bank filtration. Belgium recharges drinking water aquifers through potable ruse along with dune infiltration. Moreover, Malta

implements wastewater reuse for irrigation purposes to facilitate crop growth over a 600-hectare area (Angelakis et al., 2008).

The growth of waste reuse could potentially increase with the range of 1.3 to 14 times by the year 2025 based upon reuse estimates from 2000. However, for this achievement to certain objectives for the future of water reuse need to be met. These objectives include the recognition of water reuse as a standard method for resource management and not only as a method to mitigate water scarcity along with a framework for water reuse guidelines, regulations as well as the transfer of information. Moreover, the implementation of future water reuse projects needs to use experience from existing ones as well as financial incentives. Projects ultimately should consider the environmental, social, and economic impacts and well as benefits when considering alternatives (Angelakis et al., 2008).

II. Water Reuse Guidelines and Standards in the European Union

Even though the implementation of water reuse systems in Europe is apparent, there is a scarcity in guidelines along with standards, which is a significant impediment to their use. The limited number of guidelines includes the Council Directive's 2000/60/EC and 91/271/EEC. The 2000/60/EC directive sets up the basis of water policy actions, which indirectly acknowledges the ability of water reuse to enhance water availability. Directive 91/271/EEC implies that the implementation of water reuse technologies should occur when applicable (Fawell et al., 2016).

In addition to the council directives, the Drinking Water, Groundwater, Priority Substances, and Urban Wastewater Treatment Directives set some more indirect precedents for water reuse Fawell et al., 2016; Bixio et al., 2006). The Drinking Water Directive determines the potable water quality standards that need to be meet for consumption. The

guidelines associated with the groundwater protection is outlined in the Groundwater Directive. Moreover, the Priority Substances Directive is expecting a revision that will set forth standards concerning emerging contaminants. This directive, in turn, will influence the technology options along with the design of the system, specifically regarding any environmental buffers (Fawell et al., 2016). Lastly, the Urban Wastewater Treatment Directive requests the use of decentralized systems to diminish pollutant concentrations from households located in secluded areas. It also includes information regarding nutrient removal as well as pollutants produced from agriculture (Bixio et al., 2006)

An executive fraction of the European Union, the European Commission, helps to finance water reuse research along with the innovation of these technologies. The European Commission through the frameworks Aquarec, Reclaim Water, and Demoware outlines risk management operations for reuse. Furthermore, they promote the use of wastewater reuse systems in the enhancement of water efficiency within the European Union, specifically regarding irrigation along with the industrial application. This promotion of water reuse is seen in their document titled Water Blueprint (Fawell et al., 2016).

III. Zeta Potential

Zeta potential is the electrical charge measurement of ions when they are encompassing suspended particulates, which are usually one micron in size or less. In nature, zeta potential is generally negative and thus allows repulsion forces to be present between particles. Gravity causes larger particles to settle; however, electrokinetic charges inhibit particles less than 1 micron in size settle by preventing them from attaching to these larger masses of particulates. The zeta potential is the number in millivolts associated with the electrokinetic

charges (Bean et al., 1964). Therefore, the definition of zeta potential is also the measurement of the charge associated with particles as well as colloids (Sharp et al., 2006).

Figuring out the zeta potential involves examining particulates' velocities through a current set at a voltage within the range of 50 to 500 volts. The velocity used in this scenario is the electrophoretic mobility of the system. To determine the zeta potential, a microscope is necessary. Typically, in surface waters, the zeta potential is around -15 to -25 millivolts (Bean et al., 1964). When looking at coagulation, a zeta potential within the range of -10 millivolts to +3 millivolts is best for obtaining minimal as well as stable residuals (Sharp et al., 2006).

When looking at water quality parameters, the zeta can have some impact. For example, a negative zeta potential is beneficial for reducing turbidity in a water sample. Moreover, when alum is the coagulant used in coagulation a neutral zeta potential is advantageous for the removal of color. Moreover, color removal using ferric sulfate as the coagulant prefers the use of a slightly positive zeta potential (Bean et al., 1964). Therefore, different types of coagulants can have contrasting preferences when it comes to zeta potential and water quality.

Duan et al. examined the impact of zeta potential of coagulation using alum as the coagulant. They determined that as the concentration of coagulant increase the zeta potential decreased. When manipulating the pH of the water, they noted that at higher levels of pH, the zeta potential difference between varying coagulant dosages was smaller than when these same dosages were at a lower pH within the range of 5 to 6. Moreover, the presence of the negatively charged organics, citrate as well as oxalate, lead to a reduction in the zeta

potential along with the size of the precipitates. Furthermore, if the salt concentration increased the zeta potential associated with the alum precipitates declined (Duan et al., 2014).

Sharp et al. analyzed the impact of zeta potential when ferric sulfate was the coagulant used during coagulation. They observed that the amount of DOC, as well as turbidity, was reduced effectively when the zeta potential was within the range of -10 millivolts to +3 millivolts. Moreover, as the zeta potential shifted to negative from positive, the floc size of the precipitates increased. For example, when the zeta potential was +3.5 millivolts, the floc size was 594 ± 28 microns, whereas at a -3.3 millivolt zeta potential, the floc size was 603±24 microns. Ultimately, Sharp et al. determined that a low zeta potential leads to minimal, stable residuals when using coagulation with ferric sulfate as the coagulant (Sharp et al., 2006).

IV. Effects of Pre-Ozonation of Coagulation

a. Overview of Pre-Ozonation

Colloids and other particulates present in feed water are often small, anionic, and hydrophilic; thus, these contaminants are challenging to remove with typical coagulation processes. This problem can cause further issues in the areas of turbidity, color, odor, taste, and the presence of disinfection by-product predecessors. Cold weather can further magnify these implications as it slows down the coagulation kinetics. Therefore, the implementation of pre-oxidation processes before coagulation can enhance the coagulation's effectiveness and lessen the coagulant demand, even in cold climates or in the presence of heavy metal contamination. Pre-oxidation methods are relatively simple to operate and inexpensive compared to other pretreatment processes. This pretreatment method is effective in enhancing coagulation, especially with the use of cationic coagulants such as iron and aluminum salts, as oxidations

work by reducing the negative charges associated with the particulates in the feed water (Xie et al., 2016).

One pre-oxidation process that is effective is pre-ozonation. The application of ozone to disinfect water, reduce inorganic contaminants, regulate odor and color as well as enhance biodegradation and the removal of disinfection by-product predecessors is employed by water treatment processes for a while. In the pretreatment of coagulation, low concentrations of ozone are the most effective in improving the process as these dosages augment the reduction of colloids and particulates in the feedwater. Negative impacts are associated with the use of high ozone concentrations, such as an increase in turbidity. Therefore, optimal ozone dosages are determined before utilization and are dependent upon source water as well as charge densities of the particulates present, specifically those of humic substances. Regarding humic substances, larger charges densities require larger ozone dosages (Xie et al., 2016). In literature, ozone dosages of 0.5 to 1 g/m3 as well as ones from 0.4 to 0.8 mg O3/mg DOC are effectively improving the coagulation process, specifically regarding NOM reduction (Chiang et al., 2009). NOM removal by pre-ozonation at low dosages occurs, as ozone can reduce the size distribution by splitting larger molecules (Rodríguez et al., 2012).

Pre-ozonation with coagulation is effective in the removal of taste, color, and odor from the feed water. Bekbolet et al. (as cited by Chiang et al., 2009) determined that this pretreatment process used with coagulation can reduce the UV254 of the feedwater as well. Pre-ozonation also can reduce predecessors of disinfection by-products into trihalomethanes as well as haloacetic acids. Moreover, this pretreatment mechanism can enhance the NOM's sorption onto the hydroxides of metal coagulants through the increase in acidic functional factions present in NOM (Chiang et al., 2009). It can also improve the removal efficiency of colloids by

coagulation, particularly in feed waters that have a high presence of scavengers. (Rodríguez et al., 2012).

There are some drawbacks of using pre-ozonation as a pretreatment process for coagulation. Pre-ozonation has the potential to enhance the formation of disinfection by-products (DBPs) such as trihalomethanes, haloacetonitriles, haloacetic acids, N-nitrosodimethylamines, and halonitromethanes as well as N-DBPs and C-DBPS. The potential formation of some of these by-products increases with the use of chlorine disinfection. Furthermore, in the presence of bromide contaminated feed waters, the production of bromate occurs, which can have negative health impacts on humans (Xie et al., 2016). High concentrations of ozone can cause NOM to shift from hydrophobic to hydrophilic causing its removability to decline. Chang et al. (as cited by Chiang et al., 2009) observed that this pretreatment hindered the development of flocs (Chiang et al., 2009). Ultimately, some factors determine whether pre-ozonation positively or negatively impacts coagulation, such as feedwater characteristics, characteristics of the coagulation process, and the ozone dosage (Rodríguez et al., 2012).

b. Processes of Pre-Ozonation that Improve Coagulation

Pre-oxidation, in general, enhances the coagulation process through various mechanisms. It impairs the bonds formed amongst particulates and adsorbed organics, which results in a decrease in molecular weight. This reduction in molecular weight weakens the electrostatic barrier between the particulates and coagulants. It also enhances the adsorption of metal complexes onto alum flocs through the increase of associations with magnesium, aluminum, calcium following pre-oxidation. Bridging reactions can also occur when the particulates combine after NOM polymerization. Additionally, pre-oxidation can cause the formation of

coagulant in-situ if it breaks the metallic ion complexes. This event occurs mainly when iron or manganese are available. The decrease in charge density of anionic matter can occur because of pre-oxidation. This outcome can enhance collisions of particulates as well as coagulation. Lastly, the reduction of CO2 in the process of oxidation can cause CaCO3 to precipitate out and lead to the aggregation of particulates (Xie et al., 2012).

When using pre-ozonation, a series of processes occur that can increase coagulation's effectiveness. Pre-ozonation causes the carboxylic content to rise prompting an increase in adsorption with alum as well as with precipitates containing magnesium and calcium. The absorbed organics located on the inorganic particles decrease in size. This decrease results in the reduction of steric hindrance. Furthermore, the ozone disbands organometallic bonds which results in more effective precipitation as the metals act like coagulants to lingering organic compounds. Lastly, the oxidation and polymerization processes create bigger and more stable particulates, which increases the efficiency of the coagulation process (Farvardin et al., 1989).

c. Results from Studies Using Pre-Ozonation Before Coagulation

Chiang et al. conducted a study looking at the impacts of pre-ozonation on coagulation using a water sample from Tai-hu Lake in Taiwan. Before going through pre-ozonation and coagulation, the DOC, alkalinity, turbidity, and color of these water samples were 78±0.2 mg/l, 67±3 mg/l as CaCO3, 10±5 NTU, and 181±5 CU, respectively. Furthermore, the NOM of the water sample were approximately 25 to 35 percent hydrophilic and 65 to 75 percent hydrophobic. Based on the study conducted. Chiang et al. determined that the best ozone dosage for the Tai-hu Lake water at a pH of 9 was 0.45 mg-O3/mg-DOC to enhance the reduction of turbidity, THMFP, DOC, and UV254 (Chiang et al., 2009).

Turbidity was one of the parameters evaluated during the experiment at pH levels of 5, 7, and 9 as well as ozone dosages of 20, 40, 60, 80, and 100 mg/l. Chiang et al. observed a significant difference in turbidity following ozonation and before coagulation. Residual turbidity levels after pre-ozonation and coagulation were under 2 NTU in nearly all cases, except when the turbidity following ozonation was 16.8 NTU when the pH level was 5. The removal of turbidity was approximately 75 percent following coagulation when the turbidity levels after ozonation were lower than 5 NTU. Chiang et al. determined the residual turbidity reduced substantially following pre-ozonation and coagulation treatment at a pH of 5 and low dosages of ozone. Therefore, pH, as well as ozone concentration, have a significant impact on coagulation's ability to remove turbidity (Chiang et a., 2009).

The study also investigated the reduction of DOC following pre-ozonation and coagulation at pH levels of 5, 7, and 9 as well as ozone dosages between 0.5 and 0.85 mg-O3/mg-DOC. No considerable change in the removal of DOC was present when the alum to DOC ratio was lower than 0.6 mg/mg, and minimal removal was seen at pH values of approximately 5. However, the enhancement of DOC reduction was observed when the ratio between Al and DOC was larger than 0.6 mg/mg. Chiang et al. observed that when the coagulated dosage raised from 0.2 to 0.9 mg-AL/mg-DOC, reduction in DOC rose as well from approximately 9 to 14 percent, 7 to 30 percent, and 6 to 34 percent when the pH levels were 5, 7, and 9, respectively. Furthermore, at ozone dosages of 0.45 and 0.85 mg-O3/mg-DOC, they observed the reduction of DOC was larger when the pre-ozonation was not present when compared to when it was present. This result occurred with a pH of 5 and an alum to DOC ratio of greater than 0.6 mg/mg. Moreover, there appeared to be no considerable change in DOC reduction when pre-ozonation was used

compared to when it was not for the entirety of ozone dosages and pH values (Chiang et al., 2009).

Similar to the results for DOC reduction, the results for UV254 reduction display that at low ozone dosages there is no considerable change in this parameter by coagulation when pre-ozonation is implemented compared to when it is not implemented. However, by increasing ozone dosages, there is an increase in UV254 reduction. There was a 70 percent reduction when the dosage changed from 0.15 mg-O3/mg-DOC to 0.85 mg-O3/mg-DOC. Moreover, the trihalomethane formation potential (THMFP) was another parameter observed during this study. Chiang et al. determined that the DOC concentration following pre-ozonation as well as the SUVA were significant components in the development of trihalomethanes. They noticed that the reduction of both the THMFP and the DOC was 48 percent with just the use of coagulation. The implementation of pre-ozonation before coagulation led to a decrease in DOC reduction by 4 percent, however, the reduction of THMFP elevated by 16 percent. Therefore, with the use of pre-ozonation when the alum dosage was 100 mg/L, the DOC removal was 44 percent and the THMFP was 64 percent with the implementation of pre-ozonation compared to the 48 percent for both removals without the implementation of pre-ozonation (Chiang et al., 2009).

Rodríguez et al. determined that the ability of pre-ozonation to enhance the removal efficiency of coagulation concerning NOM was variable and contingent upon water quality attributes. For the Úzquiza Reservoir, the water source in this study, the reduction of TOC decreased with rising ozone dosages. This result is likely due to a significant portion of NOM being hydrophobic as well as the small amount of calcium hardness, which helps negate the negative impacts of pre-ozonation on coagulation. Furthermore, this result became less apparent

when they raised the coagulant dosage. Moreover, pre-ozonation was able to reduce the THMFP from 5 to 25 percent with dosages from 0.25 to 2.5 mg/l (Rodríguez et al., 2015).

Rodríguez et al. investigated the impact of pre-ozonation on coagulation, specifically regarding NOM. This study used three water sources: the Úzquiza Reservoir, a manufactured water source containing fulvic acids, and a manufactured water source containing in humic acids. The TOC concentration, hardness, and SUVA of the Úzquiza Reservoir are 2.5 mg/l, less than 10 mg/l as CaCO3, and 2.5 l/mg-m, respectively. The ozone dosages used in this study were 0.12 to 1.4 mg-O3/mg-TOC and 0.25 to 4.0 mg-O3/ mg-TOC for the Úzquiza Reservoir and the humic substances, respectively (Rodríguez et al., 2015).

Based on the results of the experiments conducted, Rodríguez concluded that concerning TOC removal, as they raised the ozone dosage the effectiveness of coagulation diminished. Thus, the TOC removal diminished as well. At ozone dosages greater than 2 mg-O3/mg-TOC, there was minimal removal. In particular, the water that was not ozonated was able to achieve TOC reduction of approximately 90 percent, whereas ozonated water with dosages greater than 2 mg-O3/mg-TOC achieved removal lower than 10 percent. Furthermore, there was a rise in turbidity with ozone dosages that exceeded 2 mg-O3/mg-TOC resulting from the increase in aluminum residual. In particular, the original turbidity of 6.80 NTU was elevated to 12.5 NTU at 2 mg-O3/mg-TOC. Regarding THMFP, pre-ozonation was able to substantially reduce it, however, the presence of TOC in the water increased as this occurred. Rodríguez et al. concluded that the negative impact that pre-ozonation had in most parameters tested during this study was likely the result of the ozone dosages being within the range that hinders TOC removal as described in the literature (Rodríguez et al., 2015).

Farvardin et al. discerned that pre-ozonation reduced the needed alum coagulant dosage by 17 percent from 13 to 30 percent. It also enhanced the water quality compared to the water quality that resulted from just using coagulation. Pre-ozonation also causes the reduction charge density of colloids during the beginning steps of oxidation. If the particulates present in the water are non-colloidal, pre-ozonation may not be an effective pretreatment option. Moreover, Farvardin et al. deduced that there is an optimal ozone dosage and that when dosages are greater than this level, pre-ozonation can become damaging (Farvardin et al., 1989).

In experiments conducted by Farvardin et al., they used a variety of natural as well as commercial humic and fulvic acids to determine the impact of pre-ozonation on coagulation, specifically dealing with humic substances. Through the sole use of alum coagulation for a 20 mg/l humic acid solution with particulate sizes ranging from 0.1 to 5 micrometers, the removal of color and ultraviolet absorbance was 89 percent and 88 percent, respectively. However, through the implementation of an optimal ozone dosage of 0.14 mg/l, the amount of alum required diminished by 13 percent and there was a 22 percent reduction in turbidity. There were minimal enhancements with the reduction in color and ultraviolet absorbance when compared to the results from using only coagulation. Regarding humic acids smaller than 0.1 micrometers, Farvardin et al. reduced the required alum dosage by 20 percent when using an optimal ozone dosage of 0.25 mg/L. Furthermore, for both sizes of humic acids, the main difference between pre-ozonated water and non-pre-ozonated water was that pre-ozonation decreased the colloidal charge density, which is a major component in determining the required alum dosage. This reduction in charge density led to the reduction of the required alum dosage (Farvardin et al., 1989).

At ozone dosages greater than the optimal dosages, humic acids are further degraded by ozone. These molecules can substantially decrease in size resulting in them no longer acting like colloidal particles. This result can negatively impact the water quality as the coagulation method changes from charge neutralization to sweep coagulation. Due to this change, the required alum dosage increases, and the coagulation process does not perform as effectively as these molecules precipitate out by adsorbing onto the surface of the aluminum hydroxide molecules (Farvardin et al., 1989).

Schneider et al. concluded that smaller ozone dosages, such as 2 mg/l, was a more effective aids in improving NOM reduction for the conditions of the study than a higher ozone dosage of 4 mg/l. At higher ozone dosages, there was an increase in the development of hydrophilic particulates, which are more difficult to remove than hydrophobic particulates through coagulation. In this study, pre-ozonation played a larger role in the removal of NOM and particulates when compared to the ability of coagulation to remove these entities. Moreover, when inspecting the effects of contact time on the reduction of turbidity, DOC, and TOC, there appeared to be no significant difference between 4 minutes compared to 28 minutes for the parameters in this study. Schneider et al. also noted that in the presence of alum coagulation, pre-ozonation decreased the removal of TOC, turbidity, and DOC using coagulant concentrations of 0.5 and 0.8 mg/l. However, by using cationic polymer coagulants, there was an enhancement in the reduction of TOC, turbidity, and DOC in the feed water using pre-ozonation (Schneider et al.,2000).

Using statistics, Schneider et al. were able to compare the differences between the removal efficiencies of coagulation versus pre-ozonation and coagulation. When looking at alum coagulation and alum coagulation with a pre-ozonation dosage of 2 mg/l, there was no

significant difference observed in the settled turbidity of the treated water as the p-statistic was 0.27, which is larger than the 5 percent benchmark. However, when observing the reduction in DOC, the p-statistic is below the 5 percent benchmark with a value of 2.7 x 10-3. This p-value indicates that pre-ozonation of 2mg/l with alum coagulation hindered the removal of DOC when compared to using only alum coagulation. Moreover, when the ozone dosage was set to 4 mg/l, the use of pre-ozonation decreased the removal of both turbidity and DOC when compared to the sole use of alum coagulation. When comparing the 2 mg/l ozone dosage with the 4 mg/L ozone dosage, the larger ozone dosage decreased the reduction in turbidity and DOC more significantly (Schneider et al., 2000).

The use of cationic polymers showed a more positive impact on the use of pre-ozonation prior to coagulation. Comparing the DOC and turbidity removal of the use of pre-ozonation with no use of pre-ozonation, the ozone dosage of 2 mg/l had an advantageous impact. The p-values associated with the comparisons between turbidity reductions and DOC reductions were 1.9x10-4 and 4.4x10-5, respectively. With an ozone dosage of 4 mg/l, pre-ozonation enhanced the reduction of turbidity and DOC as well. When comparing the two dosages, the 2 mg/l ozone dosage has a higher removal efficiency for DOC when compared to the 4 mg/l dosage. There was no discernible difference between the two with regards to a reduction in turbidity. Therefore, the 4 mg/l dosage is likely greater than the optimal ozone dose and is an over-dosage (Schneider et al., 2000).

V. Design Principles of Membrane Filtration Systems

Flux, recovery, TMP, and total membrane resistance are important concepts to know to understand the overall process of membrane filtration systems as well as the implication of

membrane fouling. The flux of the system is the flow of filtrate through the membrane surface area and is represented through equation V-1.

Equation V-1

$$J = \frac{Q_p}{A_m}$$

J is the flux with the units (liter/hour/meter^2 or gallons/day/feet^2), Q_p is the filtrate flow with the units (liters/hour or gallons/day), and A_m is the surface area of the membrane with the units of meter^2 or feet^2 (Malcolm Pirnie, Inc et al., 2005).

Temperature can impact the flux as temperature impacts the viscosity of the water. The impact of temperature on viscosity can be best depicted in equation V-2, where μ_T is the water's viscosity at a temperature and T is the water temperature in degrees Celsius.

Equation V-2

$$\mu_T = 1.784 - (0.0575T) + (0.0011T^2) - (10^{-5}T^3)$$

It is common to normalize the flux to a reference temperature, which is usually set at 20 degrees Celsius. This temperature is chosen because the viscosity of water at this temperature is approximately 1 centipoise. By normalizing the flux to a temperature, it enables more effective monitoring as the results will be independent of temperature. Therefore, it produces more comparable results (Malcolm Pirnie, Inc et al., 2005)

Normalizing the flux to a temperature of 20 degrees Celsius can take many forms based on the known parameters as well as the operating conditions. If the TMP and total membrane resistance are constant, then the normalized flux can take on the following equation:

Equation V-3

$$J_{20}\mu_{20} = J_T\mu_T$$

In this equation, J_{20} is the flux at 20 degrees Celsius; μ_{20} is the water's viscosity at 20 degrees Celsius; J_T s the actual flux of water at a temperature of T; and μ_T is the water's viscosity at a temperature of T. By substituting in 1 centipoise for μ_{20} and using the equation to determine μ_T, the flux at 20 degrees Celsius can be calculated as seen in equation V-4 where T is the actual temperature of the water (Malcolm Pirnie, Inc et al., 2005).

Equation V-4

$$J_{20} = J_T [1.784 – (0.0575T) + (0.0011T^2) – (10^{-5}T^3)]$$

The flux normalized at 20 degrees Celsius can also be expressed in terms of the temperature correction factor. The temperature correction factor or TCF is a ratio between the viscosity of the water at temperature T with the viscosity of water at 20 degrees Celsius. The definition can be seen in equation V-5 (Malcolm Pirnie, Inc et al., 2005).

Equation V-5

$$TCF = \mu_T/\mu_{20}$$

Using the TCF, the flux at 20 degrees Celsius can be written as the following equation.

Equation V-6

$$J_{20} = J_T (TCF)$$

To determine the fluxes that lead to membrane fouling, both the pressure and temperature are normalized. This flux that is both pressure and temperature normalized is called the specific flux. The specific flux, M_{20}, is expressed in equation V-7 (Malcolm Pirnie, Inc et al., 2005).

Equation V-7

$$M_{20} = J_{20}/TMP$$

TMP is the pressure gradient of the membrane in units of psi and is the active force for the movement of water through the membrane. It is the difference between the feed pressure and the filtrate pressure as signified in equation V-8 (Malcolm Pirnie, Inc et al., 2005).

Equation V-8

$$TMP = P_f - P_p$$

P_f is the feed pressure with the units (psi), and P_p is the filtrate pressure with the units (psi). However, if the mode of the microfiltration membrane system is suspension and has a recycled or wasted concentrate stream, then the feed pressure is not constant and the equation for TMP is altered as seen in equation V-9 (Malcolm Pirnie, Inc et al., 2005).

Equation V-9

$$TMP = \frac{P_f + P_c}{2} - P_p$$

P_c is the pressure of the wasted concentrate stream with the units (psi).

Similar to the flux, it is important to normalize transmembrane pressure or TMP to a specific temperature to observe the change in TMP at various fluxes without the impacts of temperature. The TMP is also typically normalized to 20 degrees Celsius due to the viscosity of water at this temperature being approximately 1 centipoise. The equation for the TMP normalized at 20 degrees Celsius can be seen in equation V-10 (Malcolm Pirnie, Inc et al., 2005).

Equation V-10

$$TMP_{20} = TMP_T \, (\mu_{20}/\mu_T)$$

In this equation, TMP_T is the transmembrane pressure when the water is at a temperature of T. It is important to note that whether the TMP or the flux is being normalized, the

normalized value is not the actual value observed during operation but rather is what the value would be at 20 degree Celsius (Malcolm Pirnie, Inc et al., 2005).

VI. Orange County Treatment Scheme

Potable water reuse is more popular as challenges with accelerating population and economic growth in certain areas lead to water scarcity. In general, water reuse technologies can provide solutions to water availability and wastewater distribution complications. For example, municipal water reuse takes wastewater, which would be released into receiving surface waters and with drinking water reuse, implements leading water treatment processes to increase drinking water reserves. Thus, the Groundwater Replenishment System (GWRS), located in Orange County, California, is the global standard with regards to potable water reuse. For more than 40 years, indirect potable water reuse systems, or potable water reuse that requires environmental buffers to facilitate the combining of reuse water with conventional water replenishments, has been used in Orange County, California. This water reuse occurred to supplement the diminishing water supplies in their coastal aquifers. The main sources of their water are local groundwater supplies, the Colorado River, the Santa Ana River, recycled water, and water supplied by northern California (Ormerod et al., 2017).

In the past, Orange County California depended upon a 15 million acre-feet groundwater basin of which between 1 and 1.5 million acre-feet was active storage. Over withdrawing from the basin as well as the inability of recharge to keep up with these demands led to the basin no longer being a viable source in the 1920s. Seawater intrusion became an issue as well resulting in seawater progressing inland to up to three and a half miles. Thus, Orange County started implanting water reuse facilities to recharge water supplies (Richardson et al., 1977). The implementation of three water reuse facilities occurred from October 1976 until the present.

These facilities are Water Factory 21 (WF-21), Interim Water Factory 21 (IWF-21), and Groundwater Replenishment System Advanced Water Purification Facility (GWRS AWPF) (Burris, 2018).

a. Water Factory 21

To manage the seawater intrusion, water scarcity, as well as rising water demands of 400,000 acre-feet for a population of 1.5 million at the time, the Orange County Water District built Water Factory 21(Richardson et al., 1977). The operation of Water Factory 21 occurred from October 1976 until January 2004 (Burris, 2018). At first, this facility, with a capacity of 15 million gallons per day, implemented advance wastewater technologies to treat secondary wastewater effluent to reuse standards (Richardson et al, 1997; Burris, 2018). The wastewater effluent coming into the facility had undergone primary and secondary treatment and had total dissolved solids concentrations ranging from 1200 to 1400 mg/l (Allen et al., 1979; Richardson et al., 1997).

The discharge of the reuse water took place at Talbert Barrier to inhibit seawater intrusion (Burris, 2018). The discharge had to satisfy drinking water guidelines due to its injection into aquifers within the Talbert Barrier (Allen et al., 1979). Thus, to meet these standards, the facility implemented lime clarification, filtration, ammonia stripping, granular activated carbon, as well as recarbonation, chlorination, a pump station, and a blending reservoir. The addition of reverse osmosis (RO) system, with a capacity of 5 million gallons per day, occurred during September 1977. This RO system contained membrane comprised of cellulose acetate as a measure to demineralize a portion of the reuse water (Burris, 2018). The RO system in Water Factory 21 also included cartridge filtration with the effective size of 25 microliters, prechlorination as well as a scaling prevention measure in the form of sodium hexametaphosphate (Richardson et al.,

1977). Furthermore, the termination of ammonia stripping transpired in 1987 when the facility discovered that the RO system, as well as nitrification occurring during secondary treatment, was able to remove ammonia. The last addition to the system was a UV advanced oxidation process in 2001 to help facilitate a reduction in organic pollutants possessing low molecular densities (Burris, 2018).

b. Interim Water Factory 21

The Interim Water Factory 21 operated from June 21, 2004 to August 8, 2006. The objectives for this facility were to generate 5 million gallons a day of potable water reuse to hinder seawater intrusion as well as function as a teaching opportunity for maintenance employees to acquire knowledge on how on the treatment processes that would be implemented into the GWRS AWPF. The water treatment processes in place at the IWF-21 were membrane filtration, reverse osmosis, UV advanced oxidation process as well as decarbonation. Using these processes, secondary effluent from the Orange County Sanitation Department was brought to portable reuse standards. This reuse combined with diluted water before being disinfected through chlorination and pumped to the injection sites (Burris, 2018).

The reconstruction of the reverse osmosis system for this treatment facility enhanced rejection rates for pollutants and mineral as well as reduced energy expenditure using polyamide membranes. These membranes were classified as thin-filmed as well as composite. The mechanism of reverse osmosis incorporated chemical pretreatment, membrane treatment as well as cartridge filtration. Post-treatment was another component and consisted of water degasification and CO_2 removal. Furthermore, the utilization of the chlorination system in place at the WF-21 in the IWF-21 resulted in the mitigation of potential biofouling problems at the injection sites (Burris, 2018).

c. Groundwater Replenishment System Advanced Water Purification Facility

January 2009 was the start date of the AWPF with a production capacity of 70 million gallons per day of potable water reuse (Burris, 2018). This system expanded with the implementation of the GWRS in May 2015, making the facility the largest AWPF in the world, specifically for potable water reuse (Burris, 2018; Wang et al., 2015). With this addition, the production capacity of the facility increased to 100 million gallons a day of potable reuse. In 2017, the average production of potable reuse was 89.6 million gallons a day. Furthermore, in 2017, the GWRS AWPF was able to satisfy all regulatory requirements as depicted in Table VI-1: 2017 Average GWRS AWPF Water Quality Results below (Burris, 2018). The bulk of the produced potable reuse from this operation is injected into the Talbert Barrier, where it percolates into basins. A small amount of the produced reuse goes to the Demonstration Mid-Basin Injection Project as well as non-potable customers (Burris, 2018).

Table VI-1: 2017 Average GWRS AWPF Water Quality Results (Burris, 2018)

Parameter Name	Units	Q1	MFF	MFE	ROF	ROP	UVP	FPW	Permit Limit
Electrical Conductivity	umhos/cm	1,610	1694[2]	1,648	1700[2]	45[2]	34	108[2]	900
Total Dissolved Solids	mg/L	957	na	962	985	18	17	50	500[3]
Suspended Solids	mg/L	4.9	5.2	<1	na	na	na	na	N/A
Turbidity	NTU	1.9	2.40[2]	0.11[2]	0.11[2]	0.04[4]	na	0.04[2]	≤0.2 / ≤0.5
Ultraviolet percent transmittance (%UVT) @254nm	%	63.7	na	67.1	na	96.68[4]	na	na	>90
pH	UNITS	7.2	7.1[2]	7.3	6.84[2]	5.52[2]	5.6	8.37[2]	6 - 9
Total Hardness (as CaCO3)	mg/L	292	na	304	287	<1	<1	33.3	240[3]
Calcium	mg/L	74.4	na	81.4	73.2	<0.5	<0.5	13.2	N/A
Magnesium	mg/L	25.8	na	24.4	25.3	<0.5	<0.5	<0.5	N/A
Sodium	mg/L	213	na	210	211	5.8	5.5	5.8	45
Potassium	mg/L	18.6	na	18.8	18.6	0.1	0.2	0.1	N/A
Bromide	mg/L	na	na	0.23	na	na	na	0.01	N/A
Chloride	mg/L	272	na	254	273	4.6	4.7	5.1	55
Sulfate	mg/L	189	na	198	197	0.2	0.1	0.5	100
Hydrogen Peroxide	mg/L	na	na	na	na	na	2.3	2.2	N/A
Bicarbonate (as CaCO3)	mg/L	na	na	164	151	7.2	4.7	35.5	N/A
Nitrate Nitrogen	mg/L	11.37	na	9.65	10.85	0.90	1.01	0.96	3[3]
Nitrite Nitrogen	mg/L	0.516	na	0.211	0.502	<0.002	0.001	0.037	1[3]
Ammonia Nitrogen	mg/L	1.7	na	1.8	2.0	0.3	na	0.2	N/A
Organic Nitrogen	mg/L	1.0	na	0.3	0.6	0.03	na	0.01	N/A
Total Nitrogen	mg/L	13.8	na	12.0	13.9	na	na	1.1	5
Phosphate Phosphorus	mg/L	0.40	na	0.52	na	na	na	<0.01	N/A
Iron	ug/L	339	na	na	131	1.0	0.5	<5	300
Manganese	ug/L	53.1	na	na	53.2	<1	<1	0.1	50
Aluminum	ug/L	7.2	na	na	4.3	0.5	0.6	0.4	200[3]
Arsenic	ug/L	<1	na	na	<1	<1	<1	<1	10
Barium	ug/L	29.7	na	na	29.4	<1	<1	<1	1,000
Boron	mg/L	0.40	na	0.42	0.40	0.25	0.25	0.25	N/A
Cadmium	ug/L	<1	na	na	<1	<1	<1	<1	5
Chromium	ug/L	<1	na	na	<1	<1	<1	<1	50
Copper	ug/L	3.9	na	na	7.6	<1	<1	<1	1,000[3]
Cyanide	ug/L	0.9	na	na	3.2	<5	na	<5	150
Fluoride	mg/L	0.93	na	na	na	na	na	<0.1	2
Lead	ug/L	<1	na	na	2.9	<1	<1	<1	15
Mercury	ug/L	<1	na	na	<1	<1	<1	<1	2
Nickel	ug/L	4.9	na	na	5.2	<1	<1	<1	100
Perchlorate	ug/L	na	na	na	na	na	na	<2.5	6
Selenium	ug/L	1.4	na	na	1.5	<1	<1	<1	50
Silica	mg/L	20.8	na	na	20.6	<1	0.6	0.3	N/A
Silver	ug/L	<1	na	na	<1	<1	<1	<1	100
Zinc	ug/L	21.1	na	na	41.5	0.3	<1	0.34	5,000
N-nitrosodimethylamine	ng/L	12.7	55.8	59.7	19.7	11.8	<2	0.9	N/A
1,4-Dioxane	ug/L	2.2	na	4.3	na	0.2	<1	<1	N/A
Total Trihalomethanes	ug/L	na	na	7.0	na	na	na	2.7	80
Dibromoacetic Acid	ug/L	na	na	na	na	na	na	<1	60,total HAA5
Dichloroacetic Acid	ug/L	na	na	na	na	na	na	<1	60,total HAA5
Monobromoacetic Acid	ug/L	na	na	na	na	na	na	<1	60,total HAA5
Monochloroacetic Acid	ug/L	na	na	na	na	na	na	<1	60,total HAA5
Trichloroacetic Acid	ug/L	na	na	na	na	na	na	<1	60,total HAA5
Apparent Color (unfiltered)	UNITS	na	na	24	31	<3	na	<3	15
Total Organic Carbon (unfiltered)	mg/L	9.00	9.68	8.13	7.99	0.10	na	0.10	0.5[3]
Surfactants (MBAS)	mg/L	0.19	na	na	0.19	<0.02	na	<0.02	0.5
Total Coliform	MPN/100 mL	1,477,235	49,626	<1	na	<1	<1	<1	2.2
Fecal Coliform	MPN/100 mL	347,719	5,309	<1	na	<1	<1	<1	N/A

Q1 Secondary Effluent (AWPF Influent) ROP Reverse Osmosis Product FPW Finished Product Water
MFF Microfiltration Feed UVF Ultraviolet UV/AOP Feed na Not analyzed
MFE Microfiltration Effluent UVP Ultraviolet UV/AOP Product N/A Not applicable

[1] For purposes of calculating annual averages, 10% of the Reportable Detection Limit (RDL) was used for all non-detect (ND) values. If all data for the period were ND, then the average is shown as "<RDL". Number of significant digits shown match those in raw data.
[2] On-line average
[3] See Appendix A for more information
[4] On-line average shown for UVF, which is effectively ROP downstream of hydrogen peroxide addition.

The original design for this facility as previously mentioned increased the production of reuse water from 15 million gallons a day to 70 gallons a day to meet the requirements of the population of 600,000 in 2008 (Ormerod et al., 2017; Wang et al., 2015). This facility replaced a portion of the treatment processes, both chemical and physical, present at WF 21 with membrane processes. The construction of the original design started in 2007, and the purposes for it were to serve as a groundwater recharge mechanism as well as a water supply source for local aquifers (Ormerod et al., 2017). This original system consisted of membrane filtration, UV advanced oxidation processes as well as reverse osmosis to produce high-quality reuse (Ormerod et al., 2017; Wang et al., 2015). This facility also implemented energy-recovery instruments, mechanisms for flow equalization, and other measures to improve upon system reliability as well

as flexibility (Wang et al., 2015). However, in 2011 they proposed a facility expansion to increase the capacity to 100 million gallons a day from 70 million gallons a day (Ormerod et al., 2017; Wang et al., 2015). The construction of the expanded facility ended in June of 2015. The main components of the expanded GWRS, which is still presently operating, are the AWPF, Talbert barrier Kraemer-Miller-Miraloma-La Plama Basins (K-M-M-L Basins), Demonstration Mid-Basin Injection (DMBI) Project, and non-potable consumers, Anaheim CCP and Anaheim Regional Transportation Intermodal Center (ARTIC) (Burris, 2018).

The updated GWRS AWPF consists of microfiltration, reverse osmosis as well as an advanced oxidation process in the form of UV disinfection with the addition of hydrogen peroxide. The process diagram of the system is seen in Figure VI-2: GWRS AWPF Process Flow Diagram below (Burris, 2018). Located before reverse osmosis, the polypropylene microfiltration membrane system reduces the presence of suspended particles and colloids, such as bacteria as well as protozoa. The modules of this system are hollow-fiber with 0.2-micron pores. The gravity feed secondary effluent flows below grade to these thirty-six membrane cells, each of them encompasses six hundred and eighty-four submerged elements. A vacuum-driven pressure system facilitates the movement of feed water through the microfiltration membrane, which has a permeate production capacity of 118 million gallons per day. This production capacity takes a 90 percent recovery rate for cycles of backwashing as well as clean-in-place processes. The clean-in-place processes utilize sodium hydroxide as well as citric acid to reduce membrane fouling and rehabilitate system performance (Burris, 2018).

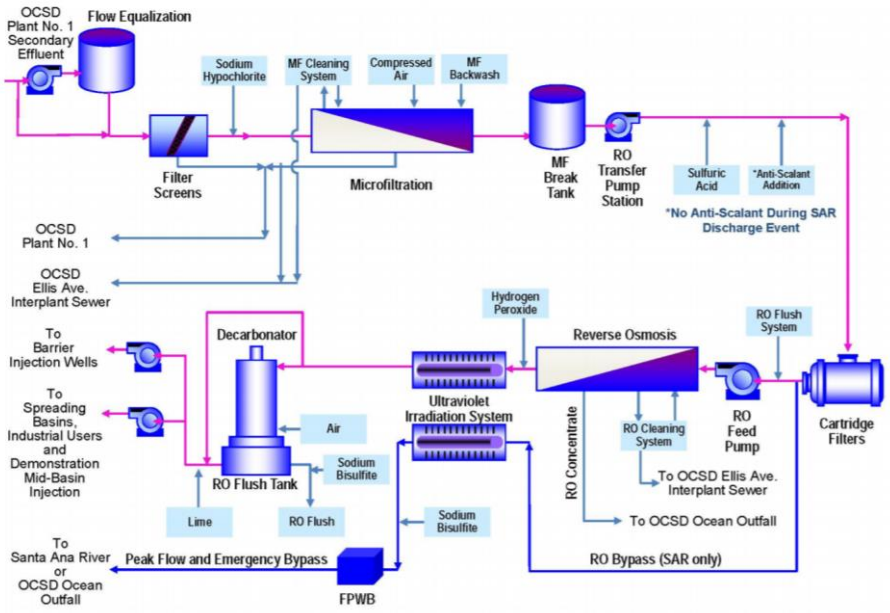

Figure VI-1 GWRS AWPF Process Flow Diagram (Burris, 2018)

Following the membrane filtration system, the influent goes through the reverse osmosis system. This system demineralizes water as well as reduces pollutant concentrations, such as viruses, inorganics, and organics. This treatment process employs polyamide membranes that are spiral wound as well as thin-film and composite. Chemical pretreatment occurs before the influent enters the system through the addition of antiscalant along with sulfuric acid and cartridge filtration, which is comprised of fourteen filters with filter sixes of 10 or 20 microns. Following pretreatment, pumps bring the feed water to the reverse osmosis system, which contains twenty-one units that all have a capacity of 5 million gallons a day. Furthermore, each unit has one hundred and fifty pressure vessels positioned as three stages (Burris, 2018).

Comprised of two main processes, the UV advanced oxidation process removes contaminants. These two main processes are the addition of hydrogen peroxide and UV radiation. Working as the main disinfectant, the UV radiation can destroy pollutants, such as N-nitrosodimethylamine, through photolysis. The formation of hydroxyl radicals occurs through the

integration of hydrogen into the system. These radicals can destroy pollutants that are resistant to photolysis through UV radiation. The UV system is closed-loop and utilizes low-pressure UV lamps that have high output associated with them. Thirteen trains comprise the entirety of the UV system, each of which has six reactors as well as an 8.75 million gallon per day capacity (Burris, 2018).

Before discharging the effluent, the water goes through decarbonation along with lime stabilization. This post-treatment enhances the hardness, alkalinity, and pH to produce more reliable and less caustic reuse water. The decarbonation process with a 72 million gallon per day capacity consists of six decarbonators. This process increases the pH of the effluent by removing the excess surplus of carbon dioxide for a fraction of the effluent. Following decarbonation, this portion of effluent combines with the rest of the effluent that did not undergo decarbonation, and the treatment process of lime stabilization occurs. The addition of calcium hydroxide during the lime stabilization process neutralizes the leftover carbon dioxide still present in the reuse water. Furthermore, this process also increases the water's alkalinity along with pH, which creates a more stable effluent. The equipment that comprises the lime destabilization system is storage silos, pumps, saturators, mixing tanks, as well as aging tanks for the slurry (Burris, 2018).

VII. In Vitro Bioassays in Water Reuse

In vitro bioassays can assess the impact of emerging contaminants, to enhance traditional chemical analysis used during the evaluation of water quality, and to minimize ambiguity in safety analysis (Simon, et al., n.d.). Furthermore, they have a significant role in the evaluation of the ecotoxicity of wastewater as well as the creation of toxicity levels for contaminants (Abba et al., 2019; Rizzo, 2011). This technology relies on a control to measure the impact of a pollutant

on an exposed organism. Some categories of bioassays used in water quality analysis include invertebrate, plants and algae, microbial, fish, and cell-based (Rizzo, 2011; Escher et al., 2013).

Invertebrate bioassays assess the contaminants' toxic impact in water matrices. Daphnia magna is the most common invertebrate bioassay implemented in wastewater quality along with water quality evaluation. Using controlled settings, the Daphnia magna is integrated into the water matrixes and following a set duration of incubation, the remaining Daphnia magna bioassays are counted. With a strong pollutant sensitivity and relatively quick reproduction timespans along with parthenogenic reproduction, Daphnia magna has many advantages to consider. Along with Daphnia magna, Artemia salina is another commonly used invertebrate bioassay. Artemia salina functions as a test entity for bioactive compounds evaluation, cyanobacterial along with algal and anthropogenic chemical exposure, and sudden toxic reactions to biochemical processes. Therefore, Artemia salina is beneficial to use in water quality analysis. Other advantages for this bioassay include commercial availability, indefinite preservation of the cyst in laboratory settings, easy application along with a low cost. Furthermore, it only needs a small amount of sample to work and can operate with high specimen production output (Rizzo, 2011).

Plant bioassays have small maintenance expenditures as well as various endpoints for evaluation including enzyme activity, rate of germination as well as biomass weight. They are effective in the assessment of inorganic as well as organic pollutant toxicity, sludge, solid refuse, polluted soils, and nanoparticles. Moreover, algal bioassays are appropriate for toxicological evaluations because of their pervasiveness and short lifespan. To count the number of algal bioassays present following the end of exposure, an automated molecule counter is operated and

the inhibition in the production of algae is the toxicity gauge. Unfortunately, the use of this bioassay can be difficult and unreproducible in some cases (Rizzo, 2011).

Another type of bioassay implemented in water quality assessment is microbial bioassays. These bioassays implement various processes depending on the ability to transform elements such as carbon, nitrogen, and sulfur, the activeness of enzymes, the presence of photosynthesis, death, as well as growth. Further parameters that can impact the process implemented include the uptake of glucose, expenditure of oxygen, and the production of luminescence. The wide range applicability of this bioassay allows it to be very useful in the characterization of water quality. One type of microbial bioassay is the AOC bioassay in which AOC stands for assimilable organic carbon. This bioassay can assess the capability of a certain water sample to encourage bacterial regrowth. With the AOC bioassay, Pseudomonas fluorescens species P17 in conjunction with Spirillum sp. species NOC are injected into the water specimen to determine the bacterial density of the sample before incubation. Consequently, the bacterial growth in these water specimens is observed during a period of incubation using plating techniques (Rizzo, 2011).

Other microbial bioassay tests include activated sludge respiration inhibition as well as luminescent. The test for the inhibition of activated sludge respiration is useful for assessing the harmfulness of chemicals to the microorganisms present in activated sludge. This assessment is done by observing the respiration rates following the exposure of a test chemical at various dosages. Generally, this test can establish the no observed adverse effect level (NOAEL) as well as the effective concentration (ECx). Luminescent microorganisms are useful for assessing toxicity as well. The most employed luminescent microorganism is Vibrio fischeri, which is a type of marine bioluminescent microorganism. This test analyzes toxicity which regards to

bacterial luminescent differences. With regards to all these microbial bioassay tests, the simplicity of them along with their relative quickness makes them advantageous to use in the analysis of toxicity (Rizzo, 2011).

To evaluate acute toxicity risks to the environment, the use of fish bioassay is an option. Fish bioassays facilitate the understanding of the impact of pollutant exposure, which could potentially occur through the discharge of wastewater effluent, to similar species. Common species of fish bioassays are rainbow trout along with bluegill sunfish. These species are highly sensitive and there is a lot of information that can characterize these species' reactions to pollutants in the natural environment. Overall, fish bioassays have exceptional sensitivity to pollutants; however, they have issues with standardization, need an extended amount of time and require training as well as equipment (Rizzo, 2011).

The use of cell-based bioassays contributes to the enhancement of information regarding pollutant processing along with the prioritization of them. They are unable to compensate for the use of regulatory in vivo assessment. However, they integrate well with water quality analysis. Escher et al. examined cell-based bioassays to determine the applicability of the use of bioassays in the evaluation of water quality, looking specifically at whether a contaminated water sample was able to produce a response and if this response was adequately small in the control specimens. With regards to the first point of assessment, Escher et al. found that for the relatively contaminated water sample, 60 positive responses were produced. Moreover, with regards to the endpoint, no blanks without solvents in them showed any responses and the procedural response showed minimal responses (Escher et al., 2013).

Escher et al. discussed the importance of having an array of bioassays when analyzing a water quality sample versus solely relying on one, which is not able to evaluate the water quality

thoroughly. This array should consist of distinct endpoints corresponding to certain water quality parameters along with more general ones like cytotoxicity. The use of indicator bioassays that deal with xenobiotic metabolisms, reactions to adaptive pressures along with endocrine disrupting compounds should be the minimum (Escher et al., 2013). Furthermore, it is also important to ensure that sample extraction is done in a manner that facilitates the effectiveness of the bioassays. Abbas et al. state that acidifying water specimens considerably changes the in vitro toxicity spectrum, specifically regarding the presence of anti-estrogenic, retinoic acid and anti-androgenic along with mutagenicity. On the other hand, sample filtration negligibly influenced the toxicity of the water specimen. Abbas et al. also found that the use of Telos C18/ENV as the water specimen extraction method at a pH level of 7 was a favorable method with regards to salvaging the toxicity of in vitro bioassays (Abbas et al., 2019). Ultimately, optimizing the sampling method is an important step in the effectiveness of bioassays to assess water quality along with the implementation of a wide range of bioassays (Abbas et al., 2019; Escher et al., 2013).